APS-LS-141 Revised
H.J. Moe
July 1991

ARGONNE NATIONAL LABORATORY
9700 S. CASS AVE.
ARGONNE, IL 60439

Advanced Photon Source: Radiological Design Considerations

Preface

In the course of developing the shielding design for the proposed Argonne Advanced Photon Source (APS), a number of internal documents treating various aspects of the shielding for the accelerating systems and storage ring were generated. In addition to the shielding calculations, estimates of radioactive and noxious gas production, induced activity in the structural components of the accelerator systems and other materials, and expected occupational and general public doses were also generated. Some of this information was needed to provide back-up documentation for information used in environmental assessments and safety analyses documents.

At the suggestion of the APS Project Director, Dr. Yanglai Cho, an effort was launched to consolidate the existing internal documents, and other information, into one document which would encompass the major design issues with respect to the radiological aspects of the machine. It was felt that such a single document would be more useful as a reference in terms of documenting the important radiological aspects of the APS design contained in the APS Preliminary Safety Analysis Report. This Light Source note is the result.

The APS Project and the author are grateful for the review of this and previous documents by Dr. Paul DeLuca, University of Wisconsin - Madison, for his helpful advice and suggestions, and for the fruitful discussion of the content of this document.

H. J. Moe

TABLE OF CONTENTS

PAGE

Preface i

Abstract ix

1.0 Introduction 1

2.0 Radiation Protection Design Objectives 1

3.0 APS Components and Parameters 1

4.0 Shielding Estimates 2
4.1 Introduction 2
4.2 Shielding Design Objectives 2
4.3 Types of Radiation Considered 5
4.4 Radiation Attenuation Parameters 5
4.5 Radiation Dose Equivalent Factors 7
4.6 Bulk Shielding Computations 8

5.0 Shielding and Dose Estimates for Linacs and Positron Converter 8
5.1 Assumptions and Parameters 8
5.2 Estimated Beam Losses in Linac System (e^- and e^+) 9
5.3 Electron Linac Shielding 10
5.4 Positron Converter Shielding 10
5.5 Positron Linac Shielding 11
5.6 Positron Beam Compression System Shielding 11

6.0 Shielding of Positron Accumulator Ring (PAR) 12

7.0 Shielding of Booster Synchrotron 14
7.1 Parameters 14
7.2 Shielding of the Booster Injection Area 15
7.3 Distributed Loss in Booster Synchrotron 16
7.4 Loss of Beam in Booster Synchrotron 16
7.5 Shielding of Booster Extraction Area 17

8.0 Storage Ring Shielding 19
8.1 Parameters 19
8.2 Continuous Loss During Beam Decay 19
8.3 Ratchet Wall Shielding 29

8.3.1 Ratchet Wall Geometry Change....29
8.3.2 Ratchet Shielding Calculations....29
8.3.3 Ratchet Wall Doors....32
8.4 Dose Rates in Module Experimental Areas....35
8.5 Shielding and Dose Rate Summary for Normal Operation....35
8.6 Skyshine Losses....35
8.7 Remarks....38

9.0 Radiological Consequences of Accidental Beam Losses....38
9.1 Linac Accidental Losses....39
9.1.1 Point Loss in Electron Linac....39
9.1.2 Point Loss in Positron Linac During Electron Acceleration....39
9.1.3 Loss Following Failure to Limit Electron Current....40
9.2 PAR Accidental Beam Loss....40
9.3 Synchrotron Accidental Beam Loss....40
9.4 Storage Ring Accidental Losses and Unusual Occurrences....40
9.4.1 Total Beam Loss at a Point....40
9.4.2 Bremsstrahlung into a Photon Beam Line....41
9.4.3 Scattered Bremsstrahlung into a Beam Line....41
9.5 Maximum Credible Incident....42
9.5.1 Scenario....42
9.5.2 Incident Parameters....43
9.5.3 Radiation Dose....43

10.0 Radioactive and Noxious Emissions....44
10.1 Introduction....44
10.2 Radioactive Gas Formation Estimates....45
10.2.1 Radioactive Emissions from the Linac System....46
10.2.2 Radioactive Emissions from the PAR and Synchrotron System....48
10.2.3 Radioactive Emissions from the Storage Ring....49
10.2.4 Average Concentration of Released Radionuclides....50
10.2.5 Radioactivity Released in Accidental Beam Losses....50
10.2.6 Dose Commitment Due to Radioactivity Released in Incidents....51
10.3 Noxious Gas Formation Estimates....53
10.3.1 Noxious Emissions in the Linac System....55
10.3.2 Noxious Emissions Due to Bremsstrahlung in the PAR and Synchrotron System....55
10.3.3 Noxious Emissions Due to Bremsstrahlung in the Storage Ring....56

10.3.4 Noxious Emissions Due to Synchrotron Radiation....56
10.3.5 Noxious Emissions Due to Synchrotron Radiation in the Synchrotron System....60
10.3.6 Noxious Emissions Due to Synchrotron Radiation in the Storage Ring....64
10.3.7 Noxious Emissions Due to Synchrotron Radiation in Experimental Enclosures....67

11.0 Activation of Accelerator Components and Other Materials....71
11.1 Introduction....71
11.2 Residual Radioactivity Estimates....72
11.3 Residual Radioactivity of the Electron Linac, Positron Linac, PAR, and Injector Region....74
11.4 Residual Radioactivity of the Converter Target....74
11.5 Residual Radioactivity of the Booster Synchrotron and the Extraction Region....74
11.6 Residual Radioactivity of the Storage Ring....75
11.7 Radioactivation of Cooling Water....75
11.8 Radioactivation of Soil....79

12.0 Bremsstrahlung Doses Produced in Vacuum Chamber Residual Gas....79
12.1 Introduction....79
12.2 Bremsstrahlung Dose Estimates for an Insertion Device....79
12.3 Bremsstrahlung Dose Rate Estimate for a Bending Magnet....81
12.4 Bremsstrahlung Dose Resulting from Loss of Vacuum....82

References....83

ADDENDUM - Review of the Radial Ratchet Wall Shielding

1.0 Introduction....A1

2.0 Upstream Bremsstrahlung Contributions....A1

3.0 Location of Additional Shielding....A7

4.0 Dose Rate in the Radial Ratchet Sections for Continuous Losses....A10

5.0 Location and Lateral Extent of the Additional Lead Shielding....A12

References....A15

List of Figures

Page

Figure 1 General layout of the Advanced Photon Source 3

Figure 2 Linac building 4

Figure 3 Layout of linac-to-PAR-to-injector-synchrotron transport line 12

Figure 4 Shielding layout for the addition of a PAR. 13

Figure 5 Geometry for Component Doses due to Continuous Loss around the Storage Ring 21

Figure 6 Bremsstrahlung Dose Distribution 23

Figure 7 GRN Dose Distribution 24

Figure 8 HEN Dose Distribution 25

Figure 9 Total Dose Equivalent Rate at Various Distances from the Positron Orbit. 27

Figure 10 Annual Dose Due to Direct Radiation and Skyshine. 28

Figure 11 General ratchet-wall dimensions 30

Figure 12 Section Through Wall in BM Ratchet Area. 33

Figure 13 Section Through Wall in ID Section. 33

Figure 14 Ratchet Wall Doors 34

Figure 15 Section View of a Shielded Beam Enclosure. 42

Figure 16 Geometry for average air path length computation 47

Figure 17 Synchrotron Radiation Spectra of Several Different Machines 57

Figure 18 Geometry for Synchrotron Radiation Trajectories in the Booster Synchrotron 60

List of Figures

Page

Figure 19 Geometry for Synchrotron Radiation Trajectory into BM2 62

Figure 20 Energy Absorption Rate in Air Due to Synchrotron Radiation in the Booster Synchrotron and Storage Ring Tunnels. 63

Figure 21 Geometry for Synchrotron Radiation Trajectories in SR 65

Figure 22 Spectral Dependence of the Absorbed Energy Rate in Air 68

Figure 23 Ozone Formation Rate in Air Versus Path Length. 69

ADDENDUM

Figure A1 Geometry for Component Doses due to Continuous Loss Around Storage Ring....A2

Figure A2 General Ratchet Wall Dimensions....A3

Figure A3 Upstream Bremsstrahlung Radiation Contribution from BM Beamline Not Intercepted by the Pb Stop or Ratchet Side Wall....A5

Figure A4 Upstream Bremsstrahlung Radiation Contribution from ID Beamline Not Intercepted by the Pb Stop or Ratchet Side Wall....A6

Figure A5 Angular Spread of Upstream Bremsstrahlung from a BM Line....A8

Figure A6 Angular Spread of Upstream Bremsstrahlung from an ID Line....A9

Figure A7 Dose Rate Due to Continuous Loss During SR Operation - 1.3 m Minimum Distance to Dose Point....A11

Figure A8 Dose Rate Due to Continuous Loss During SR Operation - 1.72 m Minimum Distance to Dose Point....A13

Figure A9 Contribution to Dose from Bremsstrahlung Spike....A14

Figure A10 Recommended Locations of Additional Lead Shielding....A16

Figure A11 Placement of Lead Shielding from a BM Beamline in Order to Shield Upstream Bremsstrahlung....A17

Figure A12 Placement of Lead Shielding for an ID Beamline in Order to Shield Upstream Bremsstrahlung....A18

List of Tables

		Page
Table 4.4.1	Attenuation Lengths	6
Table 4.5.1	Transverse Dose Equivalent Conversion Factors	7
Table 5.2.1	Estimated Losses in the Linac System Components	9
Table 7.5.1	Dose Rate for Fractional Beam Loss	18
Table 7.5.2	Average Dose Rate Using Local Shielding	18
Table 8.2.1	Annual Dose Equivalent (Direct Radiation for 8000 h Operation)	26
Table 8.5.1	Shielding and Dose Rate Summary	36
Table 8.6.1	Annual Dose Equivalent (Skyshine Radiation for 8000 h Operation)	38
Table 10.2.5.1	Maximum Energy Loss and Yield of Radionuclides in System Incident	51
Table 10.2.6.1	Standard Deviations for F Stability Class	52
Table 10.2.6.2	Estimated Effective Dose Equivalents at the Nearest Site Boundary from Radioactive Release Incidents	53
Table 10.3.7.1	Summary of Estimated Annual Noxious Gas Releases	71
Table 11.6.1	Initial Activity at Shutdown of the Important Radionuclides Contributing to the Residual Radiation	76
Table 11.7.1	Estimated Saturation Activity of Radionuclides in the Cooling Water of APS Components	78

Advanced Photon Source: Radiological Design Considerations

H. J. Moe

ABSTRACT

The Argonne National Laboratory's Advanced Photon Source (APS) will include a 200 MeV electron linac, a positron converter target, a 450 MeV positron linac, a positron accumulator ring, a 7 GeV booster synchrotron, a 7 GeV positron storage ring and a number of experimental photon beam lines utilizing synchrotron radiation.

A number of radiological design considerations for such a facility need to be addressed. In addition to shielding considerations for each of the various components and the experimental beam lines, other issues involve production of radioactive and noxious gases, induced activity in the accelerator structures and other materials, potential radiation doses during abnormal occurrences, radiation fields produced by gas bremsstrahlung, and the off-site doses to the public.

The methodology used to estimate the contributions from each of the above-mentioned issues is detailed. Estimates of the magnitude of the contribution of each component are presented, and doses, as well as released quantities, are compared to the relevant DOE and EPA requirements.

H. J. Moe
July 1991

Advanced Photon Source: Radiological Design Considerations

1.0 Introduction

A number of considerations involving the radiological aspects of the Advanced Photon Source (APS) need to be addressed. In addition to the shielding of the various accelerator components and experimental beam lines, other issues involve production of radioactive and noxious gases, induced activity in the accelerator structures and other materials, potential radiation doses during abnormal circumstances, and the off-site doses to the public need to be determined.

Bulk shielding estimates for the accelerator components have been made previously (MOE 87a, MOE 88, KNO 88). Dose estimates due to direct radiation and skyshine computed in LS-84 (MOE 87), have been recalculated for the present siting of the facility (MOE 89). This document incorporates and updates the relevant information from the previous write-ups, as well as additional material addressing the issues stated above.

2.0 Radiation Protection Design Objectives

The Department of Energy's (DOE) basic occupational exposure limit is 5 rem per year (DOE 88). However, in applying the ALARA ("as low as reasonably achievable") philosophy, the goal is to maintain exposures well below this limit. In particular, the DOE guidance in the same document states that the ALARA design objective for new facilities is to limit occupational exposures to one-fifth of 5 rem per year (~ 0.5 mrem/h for a 40-h work week). DOE Order 5400.5 (DOE 88a) limits the annual dose to members of the public to 100 mrem per year. In addition, this Order also prohibits annual doses to the public in excess of 10 mrem due to the release of airborne emissions as a consequence of DOE activities. A further requirement of 5400.5 is that actual or potential doses in excess of 10 mrem in a year to any member of the public require notification of DOE Headquarters. These dose limiting objectives and guidance have been used as the basis for establishing the adequacy of the bulk shielding design and other dose mitigation systems for the normal operations of the facility.

3.0 APS Components and Parameters

The various components of the APS are: a 200 MeV electron linac, a tungsten converter target to produce positrons, a 450 MeV positron linac, a positron accumulator ring (PAR), a

booster synchrotron to accelerate 450 MeV positrons to 7 GeV, an 1104 m circumference positron storage ring, and various photon experimental beam lines utilizing synchrotron radiation for experimental studies. The general layout of the APS facility systems is indicated in Figure 1, and a more detailed diagram of the Linac system and the PAR is shown in Figure 2. The storage ring operates at 0.1 A of circulating positron current and is expected to have a mean positron-beam lifetime of 10 h. For purposes of calculation, the circulating current is usually taken as 0.3 A and the operation time is considered 8000 h per year. The facility is located 140 m from the nearest Laboratory boundary.

4.0 Shielding Estimates

4.1 Introduction

Shielding estimates for the Advanced Photon Source (APS) have been computed utilizing the currently available design parameters. Computations of the resulting radiation fields have been made for several situations involving normal beam loss, as well as for certain postulated accidental beam losses. Whenever available, experimental data on attenuation lengths obtained at existing accelerators and light sources have been used in lieu of theoretical estimates.

4.2 Shielding Design Objectives

The occupational exposure design objective stated in DOE Order 5480.11 implies an average dose rate limit of 0.5 mrem/h, based on a 40 h work week. Sufficient concrete as a bulk shield is used to achieve reasonable global shielding of accelerator components for distributed losses in the system. Localized shielding, which may consist of iron, lead and/or dense polyethylene is used at high loss points to supplement the global shield. In some cases, exclusion zones or limited time access may be required during the operational time of the particular component in order to meet the guideline.

An additional consideration used in the shielding estimates was to limit the dose received by any individual, due to any single beam dump loss, to less than 100 mrem. This is readily accomplished with no additional shielding for the design current of 0.1 A.

Shielding considerations with respect to members of the public dictated sufficient bulk shielding to limit the sum of the direct and skyshine, or scattered, radiation contributions to < 25 mrem/y to an individual at the nearest site boundary (140 m).

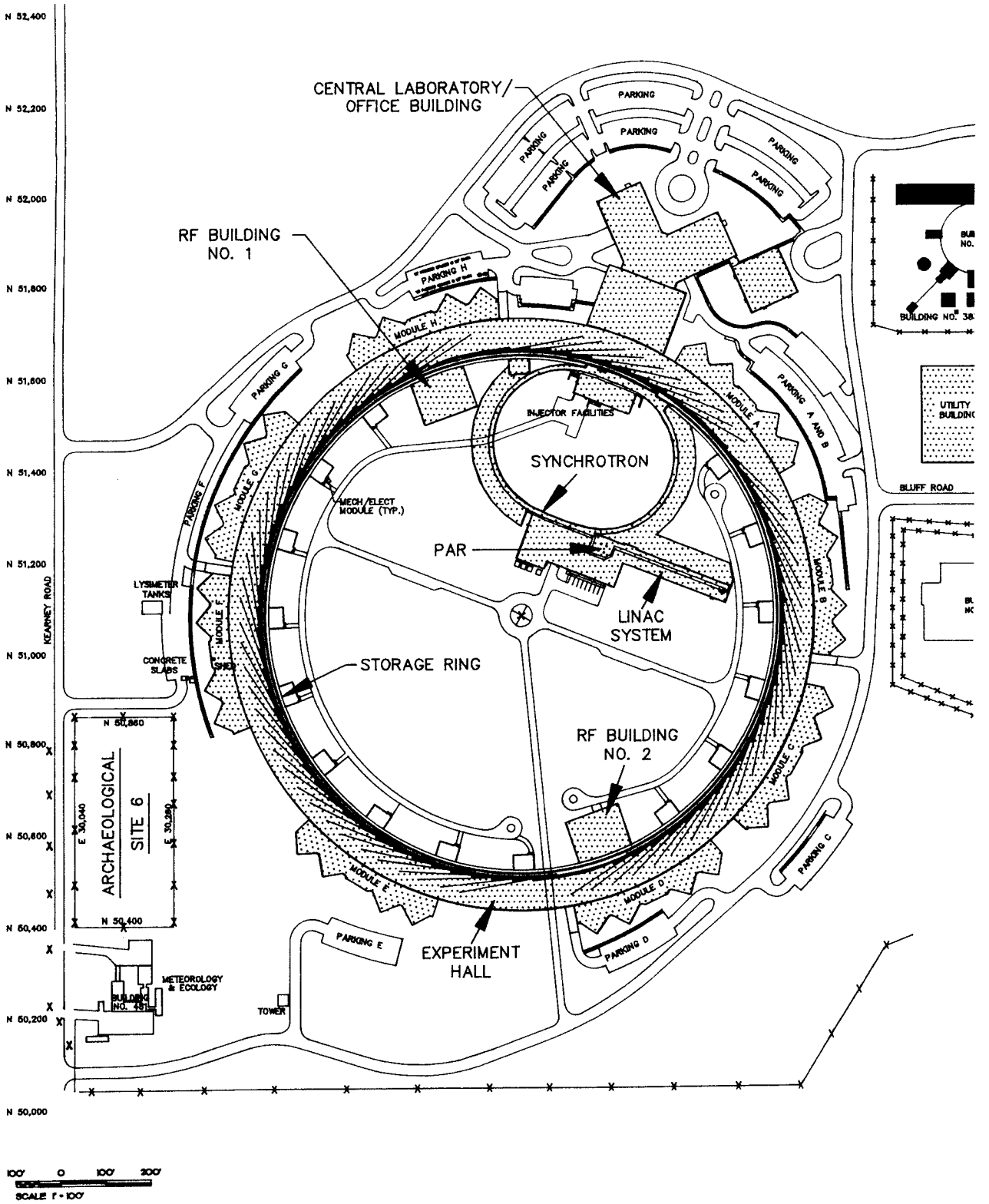

Figure 1 General layout of the Advanced Photon Source

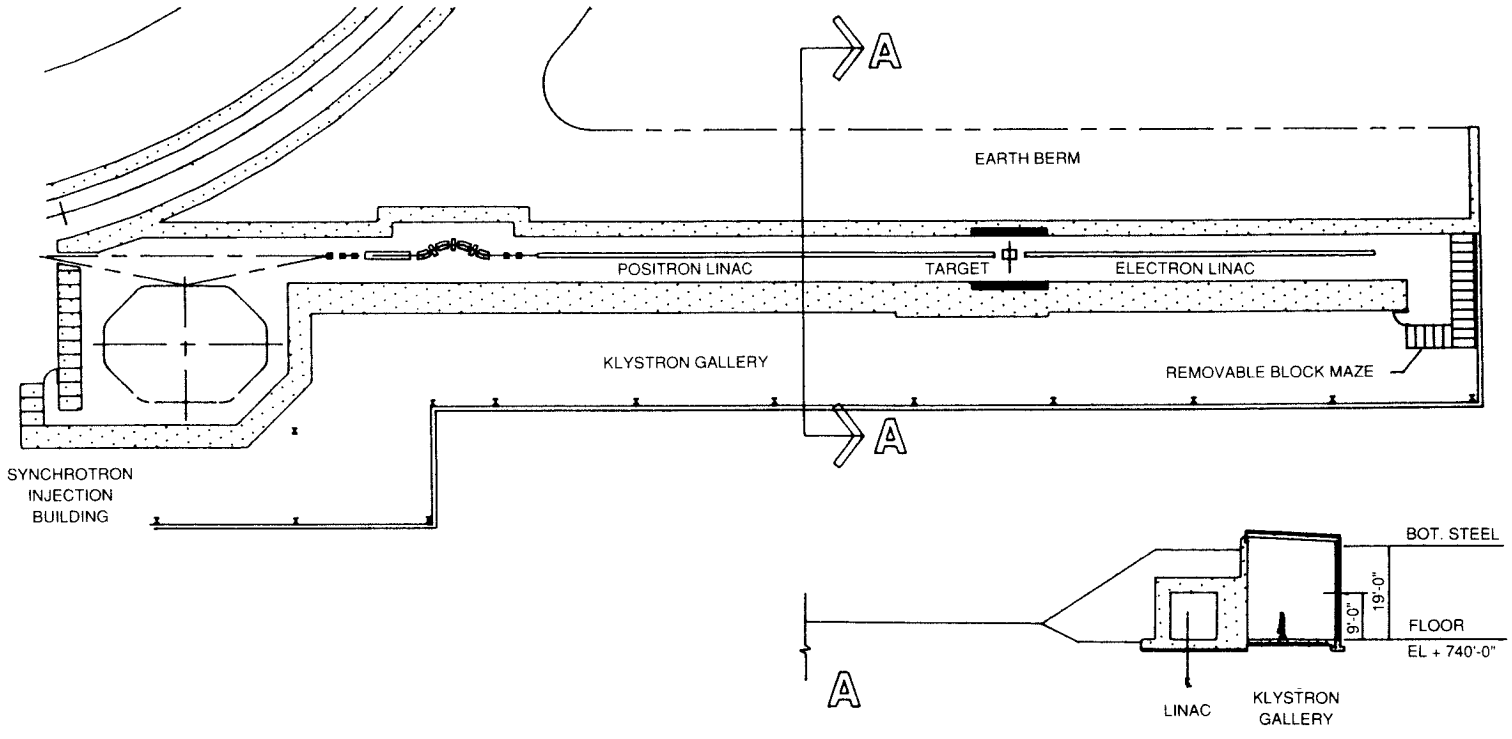

Figure 2. Linac building

4.3 Types of Radiation Considered

Depending upon the energy of the accelerated particles, one or more of three radiation components, each with differing attenuation lengths in a given medium, must be dealt with. These are bremsstrahlung (BREM), giant resonance neutrons (GRN), and high energy neutrons (HEN). High energy electrons and positrons produce photons which in turn produce more electrons and positrons which produce more photons. The electromagnetic shower which develops contains a spectrum of bremsstrahlung photons with energies up to the incident particle energy. This bremsstrahlung is highly peaked in the forward direction of the particle beam, but the transverse component cannot be neglected. Giant resonance neutrons are produced by photonuclear interactions (threshold energy in most materials in the range 7-20 MeV). They are emitted almost isotropically and have an average energy of about 2 MeV. For electrons or positrons above several hundred MeV, photons are produced with energy greater than the threshold for pion production (~140 MeV) by photonuclear reactions. The pions (π mesons) which are produced initiate nuclear cascades resulting in the production of high energy neutrons (E > 100 MeV). The high energy component is not isotropic, but in many shielding situations, only the transverse component is important. For shielding estimates in this review, both the GRN and HEN components are generally taken to be isotropic.

The bulk shielding provided for the above mentioned components will also adequately attenuate any synchrotron radiation which escapes from the vacuum chamber in which the particles are accelerated. The synchrotron radiation is produced when charged particles, in this case positrons, are bent in magnetic fields. The synchrotron radiation is composed of photons, generally in the keV energy range for the APS, and this radiation is greatly attenuated by the vacuum chamber itself. Any synchrotron radiation which escapes the vacuum chamber will also be adequately attenuated by the shielding of the tunnel.

The production of muons by electromagnetic pair production becomes possible at the threshold of 211 MeV. An additional source of muons is through decay of π mesons but this source is relatively small compared to the direct production. However, the direct rate of production of muons by bremsstrahlung is small at 7.7 GeV for a positron maximum current of 0.3 A, and the muons are highly peaked in the forward direction so their contribution is of minimal importance (FAS 84, SWA 79).

4.4 Radiation Attenuation Parameters

Information on the attenuation of bremsstrahlung, giant resonance neutrons, and the high energy neutrons by different shielding was taken from the literature, whenever available. The literature sources consulted for shielding information and shielding material attenuation lengths include ALS 67, ALS 67a, ALS 70, ALS 73, BAT 65, BAT 67, BAT 70, DIN 77, FAS 84, JEN 79, NAK 81, NCR 77, NEL 68, NEL 74, NEL 74a, PAT 73, POO 80, SCH 73, SHU 69, SUL 82, SWA 79, SWA 79a, SWA 85, TES 79, and WYC 71.

With respect to attenuation of the high energy neutrons, attenuation lengths were not available in the literature for every material of interest. In the absence of quoted values, the attenuation lengths for the high energy neutron radiation component (E > 150 MeV) were estimated from the expression:

$$\lambda = 38.5\ A^{0.3}\ g/cm,^2 \qquad (4.4.1)$$

adapted from ICRU Report 28 (ICR 78), in which A is the mass number of the attenuating material.

In all cases, an attempt was made to use conservative values for the attenuation lengths quoted in the literature. Table 4.4.1 lists the attenuation lengths for the shield materials which were used in the shielding estimates. Values for the attenuation lengths of Pb and polyethylene for the HEN component were computed from equation 4.4.1. The effective mass of polyethylene was computed according to Schaeffer (SCH 73). The bremsstrahlung attenuation length for dense polyethylene was estimated by using the minimum attenuation coefficient found in Hubbell (HUB 69).

Table 4.4.1 - Attenuation Lengths

Radiation Component	Shielding Material	Attenuation Length $\lambda(g/cm^2)$
Bremsstrahlung	Lead (density = 11.34 g/cc)	25
	Concrete (density = 2.35 g/cc)	49
	Concrete (density = 3.7 g/cc)	50
	Iron (density = 7.8 g/cc)	37
	Sand (Earth)(density = 1.6 g/cc)	70
	Dense Polyethylene (density = 1.01 g/cc)	70
Giant Resonance Neutrons	Concrete	40
	Concrete (density = 3.7 g/cc)	45
	Dense Polyethylene	6.3
	Sand (Earth)	33
	Iron (backed by H)	100
	Lead (backed by H)	161
High Energy Neutrons	Concrete	65 (E< 100 MeV) 115 (E> 100 MeV)
	Concrete (density = 3.7 g/cc)	125 (E> 100 MeV)
	Iron	138
	Lead	191 (E >150 MeV)
	Dense Polyethylene	62 (E >150 MeV)
	Sand (Earth)	90

4.5 Radiation Dose Equivalent Factors

The unshielded radiation dose equivalent factors which were used in the shielding computations were adapted from Fasso, et al. (FAS 84), with their suggested modifications. These factors for the 90° component, which relate the dose equivalent due to a given component radiation to the energy loss when positrons interact with matter, are shown in Table 4.5.1:

Table 4.5.1 - Transverse Dose Equivalent Conversion Factors

Radiation Component	Radiation Dose Equivalent Factor, F_H $\left(\frac{\text{mrem m}^2}{\text{J}}\right)$
Bremsstrahlung	2.8*
Giant Resonance Neutrons	0.63
High Energy Neutrons	0.075

*Use 28 $\frac{\text{mrem m}^2}{\text{J}}$ for the completely unshielded bremsstrahlung component.

These factors refer to the unshielded dose rates at 1 m in the transverse direction to the positron beam. As noted, in the absence of any shielding, the bremsstrahlung component will include a soft radiation component (e^+ and e^-), which is generally neglected since the above factors assume that sufficient shielding is present to assure attenuation of the particle component, ~ 25 cm of concrete (DIN 77).

In the forward direction with respect to the positron beam (0 degrees), the value of F_H for bremsstrahlung is given by

$$8.3\ E_o \quad \left(\frac{\text{mrem m}^2}{\text{J}}\right) \qquad \text{(FAS 84, SWA 79),} \qquad (4.5.1)$$

in which E_o is the initial positron energy in MeV. In general, the same values given in the table above are used for the GRN and HEN components in the forward direction.

4.6 Bulk Shielding Computations

Bulk shielding computations were based on the following expression for point losses in the various components of the APS system:

$$\dot{H} = \sum_i \frac{F_{H_i} W e^{-d/\lambda_i}}{r^2}, \qquad (4.6.1)$$

in which $\dot{H}$ has units of mrem/h, if W, the energy loss rate, is expressed in J/h, F_{H_i} is the appropriate dose conversion factor from the table, for the i^{th} radiation component, r is the source to dose point distance in m, d is the shield thickness in g/cm^2, and λ_i is the attenuation length for the i^{th} radiation component, in g/cm^2.

5.0 Shielding and Dose Estimates for Linacs and Positron Converter

5.1 Assumptions and Parameters

The revised physical parameters used to recalculate shielding for the electron linac, the positron converter and the positron linac are:

Electron Linac:

Pulse Amplitude: 1.2 A
Pulse Width: 40 ns
Pulse Repetition Rate: 24 per 1/2 s = 48 pps

Charge per Pulse: 3×10^{11} e^-/ pulse

Average Current: $I = 1.2(40 \times 10^{-9})48 = 2.3$ μA e^-
Maximum Energy: 200 MeV
Electron Beam Power at Target: 2.3 μA(200 MeV) = 460 W

Positron Converter:

Conversion Ratio: 0.0083 e^+/e^-
Transmission to Positron Linac: 60 %, which gives a net conversion of 0.005 e^+/e^-

Positron Linac:

Positron Charge per Output Pulse: 1.5×10^9 e^+/pulse
Positron Average Current: I = 11.5 nA e^+
Maximum Energy: 450 MeV
Positron Beam Power: 5.18 W

Tunnel Parameters:

Dimensions: 9' by 9'
Beam Height: 5' above floor level
Distance from Beam Line to Inner Shield Wall: 1.7 m
Length of e^- Linac: ~ 23m
Length of e^+ Linac: ~ 31m

5.2 Estimated Beam Losses In Linac System (e^- and e^+)

For the various components in the Linac system (see Figure 2), shielding computations were based upon normal operation point losses of a certain fraction of the beam power. The assumption of point losses in this and for the other accelerator systems is a prudent conservative approach which gives a maximum dose estimate. In some cases, the realization of a point loss of a beam may be unattainable, and the more likely occurrence will be a deposition along a length of a surface giving rise to a line source, in which the resulting dose would be much reduced. The point losses are indicated in Table 5.2.1 below:

Table 5.2.1 - Estimated Losses in the Linac System Components

Component	$\bar{I}$ (μA)	Loss (%)	$\bar{E}$ (MeV)	Average Power Loss (W) e^+	Average Power Loss (W) e^-
Gun Output	5.69	55	0.15		0.47
Buncher	2.56	10	100		25.6
First Linac Output	2.3	100	200		460
Second Linac Input	1.91×10^{-2}	40	60	0.46	
Transmitted	1.15×10^{-2}				

5.3 Electron Linac Shielding

In LS-90 (MOE 87), the Electron Linac shielding was determined to be 2 m of concrete, and the distance to the nearest dose point was taken as 4 m. For the Klystron Gallery side, the shielding is 2 m of concrete. On the opposite side of the linac, the shielding is part concrete, part earth berm which increases the total distance to the dose point. For the revised value of power lost, 25.6 W, the computed dose rates, utilizing equation 4.6.1, are

$$\dot{H}_{BREM} = \frac{2.8(25.6)(3.6 \times 10^3)e^{-\frac{2.35(200)}{49}}}{(4)^2} = 1.101 \text{ mrem/h}$$

$$\dot{H}_{GRN} = \frac{0.63(25.6)(3.6 \times 10^3)e^{-\frac{2.35(200)}{40}}}{(4)^2} = 0.029 \text{ mrem/h}$$

$$\dot{H}_{HEN} = \frac{0.075(25.6)(3.6 \times 10^3)e^{-\frac{2.35(200)}{65}}}{(4)^2} = 0.313 \text{ mrem/h}$$

for a total of 1.44 mrem/h, on the Klystron Gallery side. Assuming an operational time of 10 %, the average dose rate would be 0.14 mrem/h, within the guideline of 0.5 mrem/h. With the addition of localized lead shielding, the dose rate can be reduced to within the guideline even for continuous operation of the linac. With respect to the earth berm side of the shielding, the dose rate will be within the guideline without any local shielding.

5.4 Positron Converter Shielding

At the positron converter, we assume a loss of 460 W. If an additional 10 cm thickness of iron is added to the shield on the Klystron Gallery side without altering the shield thickness, the total shielding in the converter area will then be 40 cm of iron backed up by 160 cm of concrete. This added shielding will be 5 m in length, starting at the beginning of the converter area. No change in shielding will be needed on the ceiling or the earth berm shield side. For the increased shielding, the dose rates become

$$\dot{H}_{BREM} = \frac{2.8(460)(3.6 \times 10^3) e^{-\frac{7.8(40)}{37}} e^{-\frac{2.35(160)}{49}}}{(4)^2}$$

$$= 0.029 \text{ mrem/h}$$

$$\dot{H}_{GRN} = \frac{0.63(460)(3.6 \times 10^3) e^{-\frac{7.8(40)}{100}} e^{-\frac{2.35(160)}{40}}}{(4)^2}$$

$$= 0.238 \text{ mrem/h}$$

$$\dot{H}_{HEN} = \frac{0.075(460)(3.6 \times 10^3) e^{-\frac{7.8(40)}{138}} e^{-\frac{2.35(160)}{65}}}{(4)^2}$$

$$= 2.49 \text{ mrem/h},$$

giving a total of 2.76 mrem/h. For an assumed operational time of 10 %, the average dose rate would be 0.276 mrem/h which is within the guideline. The dose rate can also be further reduced by using localized lead and dense polyethylene shielding around the converter target.

5.5 Positron Linac Shielding

For the Positron Linac, the previous amount of shielding was more than adequate for the positron beam but was kept at 2 m to provide shielding for the expected losses in the accompanying electron component. For the increased intensity in the new design, the 2 m is still adequate for shielding.

5.6 Positron Beam Compression System Shielding

At the beam compression system, the loss is assumed to be 10 % of the positron beam, which amounts to 0.518 W (11.5 nA x 450 MeV x 0.1). In addition, the accompanying electron beam, assumed to be equal in magnitude to the positron beam, is entirely lost at a dump in this same region. This gives an additional loss of 5.18 W, for a total of 5.7 W. The resulting dose rates are

$$\dot{H}_{BREM} = 0.245 \text{ mrem/h}$$

$$\dot{H}_{GRN} = 0.006 \text{ mrem/h}$$

$$\dot{H}_{HEN} = 0.070 \text{ mrem/h}$$

for a total of 0.321 mrem/h. For an operational time of 10%, the average dose rate will be 0.032 mrem/h, which meets the guideline.

6.0 Shielding Of Positron Accumulator Ring (PAR)

The Transport Line from the Linac into the PAR and from the PAR into the synchrotron is shown in Figure 3. The circumference of the PAR is 30.6 m. The PAR accumulates the 24 positron pulses into a single bunch during each 0.5 s cycle of the injector synchrotron and transfers the bunch to the synchrotron (CRO 88).

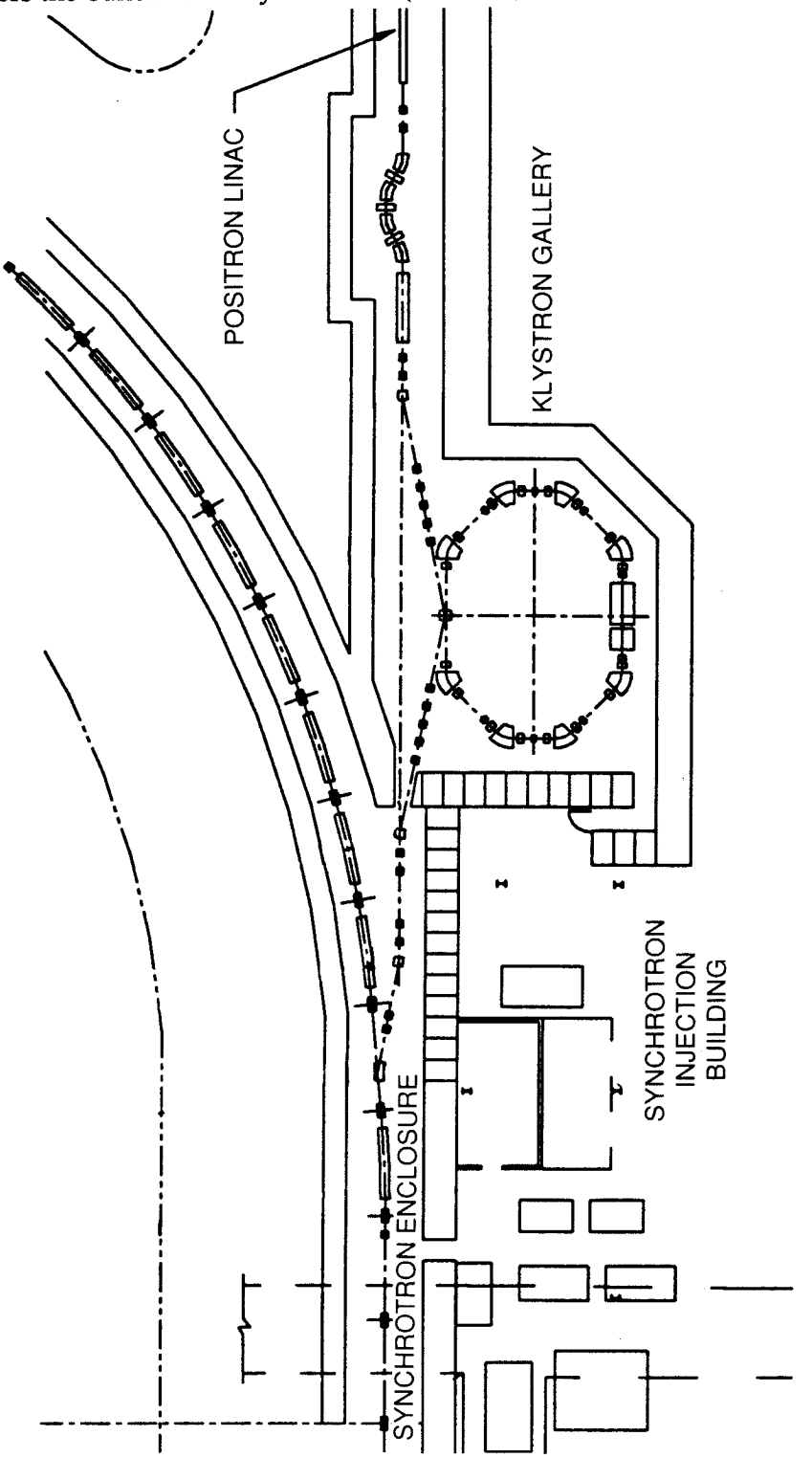

Figure 3. Layout of linac-to-PAR-to-injector-synchrotron transport line.

The shielding estimates for the PAR are based upon a total of 7.2 x 10^{10} e^+/s of energy 450 MeV being delivered to the PAR. These parameters give a beam power of 5.184 W, of which 50 % is assumed to be lost at point P in Figure 4 below. This assumption is

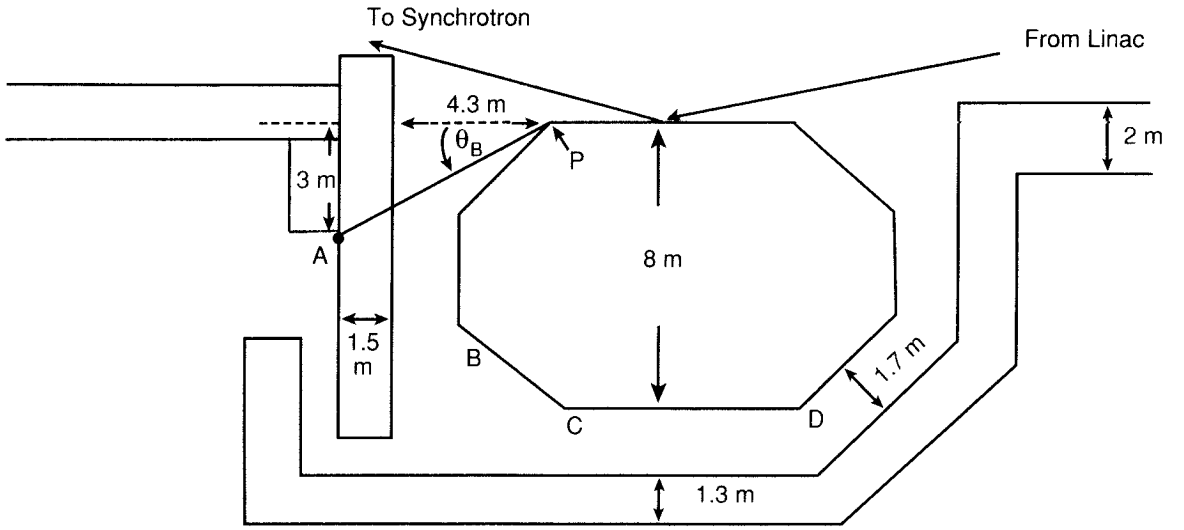

Figure 4. Shielding layout for the addition of a PAR.

based on experience at DESY which indicates that most of the loss takes place in this region and that following this, about 99 % of the remainder is delivered to the synchrotron. For the geometry shown in the figure, the forward directed bremsstrahlung will be intercepted by sufficient concrete to nullify any significant contribution to the dose rate in that direction. The nearest dose point of concern is A in the figure. To estimate the bremsstrahlung contribution at point A, the following empirical expression, adapted from Swanson, et al. (SWA 85), which expresses the angular dependence of the bremsstrahlung dose equivalent factor, was used:

$$F_{H_i} = 16.7E_o(2^{-\theta_B/\theta_{1/2}}) + 833(10^{-\theta_B/21}) + 25(10^{-\theta_B/110}) \qquad (6.0.1)$$

In which F_{H_i} is in (mrem m^2/J) at 1 m, E_o is the positron energy in MeV, θ_B is the bremsstrahlung emission angle with respect to the original positron beam direction, in degrees and $\theta_{1/2}$ is found from the expression $\theta_{1/2} E_o = 100$ MeV deg.

The first term of the expression accounts for the intense, highly peaked forward component of the bremsstrahlung, the remaining terms express the contribution as a function of θ_B. For point A in Figure 1, the distance from the loss point is 6.53 m and θ_B is taken as 27.35

degrees. The bremsstrahlung dose factor at this angle is then:

$$F_{H_{BREM}} = 16.7(450)\left(2^{-\frac{27.35(450)}{100}}\right) + 833\left(10^{-\frac{27.35}{21}}\right) + 25\left(10^{-\frac{27.35}{110}}\right)$$

$$= 55.6 \ \frac{\text{mrem m}^2}{\text{J}} \ .$$

The slant thickness through the shield is obtained from tsec 27.35°, in which t is the actual shield thickness. The dose rates for an assumed side wall shielding of 1.5 m of concrete and a 50 % loss at a point are:

$$\dot{H}_{BREM} = 3.696 \text{ mrem/h}$$

$$\dot{H}_{GRN} = 0.007 \text{ mrem/h}$$

$$\dot{H}_{HEN} = 0.037 \text{ mrem/h}$$

The total dose rate is 3.74 mrem/h, but for an operational time of 10 %, the average dose rate is reduced to 0.374 mrem/h, which is within the guidelines. Because of the increased distance from point P in Figure 4 to other dose points outside of the PAR, only 1.3 m of shielding is needed for the remaining shielding walls of the PAR.

With respect to the roof shielding of the PAR, the shielding is designed so that the area may not be occupied by personnel while the accelerator is in operation. Assuming a roof shielding of 1.0 m of concrete and a total distance of 3.22 m to the dose point, the computed total dose rate is 24.2 mrem/h on the roof directly above the point P in Figure 4. Assuming an operational time of 10 % of continuous, the average dose rate turns out to be 2.42 mrem/h. Additional local lead shielding provided around the loss points will reduce the average dose rate to within the guidelines.

Although no beam loss in the PAR is expected to result in a forward directed beam other than at point P in Figure 4, lead beam stops (10 -15 cm thick) which will greatly attenuate the bremsstrahlung component can be provided for the three positions (B, C and D) where a problem might develop.

7.0 Shielding of Booster Synchrotron

7.1 Parameters

The Booster Synchrotron is in the shape of a racetrack or ellipse, with a circumference of 368 m. The shielding, except in the injection and extraction regions, consists of 0.8 m thick

concrete-equivalent shielding. Generally, the shielding is constructed of 30 cm of concrete and enough of an earth berm covering to be the shielding equivalent of 0.8 m concrete. Since bremsstrahlung is the most prominent radiation needing shielding, the equivalence relationship is based on the equivalent bremsstrahlung attenuation. That is, the thickness of soil which is equivalent to a certain thickness of concrete is found from

$$e^{-\frac{2.35\ X(conc)}{49}} = e^{-\frac{1.6\ X(soil)}{70}}$$

$$\frac{2.35\ X(conc)}{49} = \frac{1.6\ X(soil)}{70}$$

$$X(soil) = \frac{70(2.35)\ X(conc)}{49(1.6)}$$

$$X(soil) = 2.1\ X(conc).$$

The above result implies that the required thickness of earth berm will be 105 cm for the Booster Synchrotron earth berm. In the injection and extraction regions, the shielding is concrete and is 1.5 m thick. The distance from the positron orbit to the shield wall is taken as 1.67 m. The synchrotron operates at a frequency of 2 Hz. The distance to the nearest dose point differs in each of the regions of the synchrotron and is given in the discussions below.

7.2 Shielding of Booster Injection Area

The assumed loss rate at the Injector was taken as 50 % in LS-90. Using this same assumption with the increased intensity, the power loss now becomes:

$$W = 7.2 \times 10^{10} (0.5)(450)(1.6 \times 10^{-13})(3.6 \times 10^{3})$$

$$= 9.33 \times 10^{3}\ J/h.$$

For a shield of 1.5 m of concrete and a minimum distance of 3.2 m to the dose point, the dose rates are:

$$\dot{H}_{BREM} = 1.916\ mrem/h$$

$$\dot{H}_{GRN} = 0.085\ mrem/h$$

$$\dot{H}_{HEN} = 0.302\ mrem/h,$$

which gives a total does rate of 2.3 mrem/h. For an operational time of 10 % of continuous, the average dose rate would be 0.23 mrem/h, which is within the guideline. If 10 cm of lead were used as local shielding, the photon dose rate could be reduced to about 0.02 mrem/h, and the total dose rate would then meet the guideline without averaging. At times, the loss rate at the Injector may reach 100%, such as during injecting studies or commissioning. On these occasions, the dose rate could be as high as 4.6 mrem/h at the minimum distance, but localized lead shielding of the loss points will still bring the dose rate to within the guideline.

7.3 Distributed Loss in Booster Synchrotron

For purposes of estimating the dose rate due to distributed losses in the synchrotron, it is necessary to assume that a portion of the beam is lost during each accelerating cycle. It was conservatively assumed that 2% of the beam is uniformly lost around the circumference of the synchrotron. The dose rate was then estimated by using the methodology described later in Section 8.2. This was accomplished by assuming a circle of equivalent circumference (368 m) to represent the racetrack, using a shield thickness of 1.35 m (30 cm concrete plus 105 cm of soil) and adjusting the values of the attenuation coefficients used in the expressions to reflect the equivalent attenuation of the combination shield.

The loss rate for this case is

$$\frac{7.2\times10^{10}\ e^{+}/s\left(\frac{450+7000}{2}\ \text{MeV}\right)(.02)(1.6\times10^{-13}\ \text{J/MeV})(3.6\times10^{3}\ \text{s/h})}{2\ \pi\ \text{(rad)}}$$

$$= 492\ \text{J/h rad.}$$

The average energy is used in the above expression since the positrons are accelerated from 450 MeV to 7 GeV during the cycle.

The cumulative contribution at the dose point, obtained by integrating the contribution from each loss point along the orbit, is

6.63×10^{-4} mrem rad/J. The estimated dose rate is

$$H = 6.63 \times 10^{-4}\ \text{mrem rad/J}\ (492\ \text{J/h rad}) = 0.326\ \text{mrem/h.}$$

For 10% operational time, the average dose rate will be 0.033 mrem/h.

7.4 Loss of Beam in Booster Synchrotron

For this case, consider a point loss of the positron beam ($10^{11}e^{+}$ at 7 GeV) along the circumference of the synchrotron ring (368 m). Assuming the distance of closest approach is

3.5 m and 0.8-m concrete-equivalent shielding, the dose per occurrence would be:

$$H_{BREM}: 5.52 \times 10^{-1} \text{ mrem}$$

$$H_{GRN}: 5.24 \times 10^{-2} \text{ mrem}$$

$$H_{HEN}: 1.34 \times 10^{-1} \text{ mrem}$$

The total dose per occurrence is 0.738 mrem for this beam loss. For 1000 fills of the storage ring per year, considering one occurrence for each 500 pulses in the synchrotron during filling, the number of occurrences per year would be about

$$138 \left(\text{i.e.} \; \frac{\sim 6.9 \times 10^{12} e^{+}/\text{fill (1000 fills)}}{10^{11} e^{+}/\text{pulse (500 pulses/occ.)}} \right).$$

This would result in a total dose of about 102 mrem from all occurrences, and this dose would be expected to be somewhat distributed around the synchrotron ring, since every point loss would not be expected to occur in exactly the same spot along the orbit.

7.5 Shielding of Booster Extraction Area

The Booster Extraction region presents the most formidable problem of shielding because of the high energy of the positrons. Any losses in the transfer of positrons to the Storage Ring result in the formation of a relatively large HEN component (because of the high energy of the positrons). This component is very difficult to shield, since for any material the attenuation lengths are relatively large, thereby requiring large thicknesses to realize significant attenuation. Moreover, the losses occurring in this region generally transpire within a short time period which can lead to the production of significant dose rates, which tend to be dominated by the neutron component. The attenuation length of the high energy component in concrete is 115 g/cm^2, in iron it is 138 g/cm^2, and, in lead, 191 g/cm^2. Table 7.5.1 which follows indicates the dose rates produced assuming certain fractional losses at a point. The relevant assumptions for the significant parameters are that the shield consists of 1.5 m of concrete and the minimum distance to the dose point is 3.2 m. Total beam power is obtained from:

$$W = 7.2 \times 10^{10} (7000) (1.6 \times 10^{-13}) (3.6 \times 10^{3}) = 2.9 \times 10^{5} \text{ J/h}.$$

Table 7.5.1 - Dose Rate for Fractional Beam Loss

Beam Loss Fraction	Dose Rate in mrem/h			
	BREM	GRN	HEN	TOTAL
0.5	40.9	1.3	49.5	91.7
0.4	32.7	1.1	39.6	73.4
0.3	24.5	0.8	29.7	55.0
0.2	16.4	0.5	19.8	36.7
0.1	8.2	0.3	9.9	18.4
0.05	4.1	0.1	5.0	9.2

By using local shielding (40 cm of Pb), an assuming that the operational time is 10 %, the average dose rates can be reduced to those shown in Table 7.5.2:

Table 7.5.2 - Average Dose Rate Using Local Shielding

Beam Loss Fraction	Dose Rate in mrem/h				
	BREM	GRN	HEN	Total	$\dot{H}$ (10 % OPER)
0.5	-	0.078	4.604	4.682	0.47
0.4	-	0.063	3.683	3.746	0.37
0.3	-	0.048	2.762	2.810	0.28
0.2	-	0.032	1.841	1.873	0.19
0.1	-	0.016	0.921	0.937	0.09

From the table it is evident that the HEN component contributes the majority of the radiation dose rate and that the bremsstrahlung component contribution can be made negligible if sufficient lead is supplied as local shielding. Even with the pessimistic assumption of 50 % loss at a single point, the average dose rate will still be within the guidelines for a sufficient amount of local shielding at the assumed loss point. Since it is not known what the fractional beam loss at extraction will be, the amount of local shielding, if any, that will be required cannot be exactly estimated. However, experience at DESY indicates that the losses may

even be smaller than those considered in the table above. If this proves to be the case for the APS, only a small amount of local shielding, if any, may be required. The recommended concrete shielding is 1.5 m in the extraction region, supplemented by local shielding of "hot" spots as needed. Determination of the required local shielding will be accomplished prior to operation at design current.

8.0 Storage Ring Shielding

8.1 Parameters

The methodology used to compute dose and dose rate from the storage ring is the same as that used in LS-90 (MOE 87a). The calculations assumed 80 cm thick walls of ordinary concrete (or the shielding equivalent of this) and a roof thickness of 1 meter of ordinary concrete. The circumference of the ring was increased to 1104 m, and the closest distance to the boundary was taken as 140 m.

The following assumptions were used in the recalculation of the direct radiation component:

Beam Current - 0.3 A
Circumference - 1104 m
Positron Energy - 7 GeV
Mean Lifetime of Beam - 10 h (63% loss of beam)
Shielding - 1 m normal concrete on the roof, 0.8 m of normal concrete (or equivalent) on the sides
Total Beam Energy - 7728 J
Shortest Distance to Dose Point - 1.3 m

The shielding on the outer side of the tunnel (experimental area side) is in the form of a ratchet wheel, or saw-tooth pattern, in order to increase the space available for photon beamline equipment, but for computational purposes is considered circular. The calculations should be conservative, because the distance from the positron orbit to the inside of the shielding wall does vary around the ratchet but the minimum value has been assumed for the entire perimeter.

8.2 Continuous Loss During Beam Decay

As the positron beam moves around the storage ring, there will be a continuous loss of positrons from the beam due to several different factors. Collisions of positrons with gas molecules, interactions among beam particles, and orbital excursions, all lead to positrons being lost from the beam and striking the vacuum chamber. To compute the losses around

the ring, equation 6.0.1 adapted from Swanson et al. (SWA 85), was used to estimate the variation with angle of the bremsstrahlung dose at 1 m due to positron interactions in the vacuum chamber:

$$H/W = 16.7E_o^2 \left[\theta_B^{-(\theta_B/\theta_{1/2})} + 833(10)^{-\theta_B/21} + 25(10)^{-\theta_B/110} \right],$$

in which H is in mrem, W is in joules, E_0 is the positron energy in MeV, θ_B is the bremsstrahlung angle in degrees and $\theta_{1/2} E_0 = 100$ MeV deg. The first term on the right side of the expression accounts for the highly peaked forward component of the bremsstrahlung radiation. Figure 5 illustrates the geometry for the continuous loss, assuming uniform interactions in the vacuum chamber around the circumference. As indicated in the figure, θ_B is the angle between the forward direction of the positron beam at Q and the line segment QP to the dose point P. For a positron striking the vacuum chamber at point Q, the bremsstrahlung dose (mrem/J) at P will be

$$H_{BREM} = \frac{H\, e^{-(x/\lambda_{BREM})}}{W\, (QP)^2},$$

in which H/W is evaluated for the appropriate angle θ_B, x is the slant shield thickness (g/cm^2) at that angle, and λ_{BREM} is the attenuation length (g/cm^2) for the given shield material. The contributions from each point around the orbit circumference were calculated for both the unshielded case and for 0.8 m of concrete shielding. The result is shown in Figure 6.

Isotropic emission is assumed for the two neutron components, the giant resonance neutrons (GRN) and the high energy neutrons (HEN). Their dose contributions (mrem/J) to the point P are given by

$$H_{GRN} = \frac{0.63\, e^{-(x/\lambda_{GRN})}}{(QP)^2} \quad \text{and} \quad H_{HEN} = \frac{0.075\, e^{-(x/\lambda_{HEN})}}{(QP)^2}.$$

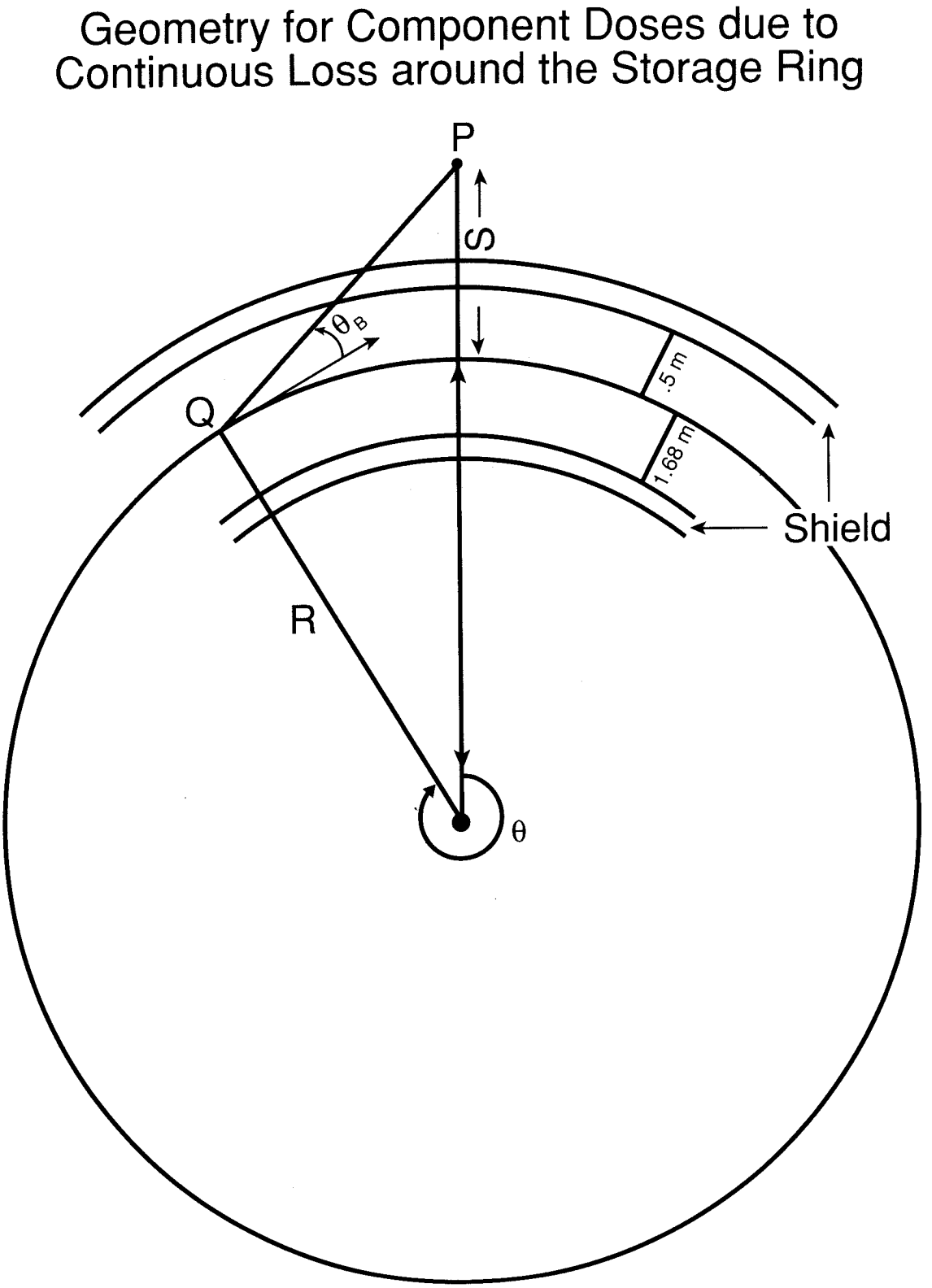

Figure 5. Geometry for Component Doses due to Continuous Loss around the Storage Ring

For the calculations using normal concrete, λ_{BREM}, λ_{GRN}, and λ_{HEN} were taken from Table 4.4.1. The individual contributions for the GRN and HEN components are shown in Figures 7 and 8, respectively.

When the contribution from each of the individual components is integrated over all angles($0^o <= \theta <= 360^o$, see Figure 5 for the designation of the angle θ), the result is the cumulative contribution from each component at the point P due to a uniformly distributed loss around the ring (mrem rad/J). For a total stored energy of 7728 J and a mean lifetime of 10 h, the energy loss rate is 77.747 J/h rad. Multiplying each of the integrated contributions by the energy loss rate and summing the results gives the total dose rate at the dose point P (mrem/h). The integrated contributions for the 0.8 m concrete shielding case are

$$H_{BREM} = 5.24 \times 10^{-4} \text{ mrem rad/J}$$

$$H_{GRN} = 2.54 \times 10^{-5} \text{ mrem rad/J}$$

$$H_{HEN} = 1.02 \times 10^{-4} \text{ mrem rad/J}$$

The resultant dose rates are

$$\dot{H}_{BREM} = 4.06 \times 10^{-2} \text{ mrem/h}$$

$$\dot{H}_{GRN} = 1.97 \times 10^{-3} \text{ mrem/h}$$

$$\dot{H}_{HEN} = 7.93 \times 10^{-3} \text{ mrem/h}$$

The total dose rate is 5.05×10^{-2} mrem/h, which is within the guideline. According to Swanson (SWA 85), the calculated results for Aladdin agreed with measurements to within about a factor of 3. The APS is a different, as well as a much larger, machine. However, the simplifying assumption of uniform beam loss along the entire circumference of the ring may not be realized. Experience at Aladdin and NSLS (SWA 85, BNL 82) indicates increased radiation levels in the vicinity of open ends of bending magnets, around the straight sections, at maximum dispersion points in quadrupole magnets, and the presence of bremsstrahlung jets at the ends of straight sections. Additional localized lead shielding for bremsstrahlung

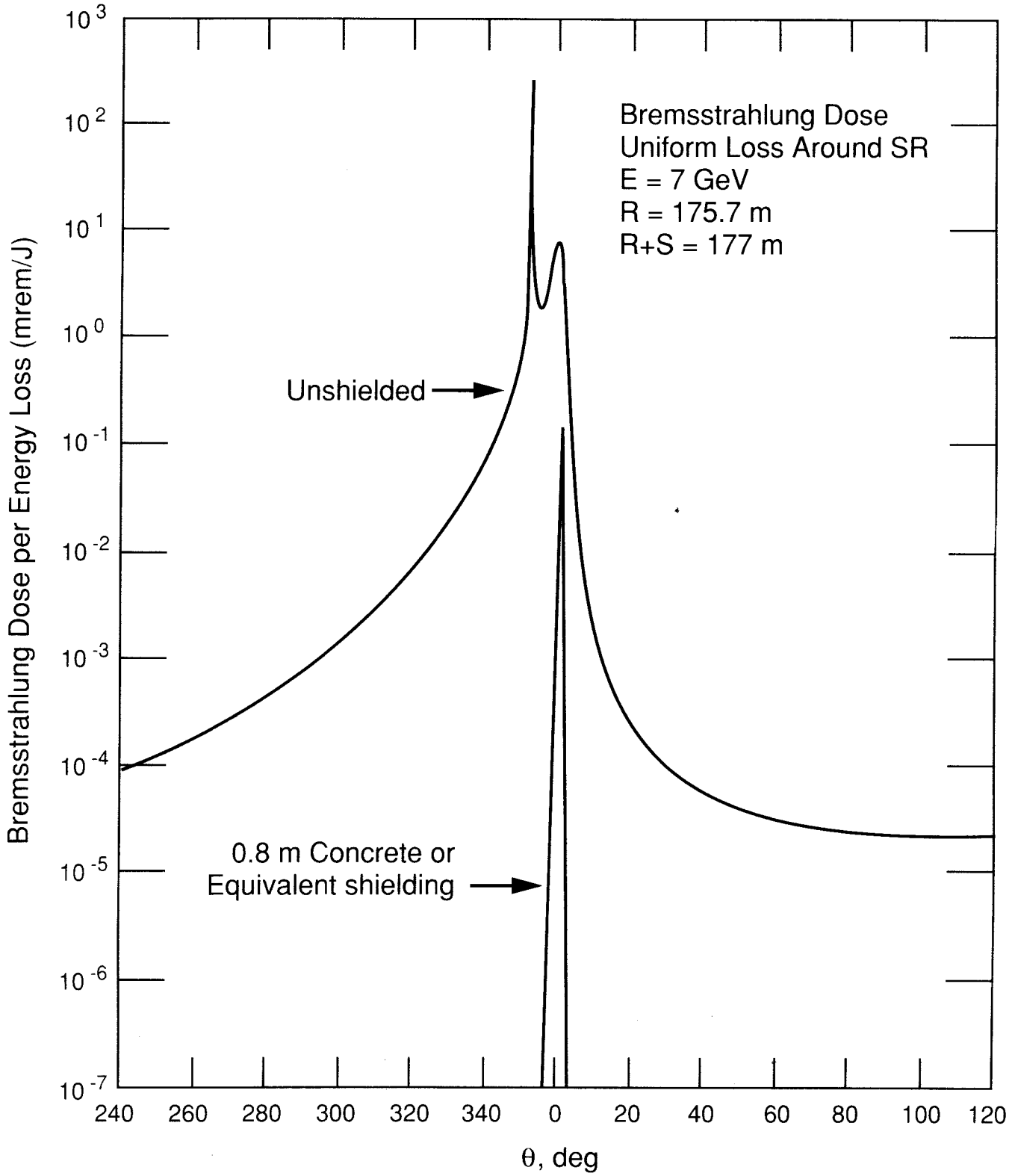

Figure 6. Bremsstrahlung Dose Distribution

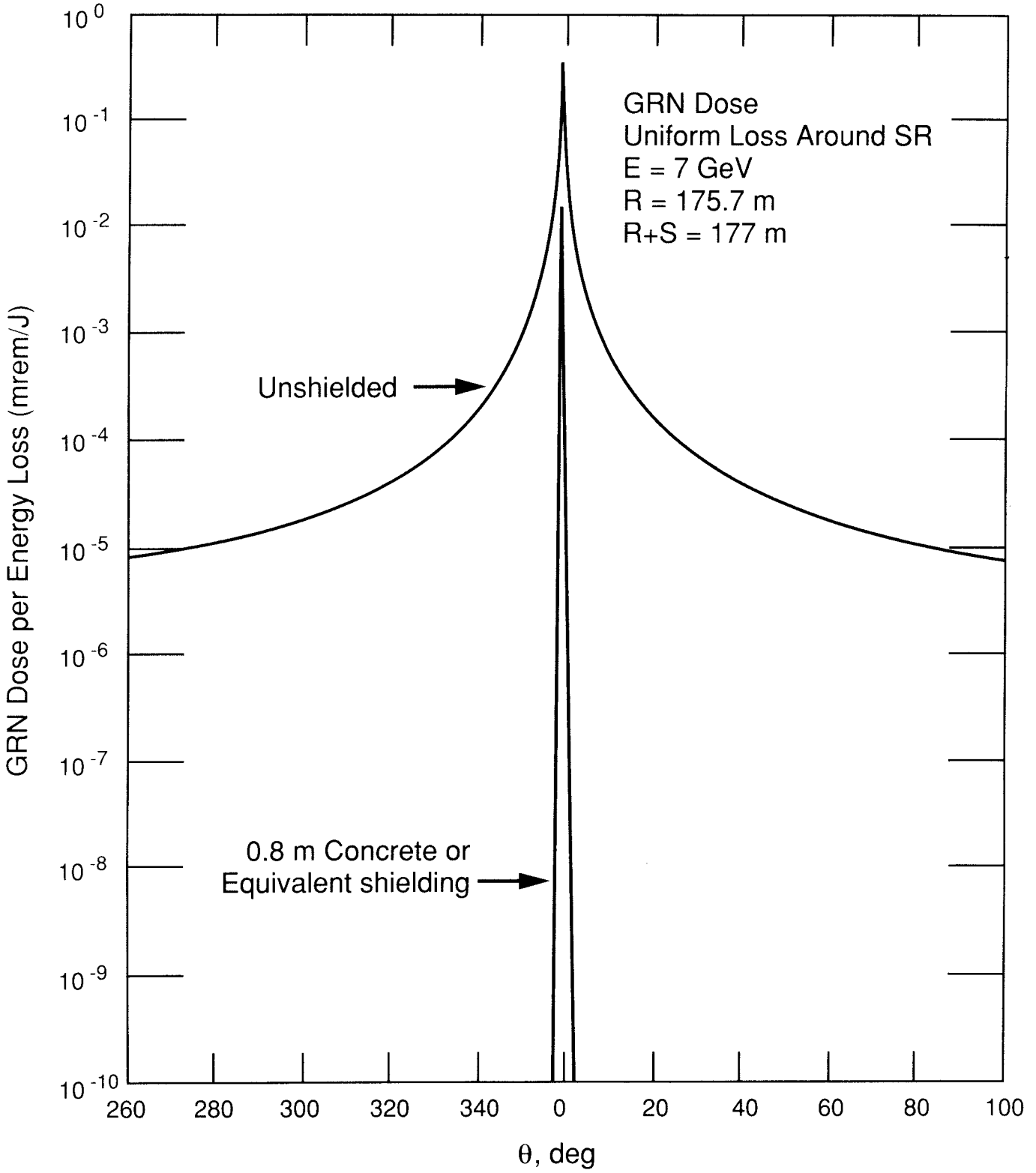

Figure 7. GRN Dose Distribution

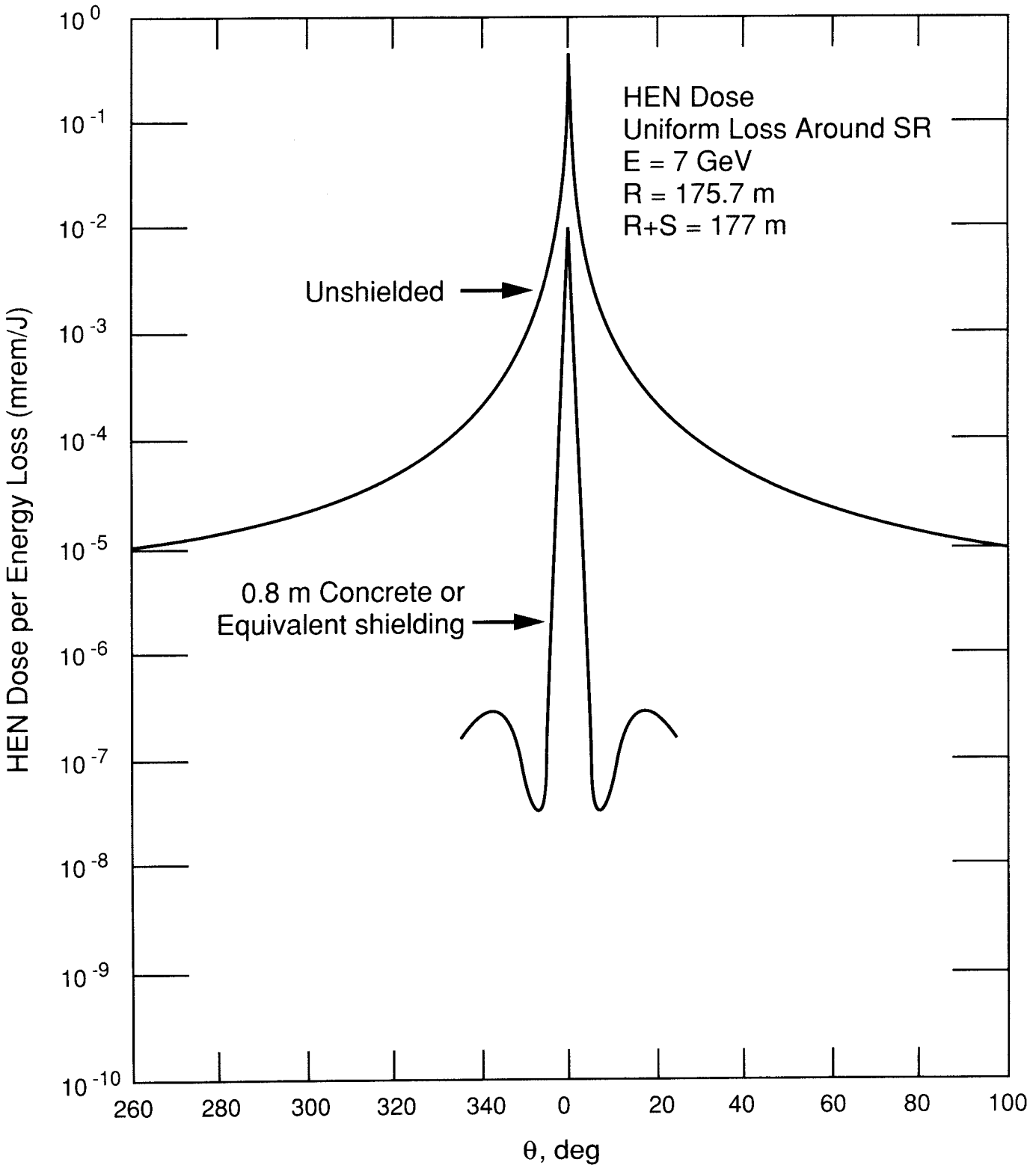

Figure 8. HEN Dose Distribution

and dense polyethylene for the high-energy neutron component may have to be provided at high-loss points in the system.

The total dose rate at various distances from the positron orbit is shown in Figure 9. Table 8.2.1 lists the annual dose equivalent from direct radiation at various distances from the positron orbit for an assumed operation time of 8000 h. These data are also plotted in Figure 10.

For estimates of the on-site annual doses, Figure 9 gives the total dose rate as a function of distance from the positron orbit. The dose rate may then be multiplied by 2000 h to obtain the estimated annual dose. For example, the dose rate at 80 m is about 5.6×10^{-4} mrem/h, so the estimated annual dose to a worker at that location would be 1.12 mrem, without correcting for any intervening shielding.

TABLE 8.2.1
Annual Dose Equivalent
(Direct Radiation for 8000 h Operation)

Distance, m	mrem/y
1.3	400.6
2	261.3
10	49.6
20	23.4
50	8.0
100	3.3
150	1.8
200	1.2
500	0.27
1000	7.8E-02
1500	3.7E-02
2000	2.1E-02
5000	3.6E-03

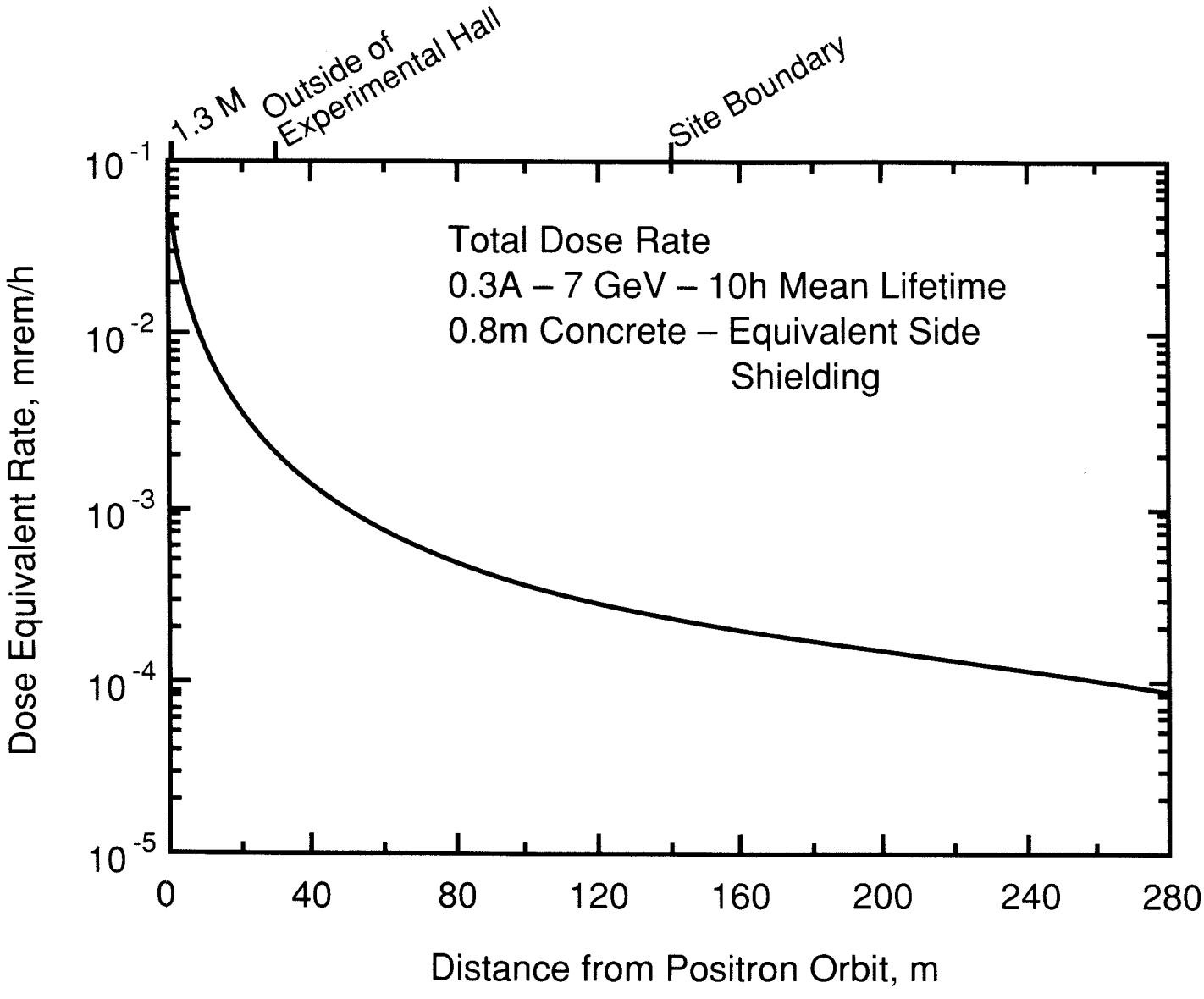

Figure 9. Total Dose Equivalent Rate at Various Distances from the Positron Orbit.

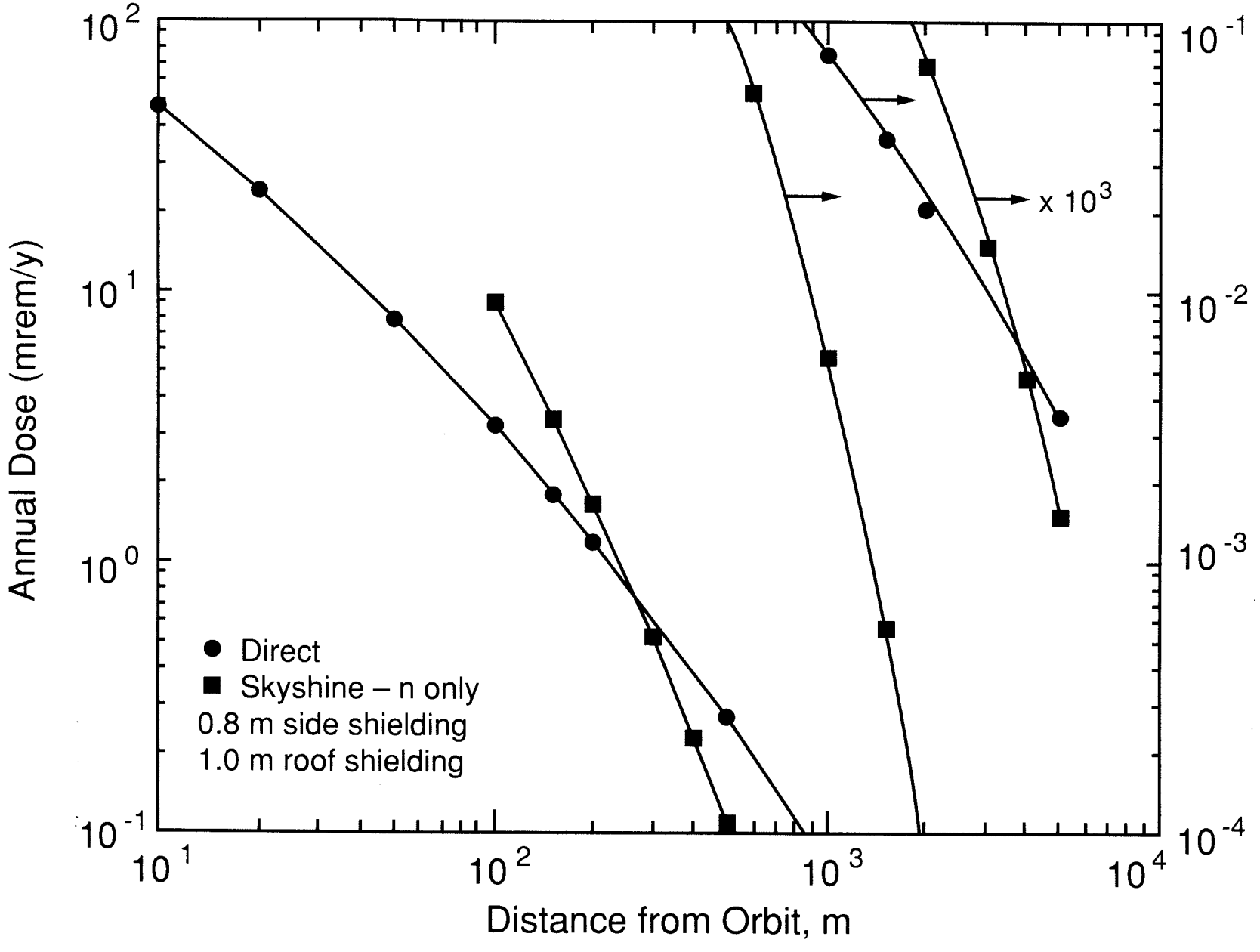

Figure 10. Annual Dose Due to Direct Radiation and Skyshine.

8.3 Ratchet Wall Shielding

8.3.1 Ratchet Wall Geometry Change

During the APS User's Subcommittee on Conventional Facilities meetings of 1987, we were urged to study changes in shield wall geometry for the Storage Ring to provide for more of the photon beam outside that shield. The shield wall position with respect to the source is a geometric function of the wall thickness, the clearance between the photon beam inside the wall (front-end area), and the corresponding clearance outside the wall. The relationship between any of these dimensions and movement of the ratchet portion of the wall (and thus the portion of the beamline outside the shield) is about one-to-eleven, so for each clearance or wall thickness inch given up, eleven inches of beamline are exposed. Unfortunately, the two clearances were considered optimal, if not minimal, and the shield wall thickness determines the radiation dose received on the operating floor and is not really a "free parameter" (KNO 88).

The first change considered using heavy concrete for the wall construction. The inner wall and roof remain normal concrete. A thickness of 0.56 meters (the shield equivalent of the 0.8 m normal concrete) is used for the outer wall. The ratchet thickness was left at 0.8 meters for several reasons: the wall encloses a lead/concrete plug of 0.8 meters total length; there is no gain in exposed beamline length when changing this dimension; and the 0.8 meter shielding length is important in attenuating the forward-angle bremsstrahlung radiation (KNO 88).

The changes made to the clearances were made in such a way so as to maintain the CDR-87 (ANL 87) clearances only in areas where front-end devices were expected to occur. The front-end-to-wall clearance of 0.8 meters was reduced to 0.5 meters while the wall ran parallel to the next upstream beamline (outside the shield) at a 0.5 meter clearance. The wall then runs parallel to the front-end at a 0.5 meter clearance until the upstream beamline clearance is reduced to 0.2 meters. At this point the outside surface of the ratchet face is placed and the above sequence is repeated with the front-end beyond that ratchet face. In this way the front-end areas retain their clearance of 0.8 meters and the initial beamline clearance is maintained at 0.2 meters. The 0.5 meter clearance inside the tunnel occurs where there are no front-end components. The 0.5 meter clearance outside the tunnel occurs where there is free access to the opposite side of the beamline.

8.3.2 Ratchet Shielding Calculations

The above thickness choice and geometry changes did not take into account the increased radiation dose received on the outside of the shield due to the wall's closer approach to the storage ring orbit. A review of the shielding estimated for the ratchet section of the Storage

Ring wall was carried out. Initially the wall shielding was computed to be 80 cm of normal concrete and the distance of closest approach was taken as 3 m, yielding a calculated dose of about 67 mrem for the case of a single point loss of the entire beam. Modification of the wall structure, relocation of the front-end components and the substitution of high density concrete for normal concrete, with an accompanying reduction in the shield thickness have made such a review prudent. Moreover, the distance of closest approach has also gotten smaller so that the possibility of an individual receiving significantly more than 100 mrem in a single dump needed investigation. A third factor affecting the dose is that the corner of the ratchet nearest the positron beam orbit has been truncated in order to provide more room (see Figure 11). This has resulted in a minimum shield thickness of 56 cm of high density concrete, as well as the shortest distance from an assumed point beam loss to the dose point.

A number of points (A, B, C, D, E and F in the figure) at 1 m intervals in the vicinity of the ratchet-like sections of the shielding were investigated. Since the wall sections differ in the bending magnet (BM) and Insertion device (ID) sections, the calculations were performed for each of these sections.

The forward directed bremsstrahlung radiation varies in intensity with the angle of emission with respect to the positron beam direction. The forward intensity for the bremsstrahlung was estimated using equation 6.0.1, adapted from Swanson (SWA 85). For each of the

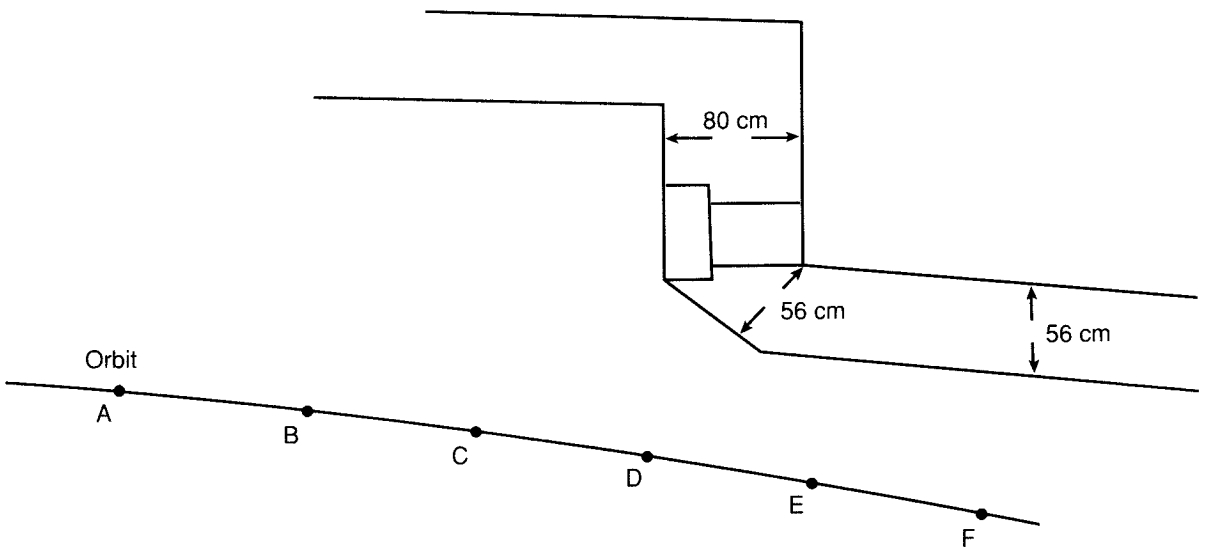

Figure 11. General ratchet-wall dimensions

points in the figure, a number of values for the parameter θ_B were used to determine the dose outside the shield. If the resultant dose outside of the shielding exceeded 100 mrem, a separate calculation to determine the distance outside of the shield at which the dose dropped to 100 mrem was performed.

Calculations for 7 GeV positrons were based on the assumption of 0.1 A of current in the ring and no additional local lead shielding placed around the ring. The attenuation lengths in high density concrete (density = 3.7 g/cc) for bremsstrahlung (BREM), giant resonance neutrons (GRN) and high energy neutrons (HEN) were taken as 50, 45 and 125 g/cm^2, respectively. These quantities represent composite parameter values obtained from the literature (ALS 73, BAT 67, DIN 77, FAS 84 and TES 79). The dose conversion factors for giant resonance neutrons and high energy neutrons are those previously used; namely, 0.63 and 0.075 mrem·m^2/J, respectively. The GRN and HEN components are assumed to be emitted almost isotropically, whereas the bremsstrahlung component has the angular dependence given by equation 6.0.1. The expressions for the dose contributed by each component, at the outside surface of the shield wall, are:

$$H_{BREM} = \frac{F_{H_{BREM}} \; W \; e^{-\frac{370(x)}{50}}}{(r + x)^2}, \qquad (8.3.2.1)$$

$$H_{GRN} = \frac{0.63 \; W \; e^{-\frac{370(x)}{45}}}{(r + x)^2}, \qquad (8.3.2.2)$$

$$H_{HEN} = \frac{0.075 \; W \; e^{-\frac{370(x)}{125}}}{(r + x)^2}, \qquad (8.3.2.3)$$

in which $F_{H_{BREM}}$ is evaluated for the appropriate angle, W = 2.3 x 10^{12} e^+(7000 MeV/e^+) (1.6 x 10^{-13} J/MeV) = 2576 J, x (m) is the slant shield thickness for the angle θ_B, and r is the distance from the relevant point loss to the inside shield wall, in m. Both x and r are functions of the angle θ_B.

Figures 12 and 13 show the results of the calculation which indicate the distance to the points outside of the shielding at which the dose is 100 mrem. These are shown as lines from the relevant loss point (A, B, C, D, E and F) to the dose point at the appropriate angle, θ_B. The angle θ_B, for a particular point loss, is found by extending the line from the loss point (A to F) to the dose point until it intersects the appropriate angle scale (A' to F') and reading the value off the scale. Angles are shown at 5° increments on the scales.

These results were obtained by increasing the value of r in the above equations, while holding x constant, and solving iteratively for the total distance at which the dose becomes equal to or < 100 mrem. In this case, r now represents the total distance in air from the loss point to the dose point in equations 8.3.2.1, 8.3.2.2 and 8.3.2.3. As seen from the figures, the dose is generally < 100 mrem for the majority of the situations investigated with the bremsstrahlung component contributing about 80% of the dose. For the few instances in which the dose exceeds 100 mrem, the distance at which the dose drops to 100 mrem is generally < 20 cm from the outside of the wall. One exception, as shown in Figure 12, is for a point loss at D in the figure, considering a BM ratchet face. For this case, θ_B equals ~ 60° and the dose is 167 mrem on the outside of the shield and drops to 100 mrem at 44 cm from the shield. None of these conditions is deemed to represent a serious hazard potential to personnel and no additional shielding for the operational current of 0.1 A is recommended.

Additional calculations were performed for the case in which the current is 0.3 A, and local lead shielding (7.62 cm) of the Storage Ring in these areas is provided. The results of these calculations indicate that with the addition of 3 inches of lead as local shielding of the Storage Ring, all doses outside of the shielding are reduced to below the administrative goal of 100 mrem. The highest dose occurring outside of the shielding under these conditions is about 81 mrem. It is planned to supply localized lead shielding in these areas to ensure that the goal of < 100 mrem is attained.

The recalculation of the estimated doses due to a beam loss at a single point in the Storage Ring System indicates that the redesigned shielding geometry, using heavy concrete for the ratchet walls is generally adequate for the parameters of no local lead shielding and an operating current of 0.1 A. For operation at 0.3 A, additional local lead shielding of 3 inches of lead will assure that all doses outside the ratchet wall shield from a beam loss at a given point, such as shown in Figures 12 and 13, will be < 100 mrem.

An additional investigation was performed for an assumed beam loss which results in forward directed bremsstrahlung which intercepts the radial portion of the ratchet wall at almost normal incidence. The results are discussed in the Addendum.

8.3.3 Ratchet Wall Doors

One further refinement made in the ratchet wall shielding is the addition of a sliding door (see Figure 14). As shown, the total thickness of this arrangement equals the total thickness of the high density concrete wall (56 cm). Each of the sections is a composite shield comprised of 5 cm of lead (Pb), 5 cm of iron (Fe) and backed by 18 cm of polyethylene. The

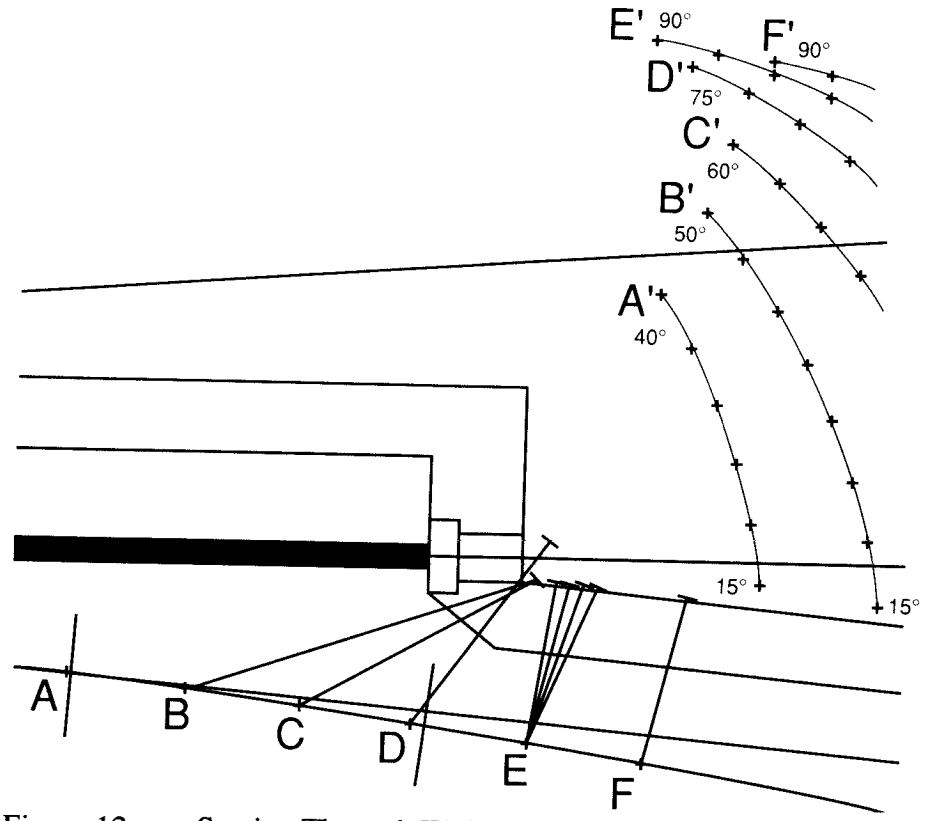

Figure 12. Section Through Wall in BM Ratchet Area.

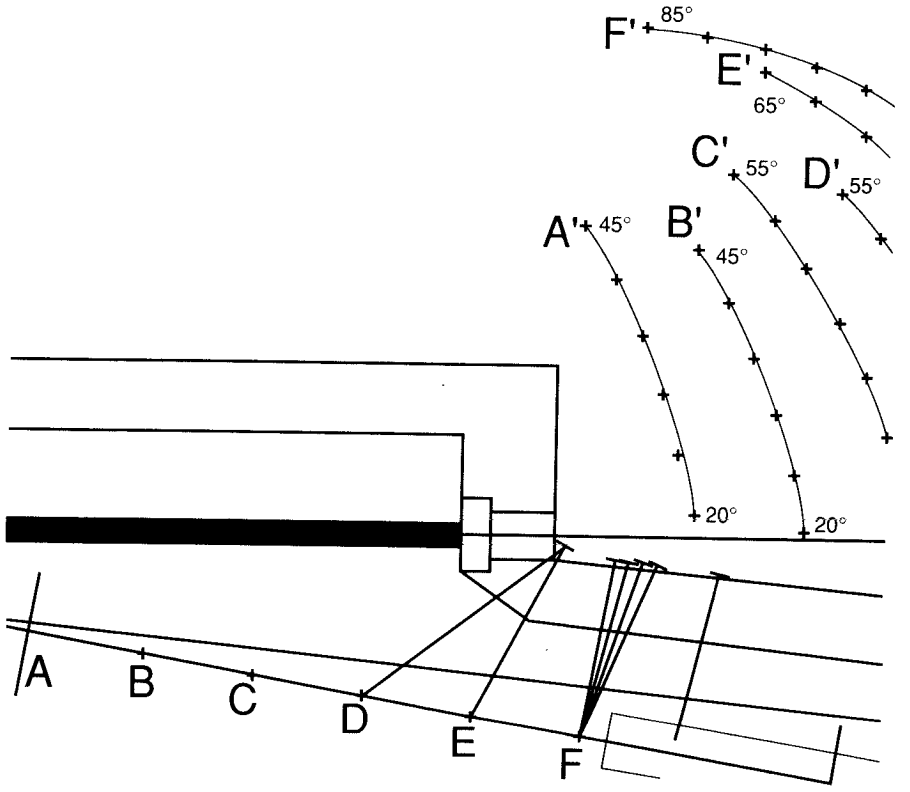

Figure 13. Section Through Wall in ID Section.

shielding ability of these sections was computed using equations 8.3.2.1, 8.3.2.2, and 8.3.2.3 from the previous discussion for the ratchet wall itself, modified to include exponential attenuation terms for each of the relevant shielding materials (Pb, Fe, polyethylene and, in some cases, high density concrete). As in the previous case, the shield was required to attenuate the radiation from a point loss along the positron orbit so that the total dose received by an individual would be < 100 mrem as the result of a dump.

Because of the differences in geometry between this case and the previous calculation; namely, the bremsstrahlung angles (θ_B in the figure) are much larger and the distances from the positron orbit to the outside of the shield are greater, the largest estimated dose is 78.5 mrem at A in the figure, assuming a current of 0.1 A. Note that for the inner door the 5 cm of Pb must have a wrap-around on the sides in order to effectively attenuate the bremsstrahlung. The dose contributions from a number of forward and backward angles were considered in order to arrive at the thicknesses of the various shielding materials in the composite.

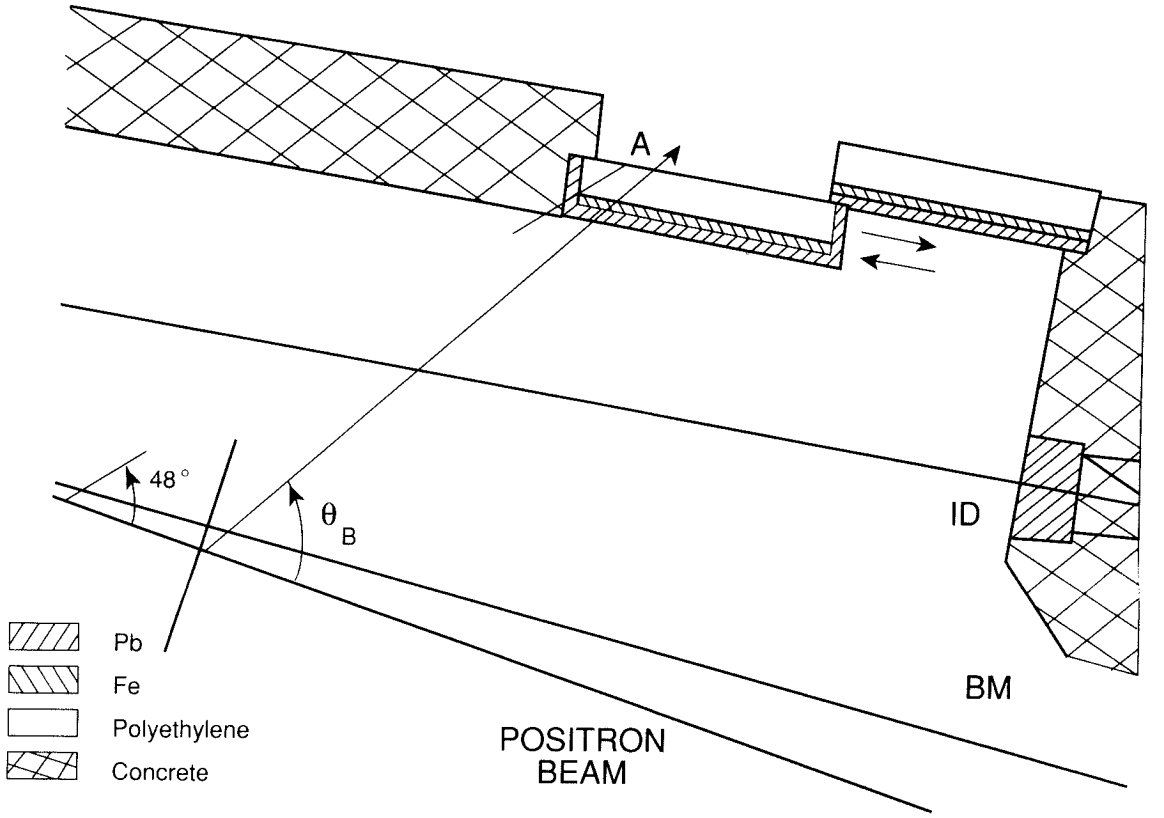

Figure 14 Ratchet Wall Doors

Utilizing data from Shure et al. (SHU 69), which indicated that a minimum of 15-20 cm of polyethylene is needed to provide adequate neutron shielding when backing up lead and iron, the thickness of polyethylene was fixed at 18 cm and the thicknesses of Pb and Fe were

varied until adequate attenuation was achieved. A minimum of 5 cm of Pb was indicated in order to keep doses below 100 mrem. For the point A in the figure, the bremsstrahlung angle was 48 degrees and the distance to point A from the orbit was 2.58 m. Slant thicknesses of the shield materials were found from t csc 40^{o}, where t is the thickness of the shield material and 40 degrees is the angle that the ratchet wall makes with the bremsstrahlung radiation for this particular example. From the figure one can see that for this case, the radiation passes through the high density concrete, lead and polyethylene, but misses the iron shielding. Since lead is the most effective shield for the bremsstrahlung radiation, the shielded doors could be made even more effective by increasing the amount of lead shielding at the expense of the iron shield. However, it may be necessary to have a certain amount of iron in the shield in order to hold the lead and polyethylene together.

8.4 Dose Rates in Module Experimental Areas

The dose rate in the module experimental areas was computed with the aid of Figure 9 which shows the various dose contributions outside of the ring at different distances, assuming uniform beam loss around the circumference. For the module areas, a nominal distance of 20 m was used for the distance of closest approach and a beam mean lifetime of 10 h was assumed. The total dose rate at 20 m is 2.9×10^{-3} mrem/h, which is within the guideline. Using this dose rate, the annual occupational dose, based upon 2000 h of exposure becomes

$$H = 2.9 \times 10^{-3} \text{ (mrem/h) } 2000 \text{ (h) } = 5.8 \text{ mrem.}$$

8.5 Shielding and Dose Rate Summary for Normal Operation

A summary of the results obtained for the bulk shielding calculations for the components of the APS, during normal operations, is shown in Table 8.5.1. In all cases, point losses of the positron beam have been assumed, so the results should be conservative.

8.6 Skyshine Losses

The term skyshine is generally used to refer to radiation which initially is directed skyward from a source, but due to scattering reactions with air nuclei, this radiation is directed back to earth (LAD 68). In the case of the APS, when the high energy component is slowed down in a shield, fast neutrons with an energy spectrum similar to giant resonance neutrons result. These neutrons and the surviving high energy component are the ones which are scattered about in air rather than effectively stopped and contribute to the skyshine effect. The radiation field produced by air scattering will be composed of both a fast neutron and a high energy neutron component. Several studies of the skyshine contribution have been done over the years and the results of these have been reviewed (ALS 81, LAD 68, NAK 81, RIN 75).

Table 8.5.1 - Shielding and Dose Rate Summary

COMPONENT	POWER LOSS (W)	DIST R (M)	SHIELD THICK. (CM)	MATERIAL	$\dot{H}$ (MREM/H)	$\dot{H}$ 10% (MREM/H)
e^- LINAC	25.6	4	200	CONCRETE AND SOIL	1.44	0.14
CONVERTER	460	4	40 160	IRON CONCRETE	2.755	0.276
e^+ LINAC	0.46	4	200	CONCRETE	-	-
BEAM COMPRESSION SYSTEM	5.7	4	200	CONCRETE	0.321	0.032
PAR	2.592	6.53	150	CONCRETE	3.74	0.374
INJECTOR REGION	2.592	3.2	150	CONCRETE	2.303	0.23
SYNCHROTRON	0.859	3.5	30 105	CONCRETE SOIL	0.326	0.033
EXTRACTION REGION	40.3	3.2	150 + Pb LOCAL	CONCRETE	4.682	0.47
STORAGE RING	0.136	1.3	80	CONCRETE	0.05	-

The skyshine contribution from scattered neutron radiation was estimated using the following assumptions:

Positrons lost in 10 h - $0.63\ (6.9 \times 10^{12}) = 4.36 \times 10^{12}\ e^+$

Neutron Fluence - 80% fast neutrons (1-2 MeV) and 20% high energy neutrons (100-400 MeV) at the dose point

Quality Factor - Values were obtained from Figure 3 of DOE Order 5480.11 (DOE 88, Section 9.f.(5))

Fluence Rate to Dose Equivalent Rate Conversion Factor -

$\bar{\phi} = 7.8$ n/cm^2 s/mrem/h for 1-2 MeV n

$\bar{\phi} = 4.6$ n/cm^2 s/mrem/h for 100-400 MeV n

$1/\bar{\phi} = 0.8/7.8 + 0.2/4.6$; $\bar{\phi} \sim 6.9$ n/cm^{2}s/mrem/h

The source term for the neutron skyshine component was computed from the high energy neutron yield 0.12 n/e, obtained from Bathow et al. (BAT 67) for 6.3 GeV e^-:

$$Q = \frac{0.12(n/e)\,4.36 \times 10^{12}\,(e)\; e^{-.02(100)}}{3.6 \times 10^{4}\,(s)} = 1.97 \times 10^{6}\ n/s \qquad (8.6.1)$$

for an assumed 10 h mean lifetime. The source term Q gives the neutrons which escape through the 1 m shielding on the accelerator tunnel roof, conservatively assuming all the neutrons are directed skyward.

An expression for estimating the fluence rate ϕ (r) at a distance r from a well-shielded accelerator (RIN 75), due to the skyshine contribution, was used to estimate the skyshine dose equivalent rate:

$$\phi\ (r) \sim \frac{a\ Q\ e^{-r/\lambda}}{4\ \pi\ r^2} \qquad (8.6.2)$$

in which a and λ are constants, ϕ (r) is the fluence rate (n/cm^{2}s), Q is the source strength (n/s) and r is the distance to the dose point (cm). Values of the constants a and λ quoted from measurements at DESY by Rindi and Thomas (RIN 75) were used in the computation. The values chosen (a = 7 and $\lambda = 3.3 \times 10^4$ cm) give the largest fluence rate (most conservative) values for the DESY measurements.

Using the conversion factor 6.9 n/cm^2 s/mrem/h, the dose equivalent rate

$\dot{H}$ becomes

$$\dot{H} = 1.59 \times 10^{5}\ \frac{e^{-(r/3.3 \times 10^{4})}}{r^2}\ \ (mrem/h), \qquad (8.6.3)$$

in which r is expressed in cm. Table 8.6.1 contains the estimates of the annual skyshine dose contribution at various distances from the positron orbit, assuming 8000 h of operation. No credit was applied for intervening shielding between the source and the dose point. Figure 10 shows the annual dose data of Table 8.6.1 plotted along with the annual dose data from direct radiation.

TABLE 8.6.1
Annual Dose Equivalent
(Skyshine Radiation for 8000 h Operation)

Distance, m	mrem/y
100	9.39
150	3.59
200	1.73
300	0.57
400	0.24
500	0.11
1000	6.31E-03
1500	5.74E-04
2000	7.42E-05
3000	1.73E-06
4000	4.32E-08
5000	1.34E-09

8.7 Remarks

From Figure 9 and Table 8.5.1, it is seen that the ALARA design criterion of < 0.5 mrem/h for occupational exposure (DOE 88, Section 9.j.(b)) is met at the distance of closest approach (1.3 m). The dose rate at this location is 0.05 mrem/h. From Figure 10, it is seen that the projected total annual dose equivalent at the new assumed boundary (140 m from the positron orbit) is about 6.25 mrem/y. This comprises ~ 2 mrem/y from direct radiation and 4.25 mrem/y from skyshine. The total annual dose is slightly lower than the estimate in LS-84 (~ 10 mrem/y), as the dose increase due to moving closer to the boundary is more than offset by removal of an arbitrary, conservative factor of 3 in the source term and the correction to the neutron quality factor. The factor was removed in the case of the source term since the equation estimates to within a factor of three, but this factor can be in either direction. The estimated total annual dose of 6.25 mrem meets the criterion of DOE Order 5400.5 (DOE 88a), which limits annual dose to the public to 100 mrem/y. This dose is also below the limit (10 mrem), contained in the same DOE Order, which requires reporting to DOE Headquarters.

9.0 Radiological Consequences of Accidental Beam Losses

A number of situations may arise in which part or all of the beam is lost in one of the accelerator component systems. Some of these have been discussed already from the standpoint of shield design parameters and expected system losses. The intent of this section

is to evaluate the estimated radiation doses from postulated accident conditions in the various systems.

9.1 Linac Accidental Losses

9.1.1 Point Loss in Electron Linac

Four protective interlock systems act to shut down the Linac within a maximum of 2 pulses. One may postulate a number of abnormal circumstances giving rise to an errant beam, but the result will be that the beam will strike the accelerator structure resulting in an assumed point loss of the electron beam. Taking the maximum energy (200 MeV) of the beam, and using 3 x 10^{11} e^-/pulse, the energy loss will be

$$E = 2(\text{pulses})(3 \times 10^{11}\ e^-/\text{pulse})(200\ \text{MeV}/e^-)(1.6 \times 10^{-13}\ \text{J/MeV})$$

$$= 19.2\ \text{J}.$$

The dose contribution from this event, assuming 2 m of concrete shielding and a distance of 4 m to the nearest dose point, and utilizing equation 4.6.1, will be

$$H_{BREM} = 2.29 \times 10^{-4}\ \text{mrem}$$

$$H_{GRN} = 5.96 \times 10^{-6}\ \text{mrem}$$

$$H_{HEN} = 6.52 \times 10^{-5}\ \text{mrem}$$

The total dose in this incident is 3.0 x 10^{-4} mrem. A loss of the beam in the positron linac would yield an even smaller dose since the number of positrons per pulse is a factor of 200 lower than that in the electron linac which more than offsets the factor of 2.25 increase in energy per particle.

9.1.2 Point Loss in Positron Linac During Electron Acceleration

The Linac system can be used as an electron accelerator alone when the tungsten target is withdrawn and certain other changes are made. For this case, the current is usually much lower so that the e^-/pulse is taken as 5 x 10^{10}, but the electrons are accelerated to 650 MeV. This gives a resultant energy loss of 10.4 J for an accident involving the loss of 2 pulses at a point before shutdown. Scaling the previous answer gives a total dose in this incident of 1.63 x 10^{-4} mrem.

9.1.3 Loss Following Failure to Limit Electron Current

One accident that could occur involves failure of the interlock to limit the electron current while accelerating electrons in the Linac system. In this incident, the electron energy is assumed to be 650 MeV, but the number of electrons per pulse could be 3×10^{11}. The energy loss in 2 pulses for this incident will be 62.4 J. The dose can again be scaled since the shielding and distance to the dose point will be the same as before. The total dose is 1×10^{-3} mrem.

9.2 PAR Accidental Beam Loss

For an accidental loss of the beam in the PAR, the system will shut down within one pulse. For this incident, a dump of 10^{11} e^+ of 450 MeV occurs at a point where the forward directed bremsstrahlung must be considered, the total shielding is 1.3 m of concrete, and the distance to the nearest dose point is 3 m. The energy loss is given by

$$E = 1 \times 10^{11}\ e^+\ (450\ \text{MeV}/e^+)\ (1.6 \times 10^{-13}\ \text{J/MeV}) = 7.2\ \text{J}.$$

Using the above parameters in equation 4.6.1, the dose components are

$$H_{BREM} = 5.9\ \text{mrem}$$

$$H_{GRN} = 2.42 \times 10^{-4}\ \text{mrem}$$

$$H_{HEN} = 5.46 \times 10^{-4}\ \text{mrem}$$

The total dose in this incident is 5.9 mrem.

9.3 Synchrotron Accidental Beam Loss

The case of a beam loss in the synchrotron was discussed in Section 7.4, and the total dose per occurrence was computed to be 0.738 mrem. Since the shutdown mechanism will be capable of closing down the system in one pulse, this is the dose an individual would receive.

9.4 Storage Ring Accidental Losses and Unusual Occurrences

9.4.1 Total Beam Loss at a Point

For the case of a total beam loss at a single point, both the transverse and radial components need to be evaluated. The transverse component was treated in Section 8.3.2. Figures 12 and 13 in that section indicate the points at which the total dose would be in excess of 100 mrem,

for a dump involving 0.1 A circulating current. As discussed in the text of that section, the largest dose that could be received by an individual right up against the shield is 167 mrem. With Pb added as local shielding, as is planned, the largest dose would be 81 mrem in this type of loss.

For the radial dose component, the closest distance to the outside of the shield is taken as about 24 m, of which 25 cm would be lead backed up by 55 cm of concrete in the ratchet section of the wall (see Figure 11). The shielding design for these sections features an 0.8-m concrete wall except for a 1.5' by 1.5' slot through the wall, centered around the axis of the photon beam line. The increased distance to the dose point, as well as the added lead shielding thickness, offset the increased bremsstrahlung in the forward direction. The neutron contribution is computed on the assumption that neutrons are formed when the bremsstrahlung strikes the shield in the ratchet section.

The distance to the dose point for the neutron component is taken as 1.5 m. The following doses are calculated from equation 4.6.1:

$$H_{BREM} = 0.66 \text{ mrem}$$

$$H_{GRN} = 14.70 \text{ mrem}$$

$$H_{HEN} = 18.98 \text{ mrem}$$

This gives a total dose per incident of 34.3 mrem.

9.4.2 Bremsstrahlung into a Photon Beam Line

It is necessary to guard against an accidental positron beam loss during injection, which could result in high energy bremsstrahlung radiation being directed down a photon beam line. This could result in very high radiation levels in the experimental area. To prevent this, a lead shutter is inserted into the photon beam line before injection begins. All beam lines require lead shutters, at least 25- cm thick in the beam direction and 10 cm transverse to the beam direction. The shutters should be located within the shield tunnel to adequately shield the neutrons produced by the electromagnetic shower in the lead.

On the assumption that 10% of the positron beam is lost, a resultant unshielded bremsstrahlung dose of 4.5×10^4 rem at 1 m, due to stopping the positron beam, would be produced in the forward direction. If this were to occur just inside of the shield wall, the total dose at the outside of the shield would be 2.76 mrem due to the attenuation by the 25 cm lead shutter and 80 cm of concrete, and an assumed distance of 1.1 m.

9.4.3 Scattered Bremsstrahlung into a Beam Line

In addition to the lead shutters in the photon beam lines, lead collars which surround the photon beam tube will need to be installed to insure that any scattered bremsstrahlung

radiation is intercepted by at least 10 cm of lead shielding. Positrons which are accidentally lost along portions of the vacuum tube produce bremsstrahlung which, when scattered, may find an optical path out to the experimental floor, other than right down a photon beam tube. Lead collars must be strategically placed around the beam pipe, and be of sufficient length to block all optical paths to the experimental floor except the one between the positron orbit and the beam tube aperture.

9.5 Maximum Credible Incident

9.5.1 Scenario

The maximum credible incident (MCI) for the APS is based upon a scenario in which the positron beam becomes unstable and "blows up" in such a way that the positron beam hits the walls of an Insertion Device. The entire beam is assumed to be converted into bremsstrahlung and the highly-peaked, forward- directed bremsstrahlung travels down a photon beam line, through the ratchet wall section of the shield without attenuation, and into a shielded enclosure (see Figure 15). This enclosure (FOE) is a shielded, interlocked enclosure such that no personnel can occupy this space if the synchrotron radiation beamline

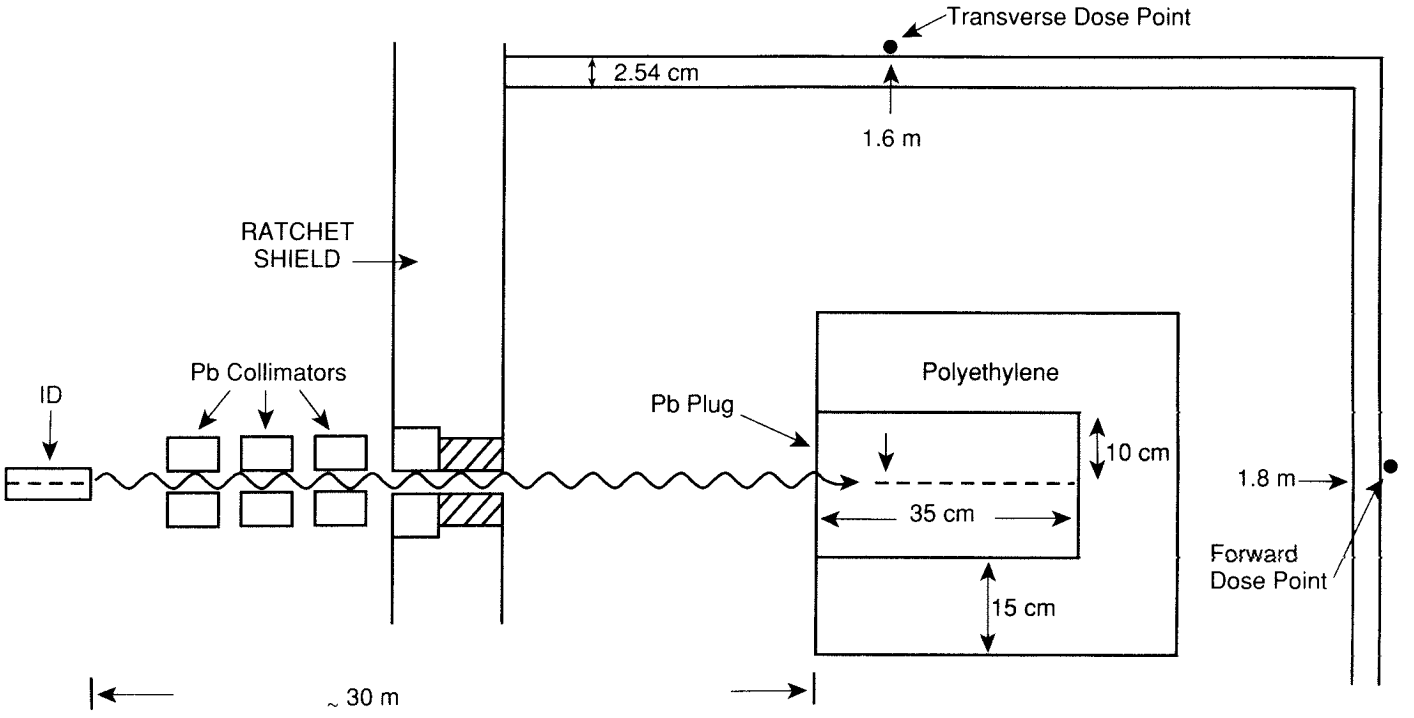

Figure 15. Section View of a Shielded Beam Enclosure.

is open. The first optical element is contained within this area, and is used to deflect the synchrotron radiation thereby changing its path. In direct line with the optical path of the synchrotron radiation from the positron orbit, is a 35 cm thick lead plug (20 cm in diameter), which is surrounded on the sides and back end by 15 cm of dense polyethylene.

For the accidental loss of the positron beam, the resulting bremsstrahlung will travel down the photon beamline and strike the lead plug. An electromagnetic shower will be produced. It is assumed that as the shower develops in the lead plug, giant resonance and high energy neutrons will be released. The plug is adequate to attenuate the shower (~ 62 radiation lengths thick) and most of the photon radiation, but is not that effective for the neutrons which are produced. The polyethylene provides effective neutron shielding of the giant resonance neutron component. Radiation escaping from the plug will be intercepted by the walls (2.54 cm Pb) of the enclosure, but an individual standing outside of the FOE could be about 1.6 m away from the plug and receive a radiation dose from the incident.

9.5.2 Incident Parameters

The total number of positrons in the beam is taken as 6.9×10^{12} (0.3 A) at an energy of 7 GeV which gives a beam energy of 7728 J (or some equivalent total energy combination of particles and energy per particle). Dose conversion factors from Table 4.5.1 and equation 4.6.1 are used to estimate the individual doses. Attenuation lengths were taken from Table 4.4.1, except for the attenuation length of the GRN component in Pb not backed up by hydrogen. The value 233 g/cm^2 was obtained from Tesch (TES 79). For the forward component of the dose, it is conservatively assumed that the shower develops in the first 5 cm of the Pb plug (~9 radiation lengths) and the photon radiation is attenuated by a total Pb thickness of 33 cm, which includes the 2.54 cm Pb shielding on the enclosure, in the forward direction and 12.5 cm of Pb total in the transverse direction. The distance to the nearest dose point in the forward direction is assumed to be 1.8 m, and in the transverse direction, 1.6 m.

9.5.3 Radiation Dose

For the parameters listed above, the dose in the forward direction is computed to be

$$H_{BREM} = \frac{8.3\ (7000)\,(7728)\ e^{-\frac{11.34(33)}{25}}\ e^{-\frac{1.01(15)}{70}}}{(1.8)^2} = 35.2 \text{ mrem}$$

$$H_{GRN} = \frac{0.63\ (7728)\, e^{-\frac{374.22}{161}}\ e^{-\frac{15.15}{6.3}}}{(1.8)^2} = 13.3 \text{ mrem}$$

$$H_{HEN} = \frac{0.075\ (7728)\ e^{-\frac{374.22}{191}}\ e^{-\frac{15.15}{62}}}{(1.8)^2} = 19.7 \text{ mrem}$$

The total dose in the forward direction is 68.2 mrem.

The doses in the transverse direction are computed for the nearest distance to the dose point, which occurs at 90 degrees to the beam direction. These doses are

$$H_{BREM} = \frac{2.8\ (7728)\ e^{-\frac{11.34(12.5)}{25}}\ e^{-\frac{15.15}{70}}}{(1.6)^2} = 23.4\ \text{mrem}$$

$$H_{GRN} = \frac{0.63\ (7728)\ e^{-\frac{113.4}{161}}\ e^{-\frac{15.15}{6.3}}\ e^{-\frac{28.4}{233}}}{(1.6)^2} = 75.2\ \text{mrem}$$

$$H_{HEN} = \frac{0.075\ (7728)\ e^{-\frac{141.75}{191}}\ e^{-\frac{15.15}{62}}}{(1.6)^2} = 84.4\ \text{mrem}$$

The total dose for the transverse radiation in this incident is 183 mrem.

The largest dose received by an individual in the MCI is 183 mrem if the individual is standing just outside the FOE at a perpendicular distance of 1.6 m from the Pb shield plug in the enclosure and a circulating current of 0.3 A "blows up" and strikes the walls of an insertion device.

10.0 Radioactive and Noxious Emissions

10.1 Introduction

Sources of radioactive and noxious gases found in air around electron or positron accelerators result from loss of particles along the accelerator system and escape of synchrotron radiation from the vacuum chamber. As previously discussed, positron losses result in bremsstrahlung formation and the interaction of this component with air results in the production of a number of radioactive products, primarily through the photonuclear reaction (γ,n) (FAS 84, KSO 82, RIN 67, SWA 79). Of the many possible radionuclides formed, only three (C-11, N-13 and O-15) are of importance in the operation of the APS. Of these three radionuclides, N-13 usually makes up about 90% of the concentration found in air (SWA 79). One other potential radionuclide, Ar-41, is formed by thermal neutron capture in argon. Since this is a second order reaction (requiring slowing down of the fast neutrons created by the bremsstrahlung and capture by argon which is < 1% abundant in air), the production of this component will be negligible.

Radioactive dust has not been a problem at other accelerators, except under unusual conditions (SWA 79, PAT 73). Irradiation of air by photon radiation below the threshold for neutron production (7-20 MeV in most materials) results in the production of ozone and oxides of nitrogen (FAS 84, NIE 82, SWA 79,WEI 87). The products ozone (O_3), nitrogen dioxide (NO_2) and nitric acid (HNO_3) are the most prominent components formed in the APS.

Estimates of the quantities of the radioactive products which are released to the atmosphere from each of the accelerator system components are developed in the following section.

10.2 Radioactive Gas Formation Estimates

The mechanism for formation of the radionuclides in air is the photoneutron interaction of bremsstrahlung with air nuclei (FAS 84, SWA 79). The (γ,n) threshold for air is 10.55 MeV, for the formation of N-13, and 15.67 MeV for O-15 (SWA 79). In addition, some C-11 is formed by photon spallation of both nitrogen and oxygen. Using the neutron yield expression given by Swanson (SWA 79a), and the effective Z of 7.26, according to Schaeffer (SCH 73), the neutron yield Y in air is

$$Y = 1.21 \times 10^{11} Z^{0.66} \text{ (n/skW)} = 4.5 \times 10^{11} \text{ (n/skW)}$$

$$Y = 4.5 \times 10^{8} \text{ (n/J)}. \qquad (10.2.1)$$

Implicit in the release of the neutron, is the formation of an unstable nucleus, which may be radioactive. We assume the yield of neutrons is also the yield of radionuclides. The change in the number of radioactive atoms present per unit time, dN/dt, is

$$dN/dt = WfY(1 - e^{-x/\lambda}) - (\lambda_R + k\,FR/V)N \text{ atoms/s},$$

in which W (watts) is the particle beam power loss, f is the fraction of particle energy which converts to bremsstrahlung and escapes into air (taken as 0.5), x is the average air path in m,λ is the attenuation length in air for bremsstrahlung in m (385 m as suggested in FAS 84), λ_R is the radioactive decay constant of the radionuclide which is formed, s^{-1} , k is a factor to account for imperfect mixing of the radionuclide in air (assumed to be 1/3), V is the volume of the region being ventilated (m^3) and FR is the ventilation flow rate (m/s). For initial conditions N = 0 for t = 0, the solution is

$$N = \frac{WfY(1 - e^{-x/\lambda})(1 - e^{-(\lambda_R + kFR/V)t}}{\lambda_R + kFR/V} \qquad (10.2.2)$$

and the activity is $A = \lambda_R N$, so that

$$A = \frac{\lambda_R W f Y (1 - e^{-x/\lambda})(1 - e^{-(\lambda_R + kFR/V)t})}{\lambda_R + kFR/V} \text{ (dis/s)}. \qquad (10.2.3)$$

Since the radionuclides which are formed all have short half-lives (< 20.5 min.), saturation is achieved quickly so that the activity at saturation becomes

$$A = \frac{\lambda_R W f Y (1-e^{-x/\lambda})}{\lambda_R + kFR/V} = \frac{(\ln 2/600)(W)(0.5)(4.5 \times 10^8)(1-e^{-x/385})}{(\ln 2/600) + FR/3V}$$

$$A = \frac{2.60 \times 10^5 W (1 - e^{-x/385})}{(\ln 2/600) + FR/3V} \text{ (dis/s)}, \qquad (10.2.4)$$

in which the decay constant (ln 2/600 s^{-1}) is for N-13 (half life ~ 10 min) which is the most abundant radionuclide formed. To obtain the estimates of the radioactivity in the various sections of the accelerator systems, equation 10.2.4 is used with the appropriate values for each system substituted for the variables in the equation. The equilibrium concentration is then obtained from

$$C = \frac{A}{3.7 \times 10^4 \text{ (dis/s}\mu\text{Ci)} V \text{ (cc)}} \text{ (}\mu\text{Ci/cc)}, \qquad (10.2.5)$$

in which V is the volume of the section being evacuated. Multiplying C by the total cc exhausted per year (during the operating time of the accelerator component) gives the estimated activity released each year of operation by that component. The sum of all contributions gives the estimated total radioactivity released from the APS.

10.2.1 Radioactive Emissions from the Linac System

The average path length in air was estimated using the geometry shown in Figure 16. The forward directed radiation is assumed to be intercepted and absorbed in the linac if the angle between the radiation and the electron beam is < 20^0. The average path length is estimated by integrating the length of the line segment AB over the range of angle θ and dividing by the integral of $d\theta$ over the same range. The value of this integral is

$$x = \frac{1.343 \int_0^{1.222} \sec\theta \, d\theta}{\int_0^{1.222} d\theta} \qquad (10.2.1.1)$$

$$= \frac{1.343}{1.222} \ln(\tan(\pi/4 + 1.222/2)) = 1.91 \text{ m.}$$

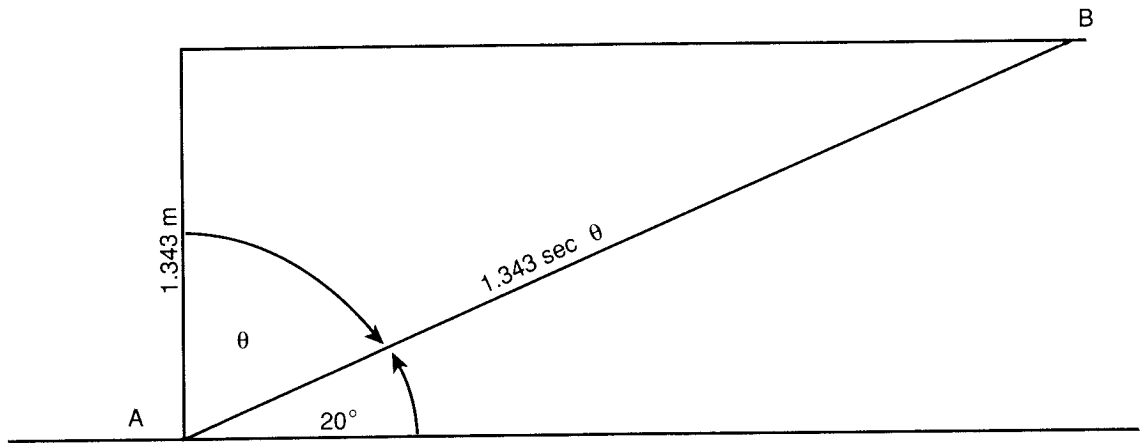

Figure 16. - Geometry for average air path length computation

The volume V for the linac system is estimated as 2.74(2.74)(70) = 525.5 m^3, and the ventilation rate (FR) is taken as 5000 cfm (2.36 m^3 /s). The loss rate W is obtained from Table 5.2.1, by summing the losses listed in the table. The value of W is 486.5 watts to which must be added 5.7 watts, which is assumed to be lost in the beam compression system, giving a total of 492.2 watts. The saturation activity is obtained from equation 10.2.4,

$$A = \frac{2.6 \times 10^5 (492.2)(1 - e^{-1.91/385})}{(\ln 2/600) + 2.36/(3)(525.5)} = 2.38 \times 10^8 \text{ dis/s.}$$

From equation 10.2.5, the concentration is

$$C = \frac{2.38 \times 10^8}{3.7 \times 10^4 (5.255 \times 10^8)} = 1.224 \times 10^{-5} \ \mu\text{Ci/cc.}$$

The volume exhausted while the system is in operation is based on using 180 min. of operation time (~ 10 % of continuous) per day for 365 days. This volume is 5000 cfm

$(2.83 \times 10^4$ cc/ft$^3)(180$ min$)(365$ d$) = 9.3 \times 10^{12}$ cc. The activity released is then

$$\text{Act. Rel.} = C(\text{volume exhausted}) \qquad (10.2.1.2)$$
$$= 1.224 \times 10^{-5} \mu\text{Ci/cc}(9.3 \times 10^{12}\text{cc}) = 1.14 \times 10^{8} \ \mu\text{Ci}$$
$$= 114 \text{ Ci.}$$

Using information contained in Table XXXb of Swanson (SWA 79) for the saturated activities of C-11, N-13 and O-15, one would expect that the released activity would be 88.6% N-13, 9.5% O-15 and 1.9% C-11. The amounts released would be 101 Ci of N-13, 10.8 Ci of O-15 and 2.2 Ci of C-11. According to the AIRDOS-EPA code, the dose at the closest boundary from these emissions (assumed to be 400 m from the Linac system) would be 0.0324 mrem due to N-13, 0.0035 mrem due to O- 15, and 0.0007 mrem from C-11. Note that when the positron conversion target is retracted, the estimated amount of radioactive gas formed will be only 6.4% of the above values. In addition, local lead shielding of the target is planned so that much of the escaping radiation will be absorbed in lead before it will be able to activate the air in the tunnel, which will reduce the amount of radioactive gas produced.

Returning to the concentration at saturation, this represents about 3x the DAC (Derived Air Concentration) for occupational exposure: 4×10^{-6} μCi/cc (DOE 88). This is the concentration while the Linac is running and no one is allowed in the tunnel. Upon stopping the Linac, this air will be exhausted and the concentration will decrease because of no further production. For the normal ventilation rate, FR/V = 0.00449 s^{-1}, the time to reduce the concentration to the DAC value will be

$$DAC = C\, e^{-(\lambda_R + FR/V)t} \qquad (10.2.1.3)$$

and

$$t = \frac{\ln(C/DAC)}{(\lambda_R + FR/V)} = \frac{\ln 3.06}{(\ln 2/600 + 0.00449)}$$

$$t = 198 \text{ s} \sim 3.3 \text{ min.}$$

After a three minute delay, entry into the tunnel would be at or below the DAC value. If the purge ventilation rate (twice the normal rate) were employed, the concentration would be reduced to the DAC value in about 1.8 min.

10.2.2 Radioactive Emissions from the PAR and Synchrotron System

The total power loss in this system was taken as 2.59 W in the PAR (see Section 6.0), 2.59 W in the Injector Region (Section 7.2), 1.6 W (2% of total Synchrotron power) as a distributed

loss around the Synchrotron (Section 7.3) and 40.3 W (50% of the power - Section 7.5) at the Extraction Region, for a total of 47.1 W. The average air path in each of these systems was estimated to be 4 m. The ventilation rate was taken to be 5500 cfm and the volume of the system 375 m^3 (only the volume of a 10 m section of both the Injection and Extraction Regions and the 30 m^3 of the PAR was used in order to be conservative). The saturated activity A is

$$A = \frac{2.6 \times 10^5 (47.1)(1 - e^{-4/385})}{(\ln 2/600) + 0.00231} = 3.65 \times 10^7 \text{ dis/s}$$

and

$$C = \frac{3.65 \times 10^7}{3.7 \times 10^4 (3.75 \times 10^8)} = 2.63 \times 10^{-6} \mu\text{Ci/cc}.$$

The volume of air exhausted during the operation time of 180 min per day, 365 days per year at a rate of 5500 cfm is 1.023×10^{13} cc. The released activity is given by equation 10.2.1.2:

Act. Rel. $= 2.63 \times 10^{-6}$ μCi/cc$(1.023 \times 10^{13}$ cc$) = 2.69 \times 10^7$ μCi

$= 27$ Ci.

Based upon the previous percentage distribution, the amounts released would be 24 Ci of N-13, 2.5 Ci of O-15 and 0.5 Ci of C-11. According to the AIRDOS-EPA code, the dose at the closest boundary (assumed to be 400 m from these systems) for these emissions would be 0.0077 mrem due to N-13, 0.0008 mrem due to O-15, and 0.0002 mrem from C-11. The saturation concentration in this system does not exceed the DAC value of 4×10^{-6} μCi/cc so that no delay in entry will be needed.

10.2.3 Radioactive Emissions from the Storage Ring

The assumed loss rate for the Storage Ring (SR) is based upon a circulating current of 0.3 A ($6.9 \times 10^{12} e^+$) at 7 GeV. The positron beam is assumed to have a mean lifetime of 10 h so the loss rate is 77.747 J/h rad (Section 8.2). When multiplied by 2π radians and divided by 3600 s/h, the power loss is 0.136 W. The average air path in the SR system was estimated to be 3 m. The ventilation rate (FR) was taken to be 900 cfm for each of 20 fans and the volume (V) of the sector was based upon a circumference of 3622 ft (1104 m)/20 = 181.1 ft (55.2 m). The tunnel width varies because of the ratchet wall so an average width of 11.56 ft (3.523 m) was used with a height of 9 ft (2.743 m), giving a total volume of 1.067×10^4 m^3. This gives an air change rate for each sector of

$$FR/3V = \frac{900}{3(60)(18842)} = 2.65 \times 10^{-4}/\text{s}.$$

The saturated activity A is

$$A = \frac{2.6 \times 10^5 (0.136)(1 - e^{-3/385})}{(\ln 2/600) + 0.000265} = 1.93 \times 10^4 \text{ dis/s}$$

and

$$C = \frac{1.93 \times 10^5}{3.7 \times 10^4 (1.067 \times 10^{10})} = 4.89 \times 10^{-10} \mu\text{Ci/cc}.$$

The volume of air exhausted during the operation time of 8000 h per year, at a total rate of 18000 cfm is 2.45×10^{14} cc. The released activity is given by equation 10.2.1.2:

Act. Rel. $= 4.89 \times 10^{-10}$ μCi/cc$(2.45 \times 10^{14}$ cc$) = 1.19 \times 10^5$ μCi

$= 0.119$ Ci.

The amount of radioactivity released in the SR is considered negligible when compared to that from the other systems. The total released per year consists of 125 Ci of N-13, 13.3 Ci of O-15 and 2.7 Ci of C-11, giving doses at the nearest boundary of 0.04, 0.0043 and 0.0009 mrem, respectively.

10.2.4 Average Concentration of Released Radionuclides

Taking the normal ventilation rates of 5000 cfm in the Linac, 5500 cfm in the Synchrotron and 18000 cfm in the Storage Ring, the total ventilation rate is 28,500 cfm. Assuming the system operates continuously, the total volume of air exhausted per day will be

Vol. Exh. $= 28500$ (ft^3/min)2.8317×10^{-2}(m^3/ft^3)1440(min/d)

$= 1.162 \times 10^6$ m^3/d.

Adding up the amount of released activity from the various contributors, without correcting for any decay during transit, the total activity released is 141 Ci/y. The average radioactivity released per day is 141/365 = 0.3863 Ci/d. The average concentration is given by

$\overline{\text{Conc.}}$ $= 0.3863/ 1.162 \times 10^6 = 3.32 \times 10^{-7}$ Ci/m^3

$= 332$ nCi/m^3.

10.2.5 Radioactivity Released in Accidental Beam Losses

Section 9 deals with a number of postulated accidental beam losses leading to radiation doses to personnel in the vicinity. Table 10.2.5.1 below summarizes the largest energy loss in a

given system for a presumed incident. Using equation 10.2.1, and assuming one half of the bremsstrahlung energy escapes to produce radionuclides in air, the yield of activated nuclei can be computed for each of these incidents. This is also listed in the table.

Table 10.2.5.1 - Maximum Energy Loss and Yield of Radionuclides in System Incident

Accelerator System	Incident	Energy Loss (J)	Yield (atoms)
Linac	Loss of e^- beam following failure to limit electron current (Sect. 9.1.3)	62.4	6.97×10^7
PAR	Loss of e^+ beam at a point -system shuts down in one pulse (Sect. 9.2)	7.2	1.68×10^7
Synchrotron	Loss of e^+ beam at a point - system shuts down in one pulse (Sect. 7.4)	112	2.62×10^8
Storage Ring	Loss of e^+ beam at a point - ring requires refill to continue (Sect. 8.3.2)	7728	1.35×10^{10}

Assuming that the decay constant for N-13 is representative of the radioactivity created, the above incidents would result in air activities of 2.2 μCi, 0.5 μCi, 8.2 μCi and 422 μCi for the Linac, PAR, Synchrotron and Storage Ring incidents, respectively.

10.2.6 Dose Commitment Due to Radioactivity Released in Incidents

The above source terms can be used to estimate the dose delivered at the nearest boundary. According to DOE Order 5400.5 (DOE 88a), the external exposure from being immersed in a semi-infinite cloud of these gases is much greater than that due to internal exposure. Taking the distance to the boundary as 140 m for the Storage Ring and 400 m for the other system components, estimating that the activity is released in one minute from each of the respective incident sites, assuming a ground-level release of the activity (i.e. no credit for a stack height), using a pessimistic wind speed of 1 m/s, and taking the most stable Pasquill Stability Class F (giving the least dispersion of the activity), the concentration $\chi(\mu$ Ci/cc) is given by the Gaussian Plume model equation, adapted from Turner (TUR 69,SLA 68):

$$\chi = \frac{Q}{6 \times 10^7 (\pi \sigma_y \sigma_z u)} \qquad (10.2.6.1)$$

The plume spread is assumed to have a Gaussian distribution in both the horizontal and vertical and Q (μCi/min) is the source release rate, σ_y and σ_z,in m, are the standard deviations of the horizontal and vertical plume concentration distributions, respectively, u is the wind speed in m/s and the constant in the denominator is a conversion to the correct units. For the F stability class, and the appropriate distances, the following values are obtained for the standard deviations:

Table 10.2.6.1 - Standard Deviations for F Stability Class

Distance, m	σ_y, m	σ_z, m
140	46	17
400	120	30.5

Using the above values in the expression 10.2.6.1, the following results are obtained:

$$\chi_{Linac} = \frac{2.2}{6 \times 10^7 (\pi)(120)(30.5)(1)} = 3.19 \times 10^{-12} \ \mu Ci/cc$$

$$\chi_{PAR} = \frac{0.5}{6 \times 10^7 (\pi)(120)(30.5)(1)} = 7.25 \times 10^{-13} \ \mu Ci/cc$$

$$\chi_{Sync} = \frac{8.2}{6 \times 10^7 (\pi)(120)(30.5)(1)} = 1.19 \times 10^{-11} \ \mu Ci/cc$$

$$\chi_{SR} = \frac{442}{6 \times 10^7 (\pi)(46)(17)(1)} = 2.86 \times 10^{-9} \ \mu Ci/cc$$

These concentrations have not been adjusted for decay of the radionuclides in transit. DOE Order 5400.5 (DOE 88a), in Figure III-3, gives the concentration which delivers an annual effective dose equivalent of 100 mrem for continuous immersion in the given concentration. The value for N-13 is 2 x 10^{-8} μCi/cc. Exposure to this concentration of N-13 for 24 h per day, 365 days per year results in an effective dose equivalent of 100 mrem. The dose delivered as a result of the various incidents can then be found from

$$Dose_{Incid.} = \frac{\chi_{Incid}(t)}{2 \times 10^{-8} (24)(365)} (100 \text{ mrem}), \qquad (10.2.6.2)$$

in which t is the time of exposure, in h, following the release. Although the release duration should be quite short, the assumption of 1 h exposure time is made. This assumption leads to conservative estimates of the effective dose equivalents, at the nearest site boundary, due to the release of radionuclides in an incident. The annual effective dose equivalent estimates which result can be found in Table 10.2.6.2.

Table 10.2.6.2 - Estimated Effective Dose Equivalents at the Nearest Site Boundary from Radioactive Release Incidents

Incident	H_{eff}, mrem
Linac	1.8×10^{-6}
PAR	4.1×10^{-7}
Synchrotron	6.8×10^{-6}
Storage Ring	1.6×10^{-3}

10.3 Noxious Gas Formation Estimates

The basis of the formation of ozone (O_3) and other noxious gases (nitrogen oxides) in air is photon irradiation of the air molecules (FAS 84, GOE 81, NIE 82, SWA 79, WEI 87), causing dissociation of oxygen molecules, leading to an active free atom of oxygen attaching to an oxygen molecule. Ozone also reacts with other materials formed in air, such as nitrogen oxide, to form nitrogen dioxide (NO_2), which reacts with water vapor in air to form nitric acid (HNO_3)(FAS 84). The radiolytic yield of these products is expressed by the quantity, G, which is the number of molecules formed per unit energy absorbed. These values are usually given as molecules per 100 eV absorbed. Because of its low Threshold Limit Value (TLV) of 0.1 parts per million (ppm) for occupational exposure conditions (8 h per day, 40 h per week) (WEI 87, ACG 88), and its high production rate relative to the other products, ozone is the most important of the noxious products. Ozone is also chemically active and decomposes spontaneously with a chemical half life of about 50 min. In addition, ionizing radiation acts to break up ozone molecules which reduces the concentration. This latter effect can be important for the high radiation fields associated with synchrotron radiation.

The TLV values (ACG 88) for NO_2 and HNO_3 are much higher at 3 and 2 ppm, respectively, than that of ozone. Estimates of the production of O_3, NO_2, and HNO_3 are based upon the G values of 10, 4.8 and 1.5, respectively (SWA 79, FAS 84). Adapting the expression from

Goebel (GOE 81), the change in the number of ozone atoms present per s, dN/dt, is

$$dN/dt = PG - \alpha N - (KP/V)N - (kFR/V)N, \qquad (10.3.1)$$

in which

P = power absorbed in air, eV/s
FR = ventilation rate, cc/s
V = volume irradiated, cc
k = constant which accounts for imperfect mixing = 1/3
α = chemical decay constant = 2.31×10^{-4} /s
K = constant expressing destructive effect of radiation on ozone = 1.4×10^{-16} (GOE 81) to 5×10^{-18} (WEI 87) cm^3/eV
G = number of ozone molecules formed per eV = 0.1 mol/eV.

The solution of the equation for initial conditions N = 0 when t = 0 is

$$N = \frac{PG}{(\alpha + KP/V + FR/3V)} (1-e^{-(\alpha + KP/V + FR/3V)t}). \qquad (10.3.2)$$

Since the TLV is given in ppm, it is desirable to express the number of ozone molecules in terms of that unit, and

$$C_{O_3} = \frac{N \text{ (mol ozone)}}{V\text{(cc of air)}\ 2.463 \times 10^{13} \text{(mol ozone/(cc of air)ppm)}} \qquad (10.3.3)$$

The power absorbed, P, for the case of bremsstrahlung resulting from loss of particles may be expressed as

$$P = (Wfx/\lambda)(6.25 \times 10^{18} eV/J), \qquad (eV/s) \qquad (10.3.4)$$

in which W (watts) is the particle beam power loss, f is the fraction of particle energy which converts to bremsstrahlung and escapes into air (taken as 0.5), x is the average air path in m (Section 10.2.1), and λ is the attenuation length in air for bremsstrahlung in m (385 m as suggested in FAS 84). Combining equations 10.3.2, 10.3.3 and 10.3.4, and taking the more conservative value of $K = 5 \times 10^{-18}$ cm^3 /eV (WEI 87), one arrives at

$$C_{O_3} = \frac{33Wx\ (1-e^{-(0.000231+0.0041Wx/V+FR/3V)t})}{V(0.000231 + 0.0041Wx/V + FR/3V)} ppm. \qquad (10.3.5)$$

Multiplying ppm by 10^{-6} and by the total cc of air exhausted per year (during the operating time of the accelerator component) gives the estimated cc of O^3 released each year of operation by that component.

Multiplying the estimated cc of ozone released, by the density of ozone (1.964×10^{-3} g/cc), yields the mass of ozone released in a year. The sum of all contributions gives the estimated total ozone released due to bremsstrahlung radiation. Estimates of the release of nitrogen dioxide and nitric acid may be obtained by scaling the ozone release values by the G value ratios.

10.3.1 Noxious Emissions in the Linac System

The noxious components formed in the linac system are assumed to be due only to the ionizing radiation created by bremsstrahlung. Using the parameters from Section 10.2.1 for W, x, V and FR for the linac system, in equation 10.3.5, and making the conservative assumption that saturation is reached, gives

$$C_{O_3} = \frac{33(492.2)(1.91)}{5.255\times10^{8}(0.000231 + \sim 10^{-8}+0.001491)} = 0.034 \text{ ppm.}$$

Even assuming saturation which is not expected to be reached in the operation time of the Linac, the ozone concentration is below the TLV of 0.1 ppm. Although no delay is needed for entry to the tunnel because of the ozone concentration, continued operation of the ventilation in normal mode would reduce the ozone concentration in the tunnel to 0.002 ppm in about 10 minutes. As was mentioned in the case of radioactive gas formation, the amount of ozone and other noxious gases produced would only be about 6% of the above values if the positron converter target is retracted. Also, local lead shielding of the target will reduce the amount of photon energy which escapes into air.

The estimated annual release of ozone is

$$\text{Ozone released} = 0.034\,(\text{ppm})\,1\times10^{-6}\left(\frac{\text{cc ozone}}{\text{cc air}}\right)9.3\times10^{12}\,(\text{cc air})$$

$$= 3.162\times10^{5}\,(\text{cc})\,1.964\times10^{-3}\,(\text{g/cc}) = 621 \text{ g.}$$

Based upon the ratio of G values, the estimated release of NO_2 is approximately 298 g and that of HNO_3 is approximately 93 g. Concentration values, in ppm, for these two products can be estimated by scaling the ozone concentration by the ratio of the G values.

10.3.2 Noxious Emissions Due to Bremsstrahlung in the PAR and Synchrotron System

For the portion of noxious gases formed in the PAR and the synchrotron by bremsstrahlung, the information in Section 10.2.2 can be utilized in equation 10.3.5. With the appropriate values of W, x, V and FR for the synchrotron system and the assumption of saturation conditions, one arrives at

$$C_{O_3} = \frac{33(47.1)(4)}{3.75\times10^{8}(0.000231+2\times10^{-9}+0.002307)} = 6.5\times10^{-3}\ \text{ppm}.$$

The estimated annual release of ozone is

$$\text{Ozone released} = 0.0065\,(\text{ppm})\,1\times10^{-6}\left(\frac{\text{cc ozone}}{\text{cc air}}\right)1.1023\times10^{13}\,(\text{cc air})$$

$$= 6.65\times10^{4}\,(\text{cc})\ \ 1.964\times10^{-3}\,(\text{g/cc}) = 131\ \text{g}.$$

Based upon the ratio of G values, the estimated release of NO_2 is approximately 63 g and that of HNO_3 is approximately 20 g.

10.3.3 Noxious Emissions Due to Bremsstrahlung in the Storage Ring

Using the information contained in Section 10.2.3 concerning the parameters for the SR, and assuming saturation, equation 10.3.5 becomes

$$C_{O_3} = \frac{33(0.136)(3)}{1.067\times10^{10}(0.000231+\sim10^{-13}+0.000265)} = 2.5\times10^{-6}\text{ppm}.$$

The estimated annual release of ozone is

$$\text{Ozone released} = 2.5\times10^{-6}\,(\text{ppm})\,1\times10^{-6}\left(\frac{\text{cc ozone}}{\text{cc air}}\right)2.45\times10^{14}\,(\text{cc air})$$

$$= 6.13\times10^{2}\,(\text{cc})\,1.964\times10^{-3}\,(\text{g/cc}) = 1.2\ \text{g}.$$

Based upon the ratio of G values, the estimated release of NO_2 is approximately 0.6 g and that of HNO_3 is approximately 0.2 g.

The total estimate for the annual noxious gas production due to bremsstrahlung is 753 g of O_3, 362 g of NO_2 and 113 g of HNO_3.

10.3.4 Noxious Emissions Due to Synchrotron Radiation

In addition to the noxious gas production by bremsstrahlung, synchrotron radiation which escapes through the wall of a vacuum chamber or through a beryllium window will also produce ozone and other noxious gases in air. Although the vacuum chamber absorbs much of the synchrotron radiation, the intensity (photons/s) is great enough so that sufficient photons, in the energy range above about 80 keV, escape absorption in the vacuum chamber wall and emerge into the tunnel. These photons irradiate air to produce ozone and also may produce a high enough radiation field in the vicinity of electronic components to represent a potential for damage to these components (DIN 82, DIN 85).

The synchrotron radiation arises when electrons or positrons are bent in a magnetic field. Because the change in direction represents an acceleration, there is a probability that the particle may emit a photon. An early treatment of synchrotron radiation can be found in Schwinger (SCW 49, SCW 73). More recent discussions dealing with storage ring aspects can be found in the literature (ANL 86, GOD 68, GRE 76, SAB 73, SHE 85). From a radiation dosimetry aspect, the distribution of the synchrotron radiation within the vacuum chamber is important (KIM 86, TAZ 84) as well as the nature and thickness of the attenuating material of the chamber. Synchrotron radiation is emitted as a continuous spectrum of photon energies (Figure 17 illustrates synchrotron radiation spectra from a number of facilities). The source strength of the synchrotron radiation is determined by the

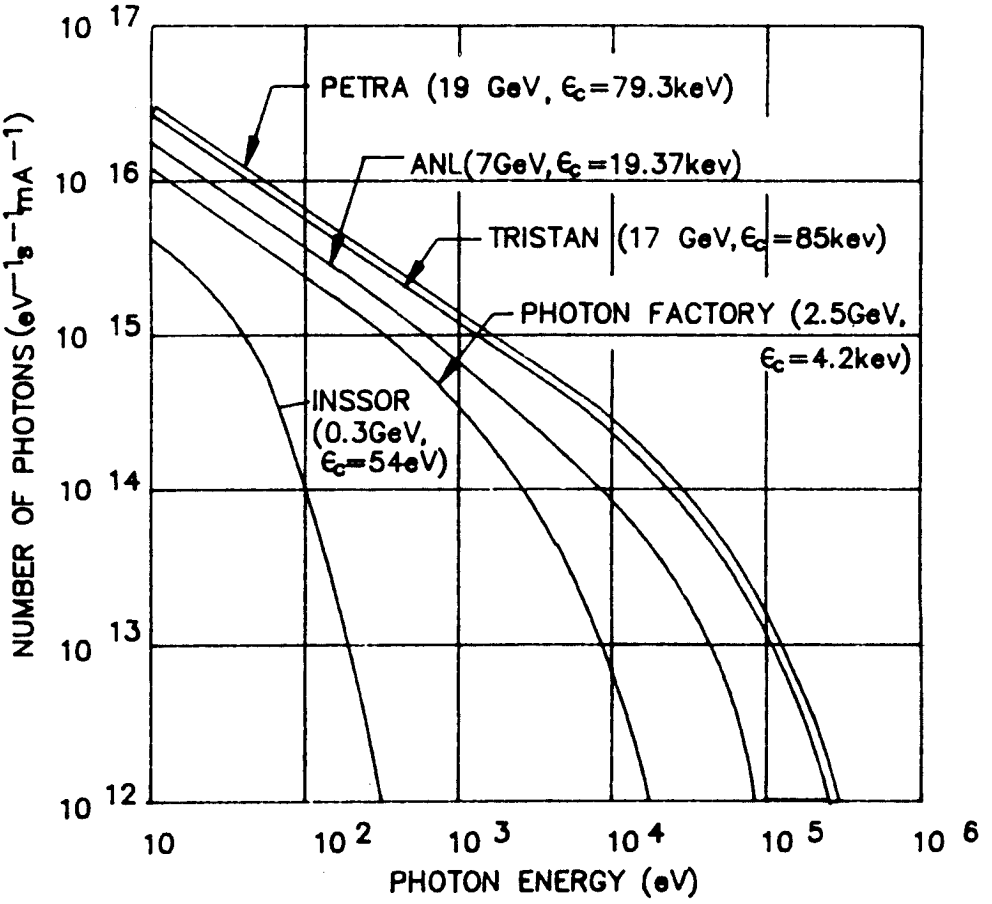

Figure 17. Synchrotron Radiation Spectra of Several Different Machines.

energy of the positron, the bending radius of the magnet and the critical energy of the synchrotron radiation spectrum. An important parameter associated with the synchrotron radiation is the critical energy. The critical energy represents the energy at which half of the power is emitted above, and half below, this value. As the critical energy is increased, the

number of higher energy photons in the spectrum becomes more important since these are more penetrating and may actually pass through the vacuum chamber wall. The fraction of the photons which penetrate the wall of the chamber may be small, but the number of available photons in the beam is quite large so that a significant number of photons may penetrate the wall. Once the photons enter the tunnel, irradiation of air occurs over the path length traveled by the photon.

For the estimates of noxious gas production in this section, the particle energy is assumed to be 7 GeV, the critical energy is taken as 19 keV for the storage ring and the synchrotron, and the radius of the bending magnet was assumed to be 38.9611 m in each case. These assumptions give a conservative result for the synchrotron calculation since the energy of the positron varies from 450 MeV to 7 GeV during acceleration but the full energy value was used. Because the energy in the PAR is only 450 MeV, noxious gas production in the PAR will be negligible. However, the potential for synchrotron radiation beams irradiating air in the experimental enclosures (often called hutches) necessitates estimating the contribution from this source.

Equation 10.3.1 expressing the formation rate of ozone can be used for that produced by the synchrotron radiation. In the case of synchrotron radiation, the expression for the power absorbed in air, P, must be modified from that given in equation 10.3.4. In addition, the constant, K, expressing the destructive effect of radiation on ozone, is a more important factor for the high intensity synchrotron radiation and for small irradiation volumes. According to Green (GRE 76,p.1-9), the number of photons, $(\partial N(\epsilon,t,I,\theta)/\partial\epsilon\,\partial t\partial I\partial\theta)$, per eV per s per mA per mrad in the horizontal, for the entire opening angle ψ, is given by

$$\frac{\partial N(\epsilon,t,I,\theta)}{\partial\epsilon\,\partial t\partial I\partial\theta} = 4.2419 \times 10^{16}\, R/(\gamma)^2 \int_y^\infty K_{5/3}(\eta)\,d\eta, \qquad (10.3.4.1)$$

in which R is the radius of the bending magnet, $\gamma = 7000/0.511$, $y = \epsilon/\epsilon_c = \epsilon/19000$, ϵ is the energy of the photon, eV, and $K_{5/3}(\eta)$ is a modified Bessel function (ABR 64, WAT 48). When values are substituted for the parameters, and using

$$N(\epsilon) = \frac{\partial N(\epsilon, t, I, \theta)}{\partial\epsilon\,\partial t\partial I\partial\theta},$$

the expression becomes

$$N(\epsilon) = 8.8067 \times 10^9 \int_y^\infty K_{5/3}(\eta)\,d\eta \left(\frac{ph}{eV\ s\ mA\ mradh}\right). \qquad (10.3.4.2)$$

If one multiplies $N(\epsilon)d\epsilon$ by ϵ and $e^{-(\mu/\rho)_m(\rho)_m(x_m/\sin\theta)}$, the result will be the (eV/s mA mradh) which is coming through the wall material m of density ρ, slant thickness x/ sin θ, and mass attenuation coefficient (μ/ρ). The angle θ is the angle at which the synchrotron radiation strikes the vacuum chamber wall. The energy absorbed in the air path, t cm, is

$$N(\epsilon)\epsilon d\epsilon\ e^{-(\mu/\rho)_m(\rho)_m(x_m/\sin\theta)}(1 - e^{-(\mu_{en}/\rho)(\rho_{air})t}),$$

in which (μ_{en}/ρ) is the mass energy absorption coefficient in air, in cm^2/g, and ρ_{air} is the density of air, g/cc.

If the expression is then integrated over all values of ϵ, the final result is the total energy absorbed in the air path due to all the photons in the spectrum:

$$\frac{\partial N(t,I,\theta)}{\partial t\partial I\partial\theta} = 8.8067 \times 10^9 \int_0^\infty e^{-(\frac{\mu}{\rho})(\rho)(\frac{x}{\sin\theta})}(1 - e^{-(\frac{\mu_{en}}{\rho})(\rho)t_{air}}) \times \epsilon d\epsilon \int_y^\infty K_{5/3}(\eta)d\eta. \qquad (10.3.4.3)$$

Making a change of variables based upon $y = \epsilon/\epsilon_c$, the final form becomes

$$\frac{\partial N(t,I,\theta)}{\partial t\partial I\partial\theta} = 3.179 \times 10^{18} \int_0^\infty e^{-(\frac{\mu}{\rho})(\rho)(\frac{x}{\sin\theta})}(1 - e^{-(\frac{\mu_{en}}{\rho})(\rho)t_{air}}) \times y dy \int_y^\infty K_{5/3}(\eta)d\eta \cdot (\frac{eV}{s\ mA\ mradh}) \qquad (10.3.4.4)$$

To evaluate the integral of the modified Bessel function in equation 10.3.4.4, one may make use of the series expansion found in Kostroun (KOS 80). To obtain a solution to equation 10.3.4.4, it is necessary to perform a numerical integration over the variable y. Mass attenuation and mass energy absorption coefficients for the various materials found in the windows, vacuum chambers and air are available in the literature (BRO 78, HUB 80, JAC 81).

Multiplying the above result by the current (mA) and the number of radians in the horizontal plane (mradh) gives the power absorbed, P, in eV/s:

$$P = \frac{\partial N(t,I,\theta)}{\partial t\partial I\partial\theta}(I)(\theta)\quad(\frac{eV}{s}). \qquad (10.3.4.5)$$

Rewriting equation 10.3.5 to account for the difference in the absorbed power in the case of the synchrotron radiation relative to that from the bremsstrahlung, one arrives at an expression for the ozone production due to synchrotron radiation:

$$C_{O_3} = \frac{4.06 \times 10^{-15} P(1-e^{-(0.000231 + KP/V + FR/3V)t})}{V\ (0.000231 + KP/V + FR/3V)} \text{ ppm.} \qquad (10.3.4.6)$$

Multiplying ppm by 10^{-6} and the total cc of air exhausted per year (during the operating time of the particular accelerator component), gives the estimated cc of ozone released each year. Multiplying the estimated cc by the density of ozone (1.964×10^{-3} g/cc), yields the estimated mass (g) of ozone released in a year. The sum of all contributions gives the estimated total ozone released by the synchrotron radiation. When this total is added to that released due to bremmstrahlung, the total ozone released by the APS is obtained.

10.3.5 Noxious Emissions Due to Synchrotron Radiation in the Synchrotron System

In the proper evaluation of equation 10.3.4.4 to obtain the power absorbed in air, the air path, t, varies with the emission angle of the synchrotron radiation emanating from a bending magnet. Assuming the synchrotron orbit can be approximated by a circle of radius 53.476 m, and the transverse distance from the orbit to the shielding wall is 1.067 m, the total tangential path inside the synchrotron is estimated to be 10.736 m. The air path will be less than this because of the varying path of the synchrotron radiation within the vacuum chamber. Using the geometry scheme presented in Tazzari (TAZ 84) and illustrated in Figure 18, one may

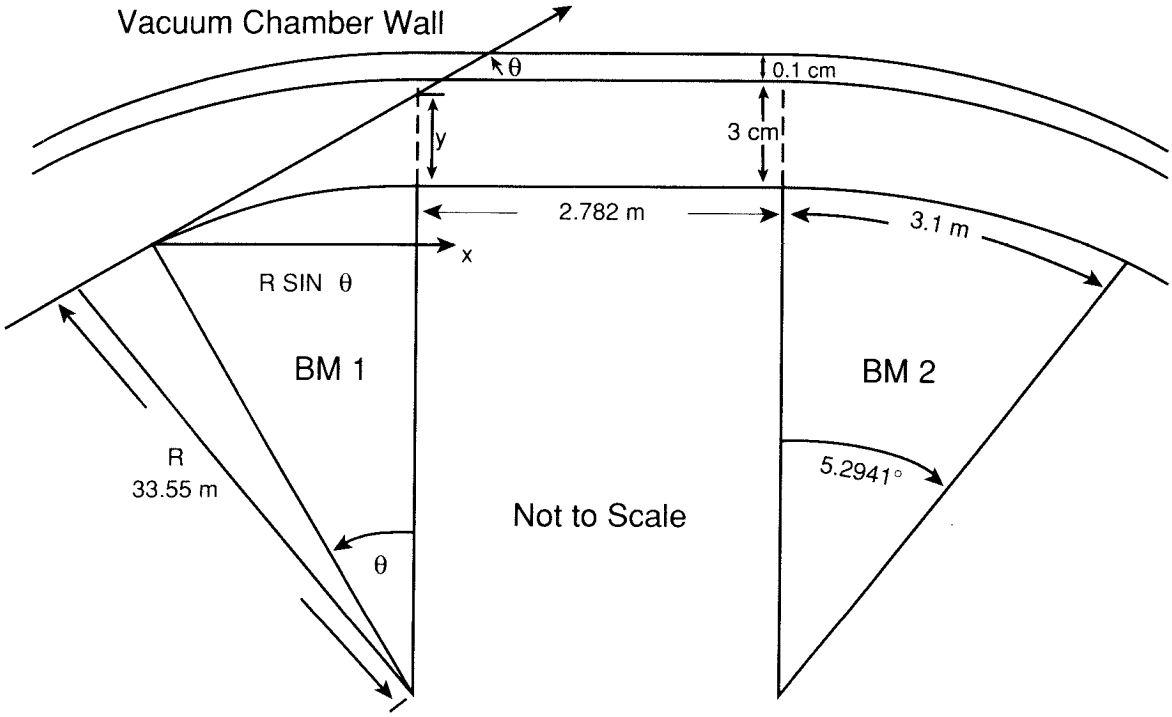

Figure 18 Geometry for Synchrotron Radiation Trajectories in the Booster Synchrotron

solve for the distance traveled by the synchrotron radiation before it emerges into air. When this distance is subtracted from the 10.736 m, one obtains the approximate value of the air path distance.

The vacuum chamber for the Booster Synchrotron is a stainless steel oval which is 1 mm thick, whose major axis is 6 cm long and minor axis 3.7 cm long (ANL 87). There are 68 dipole magnets of length 3.1 m of strength 0.696 T at 7 GeV. The radius of the magnets is 33.55 m and the bending angle of the dipoles is 5.2941^{o} (92.4 mrad). The length of the straight sections following the magnets is 2.782 m. As the positrons enter the magnet, they are continually bent by the magnetic field over an arc of 5.2941^{o}, emitting a "fan" of synchrotron radiation which intercepts the stainless steel vacuum chamber wall at various distances downstream of the emission point. Because of the very shallow angles involved, the slant thickness through the chamber wall is very much increased over the straight-through thickness and the shielding effect is enhanced. With reference to Figure 18, our concern is in the radial plane only, because of the narrow cone into which the radiation is emitted. Radiation from BM1 is emitted at some angle θ as indicated in the figure. The distance y, in the radial direction, from the orbit in the magnet and the following straight section is given by

$$y = (x + R \sin\theta)\tan\theta - R\,(1 - \cos\theta) \quad \text{(cm)}, \qquad (10.3.5.1)$$

in which R is the radius of the magnet in cm (3355 cm) and x (cm) is the distance into the straight section at which the synchrotron ray is displaced a distance y from the orbit. As shown in the figure, the value of y such that the ray just strikes the chamber wall is 3 cm and the value of y = 3.1 cm indicates when the attenuated ray leaves the chamber and continues on through air. The path in the vacuum chamber for a given angle θ for which y = 3.1 cm is given by

$$path_{v} = (x + R \sin\theta)\sec\theta \ . \qquad (10.3.5.2)$$

The air path used for the estimates is then 1073.6 - $path_{v}$, until the synchrotron radiation leaves the straight section. Following the straight section is another bending magnet BM2, and rays that are emitted near the end of BM1 (when θ is very small) may traverse the entire length of the straight section without colliding with the vacuum chamber wall. This radiation will continue on through BM2, through the stainless steel wall of the chamber and out into air. A portion of the path in the vacuum chamber can be computed by equation 10.3.5.2, the remainder may be estimated based upon the geometry in Figure 19.

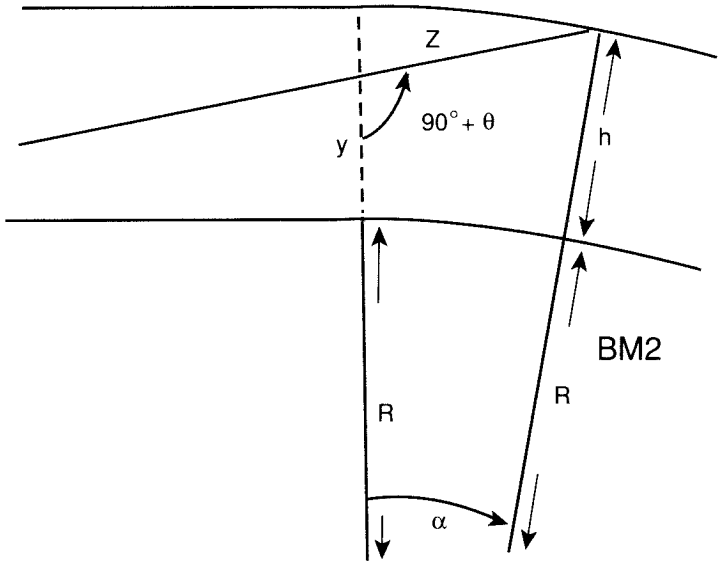

Figure 19 Geometry for Synchrotron Radiation Trajectory into BM2

Initially, the value of y is computed for a value of x which represents the end of the straight section (x = 2.782 m), and the value of the path in the vacuum chamber, $path_V$, up to that point is also computed. The remainder of the path in the vacuum chamber is estimated with the use of the geometrical arrangement shown in Figure 19. The objective is to evaluate z in the figure. Using the computed value of y at the end of the straight section, and the known value of h (the distance from the orbit to the vacuum chamber wall), one may write the the relationship

$$\frac{R + h}{\sin\,(90^{o}+\theta)} = \frac{R + y}{\sin\,(90^{o}+\theta-\alpha)} \,. \qquad (10.3.5.3)$$

From relationship 10.3.5.3, the value of the angle α can be found. Referring to the figure, the length of z is then found from

$$\frac{Z}{\sin\,\alpha} = \frac{R + h}{\sin\,(90^{o}+\theta)} \,. \qquad (10.3.5.4)$$

The total path in the vacuum chamber is then $path_V + z$. This value may then be subtracted from 1073.6 cm to find the path in air. The value of the slant thickness for the stainless steel wall was approximated by assuming initially that the slant thickness equals x/sin θ , in which x is the straight-through thickness and θ is the angle of emission from the bending magnet. For radiation passing through BM2, equations 10.3.5.3 and 10.3.5.4 were used to obtain the wall thickness. The air path and the slant thickness through the stainless steel as a function of θ were used to determine the energy absorbed in air from the synchrotron radiation (equation 10.3.4.4), and this distribution is plotted in Figure 20. The integral of this distribution over all θ gives the eV/s mA absorbed in air from one bending magnet in the

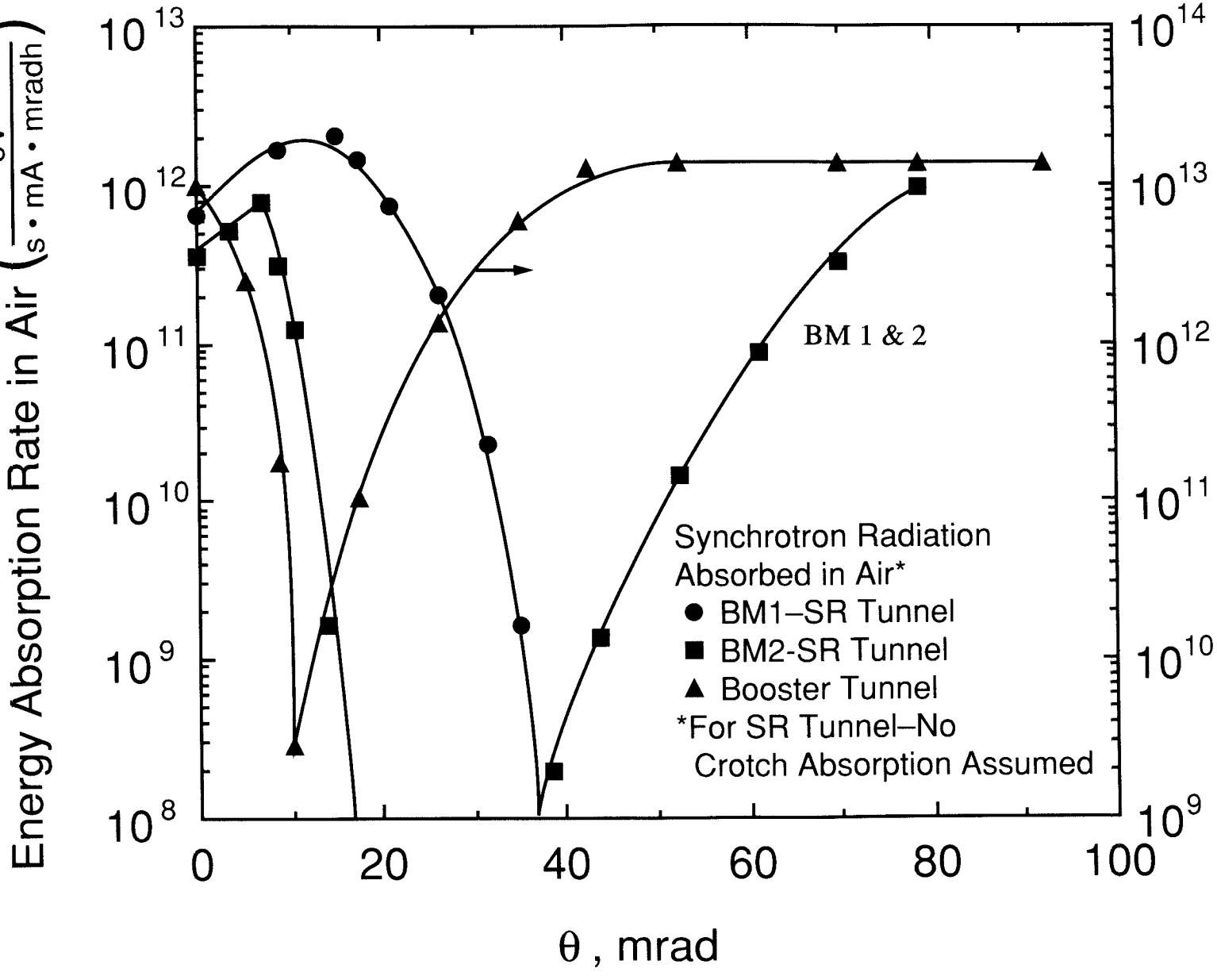

Figure 20. Energy Absorption Rate in Air Due to Synchrotron Radiation in the Booster Synchrotron and Storage Ring Tunnels.

synchrotron. When multiplied by the value of the circulating current in mA, one gets the total contribution from all the positrons which are available during the accelerating cycle (eV/s). Because of the symmetry of the system, the total contribution will be equal to the total number of magnets (68) times the integral of the distribution.

The integral of the distribution in Figure 20 is 8.716×10^{14} (eV/s mA). The current in the synchrotron is calculated from

$$I = \frac{7.2 \times 10^{10} (e^+) \; 3 \times 10^{8} \; (m/s)}{368 \; m \; (6.25 \times 10^{15} \; e^+/s \; mA)} = 9.4 \; mA$$

The total power absorbed in air from one bending magnet is

$$P = 9.4 \; mA (8.716 \times 10^{14} \; eV/s \; mA) = 8.19 \times 10^{15} \quad (eV/s),$$

and the total power from 68 magnets is = 5.57×10^{17} (eV/s).

The ozone production by the synchrotron radiation in the Booster Synchrotron tunnel, assuming that the saturation concentration has been reached, is estimated from equation 10.3.4.6 to be

$$C_{O_3} = \frac{4.06 \times 10^{-15} (5.57 \times 10^{17})}{2.763 \times 10^{9} (0.000231 + \sim 10^{-9} + 0.000313)} = 0.0015 \; ppm.$$

Since this concentration is well below the TLV of 0.1 ppm, no delay in entering the Booster Synchrotron tunnel following shutdown is anticipated from the standpoint of the ozone concentration.

The estimated annual release of ozone from this source is

$$\text{ozone released} = 0.0015 (ppm) \, 1x10^{-6} \left(\frac{cc \; ozone}{cc \; air}\right) 1.023x10^{13} (cc \; air)$$

$$= 1.53x10^{4} (cc) \, 1.964x10^{-3} (g/cc) = 30 \; g.$$

Based upon the ratio of G values, the estimated release of NO_2 is approximately 14 g and that of HNO_3 is approximately 4.5 g.

10.3.6 Noxious Emissions Due to Synchrotron Radiation in the Storage Ring

The geometry scheme in the Storage Ring for BM1 is shown in Figure 21. Utilizing details from ANL-87-15 (ANL 87), the vacuum chamber is made out of aluminum, 1.6 cm thick in the region where the synchrotron radiation will strike the chamber, and the radial distance

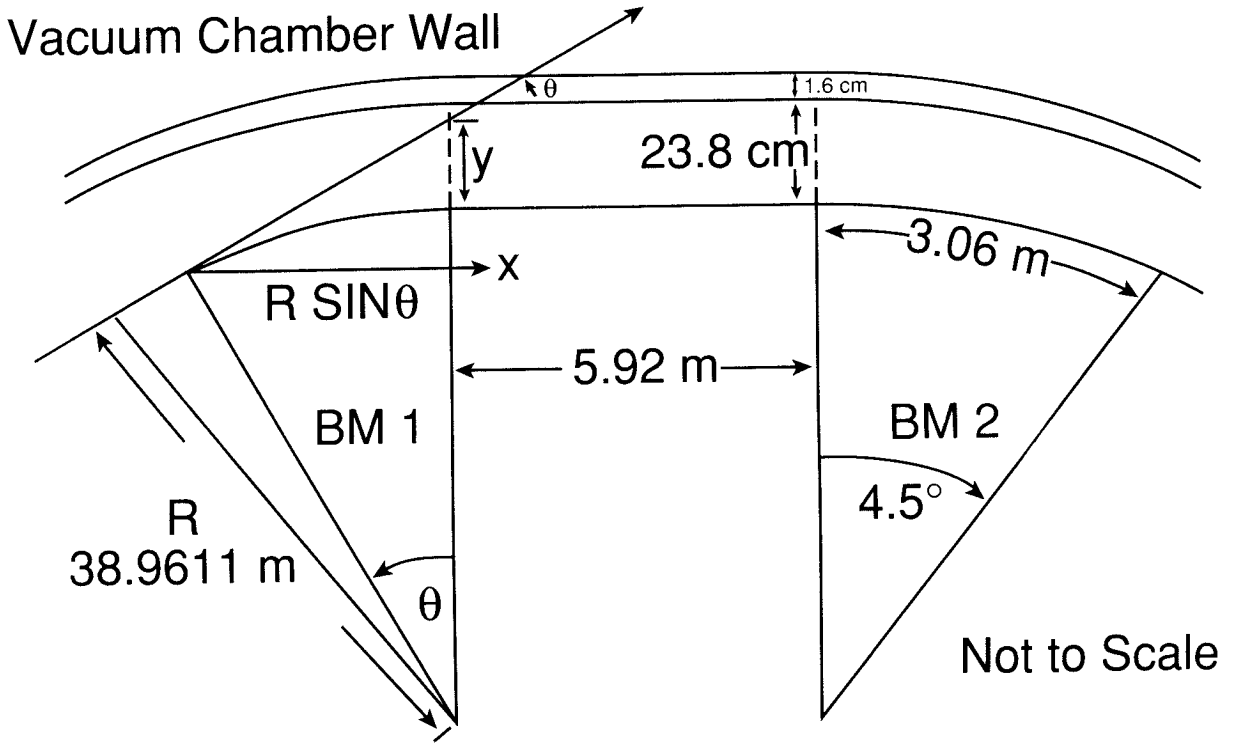

Figure 21. Geometry for Synchrotron Radiation Trajectories in SR

from the orbit to the chamber wall is 23.8 cm. There are 80 dipole magnets of length 3.06 m and bending radius 38.9611 m. The bending angle is 4.5^{o} (78.54 mrad). The length of the straight section following BM1 is taken as 5.92 m.

The storage ring orbit can be approximated by a circle of radius 175.7 m, but because of the serpentine nature of the outer ratchet wall, the distance from the orbit to the shielding wall varies so the total tangential path length also varies. For purposes of this estimate, the nominal value of 22 m was used. As was the case in the Synchrotron, the slant thickness through the Al wall of the chamber is very much increased over the straight-through thickness which provides additional shielding. One may use equations 10.3.5.1, 10.3.5.2, 10.3.5.3 and 10.3.5.4 to determine the path of the synchrotron radiation in the vacuum chamber, as in the Synchrotron case, and the air path is determined for a given angle of emission by subtracting the path in the vacuum chamber from 2200 cm. The slant thickness was calculated in the same manner as for the Synchrotron vacuum chamber. The air path and the slant thickness through the aluminum as a function of θ were used to determine the energy absorbed in air from the synchrotron radiation (equation 10.3.4.4), and this distribution is plotted in Figure 20 for BM1. The geometry for BM2 differs from that shown in Figure 21 for BM1 in that BM2 is followed by a longer straight section. This leads to

increased absorption of the synchrotron radiation at the shallower angles. The distribution of the rate of energy absorbed from the synchrotron radiation from BM2 is also shown in Figure 20. The integral of these distributions over all θ gives the eV/s mA absorbed in air from each bending magnet in a sector of the Storage Ring. The sum of these integrals gives the eV/s mA for a sector. The total energy absorption rate is equal to the number of sectors (40) times the sum for one sector. The sum of the integrals of the distributions from BM1 and BM2 in Figure 20 is 5.3024×10^{13} (eV/s mA). The circulating current is taken as the design current 0.1 A, so the total absorbed power from the 40 sectors will be

$$P = 100\ \text{mA}(5.3024 \times 10^{13}\ \text{eV/s mA sector})40\ \text{sectors}$$

$$= 2.12 \times 10^{17}\ (\text{eV/s}).$$

The ozone production by the synchrotron radiation in the Storage Ring tunnel, when the saturation concentration has been reached, is estimated from equation 10.3.4.6 to be

$$C_{O_3} = \frac{4.06 \times 10^{-15}(2.12 \times 10^{17})}{1.067 \times 10^{10}(0.000231 + \sim 10^{-10} + 0.000265)} = 0.00016\ \text{ppm}.$$

Since this concentration is well below the TLV of 0.1 ppm, no delay in entering the Storage Ring tunnel following shutdown is anticipated from the standpoint of the ozone concentration.

The estimated annual release of ozone from this source is

$$\text{ozone released} = 0.00016(\text{ppm})1\text{x}10^{-6}\left(\frac{\text{cc ozone}}{\text{cc air}}\right)2.45\text{x}10^{14}(\text{cc air})$$

$$= 3.92\text{x}10^{4}(\text{cc})1.964\text{x}10^{-3}(\text{g/cc}) = 77\ \text{g}.$$

Based upon the ratio of G values, the estimated release of NO_2 is approximately 37 g and that of HNO_3 is approximately 12 g. However, the calculation above does not take into account the use of absorber crotches in the ring to intercept and absorb synchrotron radiation so that it will not penetrate the chamber. The crotches and end absorbers are estimated to intercept 90 - 95% of the synchrotron radiation (ANL 87). If one assumes that 80% of the synchrotron radiation is intercepted and absorbed before it can get out of the chamber, the estimated releases are then 15.4 g of O_3, 7.4 g of O_3, 7.4 g of NO_2, and 2.4 g of HNO_3.

10.3.7 Noxious Emissions Due to Synchrotron Radiation in Experimental Enclosures

Synchrotron radiation is guided by photon beam tubes from the bending magnets into enclosures where it passes through a window, often of beryllium, and is directed to the first optical element. In making the transition from the Storage Ring to the experimental stations, the beam of synchrotron radiation may pass through an air path. When the beam consists of the entire spectrum of photons passed by the window, it is referred to as a "white" beam. The cutoff energy that determines whether a photon gets through the window will depend upon the thickness and material composition of the window. If the synchrotron radiation is allowed to pass through an air path in the enclosure, ozone will be produced. One may estimate the power absorbed per mA per mradh in an air path of t (cm) length, by using a modified equation 10.3.4.4. If one replaces x/sin θ by the straight- through thickness x (cm) of the window, then one may use this modified equation to solve for the power loss in air per mA per mradh. A typical distribution for the power loss is shown in Figure 22 in which the F (y) evaluated from the equation is plotted against u = ln y in order to better indicate the spectral region which contributes the most to the absorbed energy rate. Upon performing the integration indicated in the modified equation 10.3.4.4, the total power absorbed is then given by equation 10.3.4.5,

$$P = \frac{\partial N(t, I, \theta)}{\partial t \partial I \partial \theta} (I)(\theta) \qquad (eV/s).$$

For the purpose of the estimate, the window is assumed to be Be of thickness equal to 0.05 cm (density = 1.848 g/cc). The actual air path for any experimental arrangement is a poorly known quantity, so a number of calculations were made to determine the energy loss rate and the formation rate of ozone (mol/s) as a function of various air paths. The parameters used in this calculation were a positron beam energy of 7 GeV, a positron beam current of 100 mA, and a horizontal acceptance angle of 2 mradh for the synchrotron radiation. The critical energy was taken as 19 keV and the radius of the bending magnet was 38.9611 m. The results of the calculations are plotted in Figure 23 where the ordinate value is the product PG. From the steep rise in the curve for even very small air paths, one can see the need to reduce to a minimum, if not totally eliminate, any air path in the enclosure. For example, assuming a 10 cm air path, an enclosure volume of 30 m^3, a ventilation rate of 200 cfm, and taking the value of PG from the curve (~ 4.5×10^{18} mol/s), the concentration at saturation is obtained from a modified equation 10.3.4.6:

$$C_{O_3} = \frac{4.06 \times 10^{-14} (4.5 \times 10^{18})}{3 \times 10^{7} (0.000231 + 0.000008 + 0.001049)} = 4.73 \text{ ppm}.$$

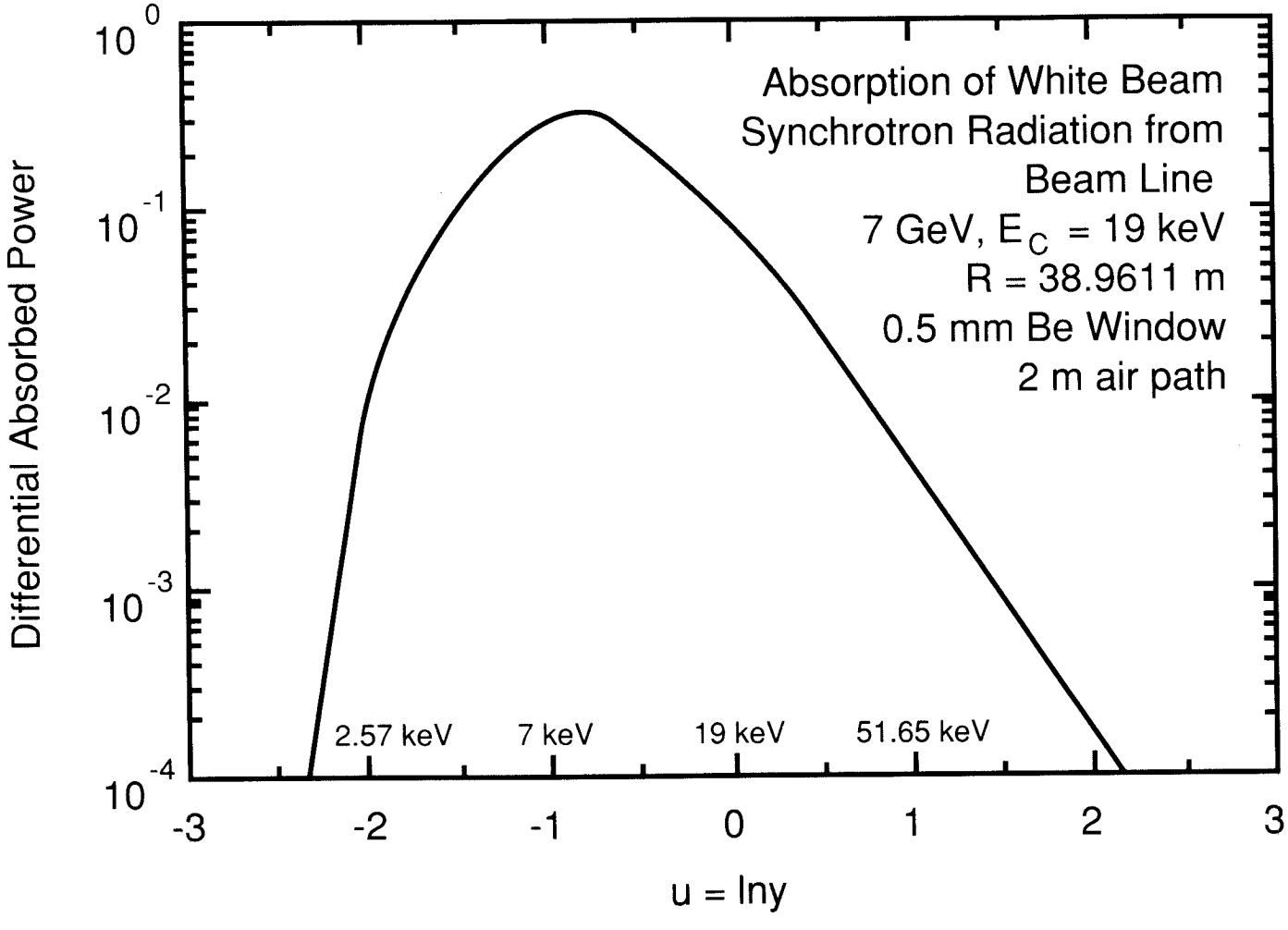

Figure 22. Spectral Dependence of the Absorbed Energy Rate in Air

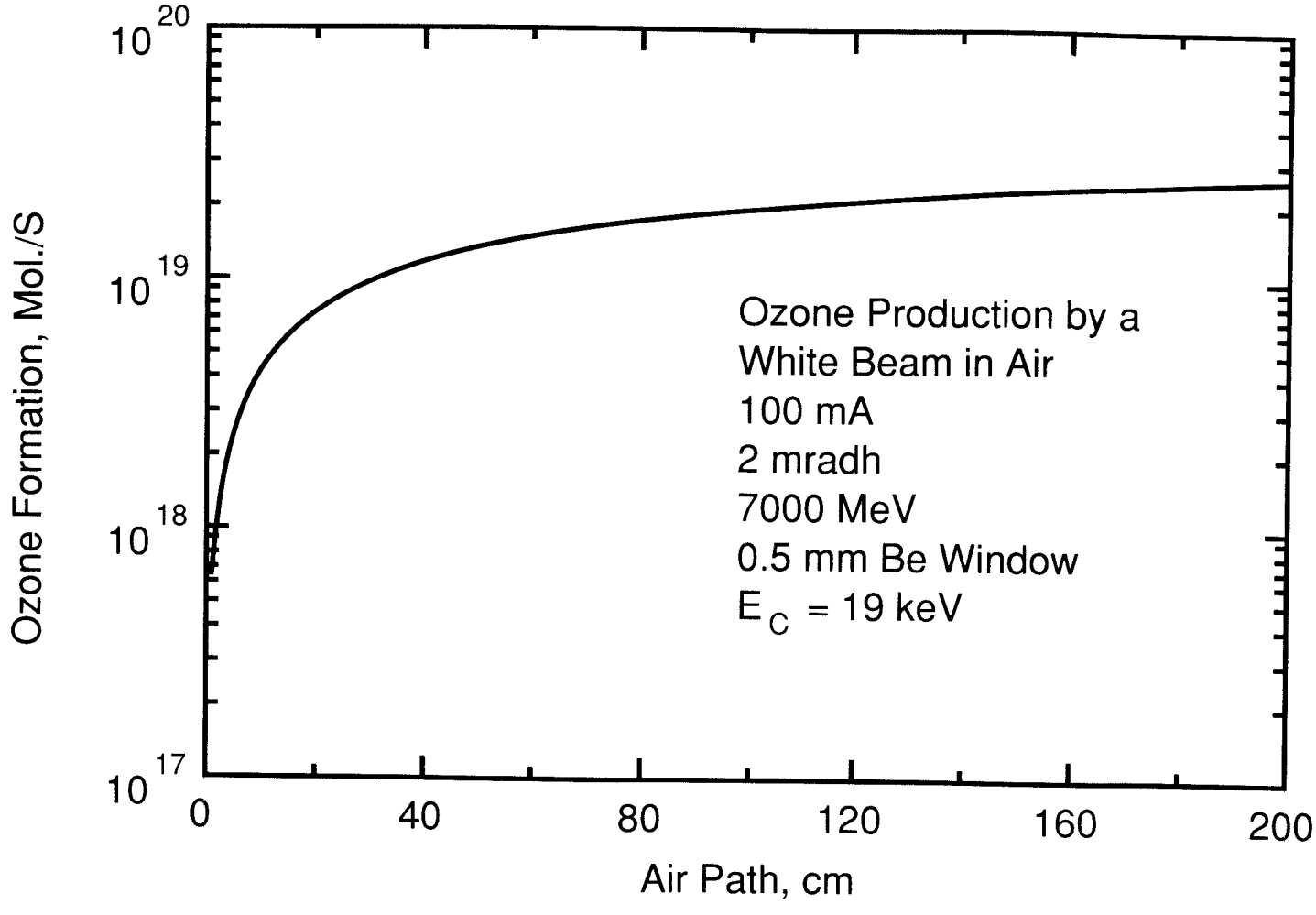

Figure 23. Ozone Formation Rate in Air Versus Path Length.

In this case the concentration in the enclosure will build up to almost 50 x the TLV. Following shutdown, the time to reduce the concentration to 0.1 ppm is

$$0.1 = 4.73\, e^{-(0.000231 + 0.003147)t}$$

$$t = \frac{3.8565}{0.00338} = 1141 \text{ s} = 19 \text{ min.}$$

For this example, both the concentration of the ozone and the time delay to exhaust the enclosure are undesirable. The ventilation rate can be increased, but too large an increase in the flow rate could create an imbalance in the ventilation for the Storage Ring building.

A number of remedies are available: localized ventilation using a shroud just above the beam, fill any voids with an inert gas which will remove more of the low energy photons (WEI 87), or enclose the path in a vacuum to reduce the number of air molecules.

On the assumption that sound practice will all but eliminate the smallest of air paths, the estimate of the ozone released is based upon an equivalent air path of 2 cm., a current of 100 mA, an acceptance angle of 2 mradh, an enclosure size of 30 m^3 and a ventilation rate of 1000 cfm. The product PG for a 2 cm path is 1.14×10^{18} mol/s. The saturation concentration for the above parameters is

$$C_{O_3} = \frac{4.06 \times 10^{-14}(1.14 \times 10^{18})}{3 \times 10^{7}(0.000231 + 0.000001 + 0.005244)} = 0.28 \text{ ppm.}$$

Since this value is above the TLV, the time to reduce the concentration to 0.1 ppm is

$$0.1 = 0.28\, e^{-(0.000231 + 0.015732)t}$$

$$t = \frac{1.03}{0.016} = 64.4 \text{ s} \sim 1 \text{ min.}$$

The estimated annual release of ozone from this source is

$$\text{ozone released} = 0.28(\text{ppm})\, 1 \times 10^{-6} \left(\frac{\text{cc ozone}}{\text{cc air}}\right) 1.36 \times 10^{13} (\text{cc air})$$

$$= 3.8 \times 10^{6} (\text{cc})\ 1.964 \times 10^{-3} (\text{g/cc}) = 7463 \text{ g.}$$

This is the estimated release from one enclosure. The total number of such enclosures is unknown at this time. Until a better estimate of the number of enclosures which may have an air path can be made, the above result represents the best available estimate. Based upon the

ratio of G values, the estimated release of NO_2 is approximately 3582 g and that of HNO_3 is approximately 1119 g. From the previous results, one may conclude that the most significant source of ozone production will be that from the "white" beam enclosures.

The results from the various calculations concerning noxious gas production by bremsstrahlung and synchrotron radiation have been summarized in Table 10.3.7.1.

Table 10.3.7.1 Summary of Estimated Annual Noxious Gas Releases

Accelerator Component	Ozone (g)	Nitrogen Dioxide (g)	Nitric Acid (g)
Linac			
Due to Bremsstrahlung	621	298	93
Due to Synchrotron Rad.	-	-	-
Synchrotron System			
Due to Bremsstrahlung	131	63	20
Due to Synchrotron Rad.	30	14	4.5
Storage Ring			
Due to Bremsstrahlung	1.2	0.6	0.2
Due to Synchrotron Rad.	15.4	7.4	2.4
Experimental Enclosures			
Due to Bremsstrahlung	-	-	-
Due to Synchrotron Rad.	7463	3582	1119
Totals	8262	3965	1239

11.0 Activation of Accelerator Components and Other Materials

11.1 Introduction

As discussed in Section 10.2, the photoneutron interaction of bremsstrahlung with the nuclei of materials leads to the formation of radioactive products in the air. This same interaction produces the major portion of activated components in the accelerator structures. The

particular radionuclides which are produced will depend upon the (γ,n) and photospallation cross sections for the various materials which are present in the structures. Those components which absorb most of the bremsstrahlung will be the most likely sites for finding activation products. In particular, the tungsten converter target, which absorbs a large amount of the bremsstrahlung, will become very activated. In the other parts of the accelerator structure, collimators, beam dumps, injection and extraction points are other likely sites of activation (GOL 76, BAR 69). The radioactive materials which are formed have a range of half lives from seconds to more than 10^5 years (SWA 79). The intensity of these radioactive products at some time following a shutdown is a function of the composition and amount of a given target material present, the cross section for the reaction and the half life of the radioactive product. The materials of interest for the APS system are aluminum, copper, iron in steel, and tungsten. The radioactivity builds up during the operation of the accelerator, and when the accelerator is shut down, there is an initial rapid decay of the shorter-lived materials, followed by a slower decay of the intermediate half life materials, finally leaving only the residual longer-lived components.

In terms of the initial radioactive material which will survive for a year or more, following shutdown and no further operation, the radionuclides Fe-55, Mn-54, Co-60, Ni-63, Ta-182, W-181, Na-22, and Al-26 are the main contributors. These longer-lived components will constitute the residual radioactivity of the facility and will influence the disposition of the facility components. Although many radionuclides will be formed during each cycle of operation, most of these will quickly decay away so that only those listed above will be important.

11.2 Residual Radioactivity Estimates

An estimate of the activity of a radionuclide formed in a particular material can be obtained with the use of equation 10.2.1,

$$Y = 1.21 \times 10^{11} Z^{0.66} \text{(n/skW)} = 1.21 \times 10^{8} Z^{0.66} \text{(atoms/sW)},$$

modified by a factor which accounts for the abundance of the particular target isotope of the given element, which becomes activated to the radionuclide. As in Section 10.2, we assume that the yield of neutrons is also the yield of radionuclide atoms. This may be expressed as

$$Y' = FY = 1.21 \times 10^{8} FZ^{0.66} \text{ (atoms/sW)}, \qquad (11.2.1)$$

in which F is the fractional abundance of the isotope and Z is the atomic number of the element. For example, copper activation (Z = 29) is the result of activation of Cu-63 (F = 0.691) and Cu-65 (F = 0.309), leading to a number of radionuclides: Co-58, Co-58m, Co-60, Ni-63, Cu-61, Cu-62, and Cu-64 (SWA 79). Most of these radionuclides have half lives of a few minutes to a few hours so they decay away quickly and do not contribute to any long

term residual radioactivity. However, Co-60 and Ni-63, with half lives of 5.27 y and 92 y, respectively, will be important with respect to the residual radioactivity in the system.

The change in the number of radioactive atoms of a given species present per unit time, dN/dt, is given by

$$dN/dt = Wf'Y' - \lambda_R N \qquad \text{(atoms/s)},$$

in which W (watts) is the particle beam loss, f'is the fraction of the particle energy which converts to bremsstrahlung and is absorbed in the material being activated (taken as 0.5), and λ_R is the radioactive decay constant of the radionuclide which is being formed, s^{-1}. For the initial conditions, N = 0 for t = 0, the solution is

$$N = \frac{Wf'Y'}{\lambda_R}\,(1 - e^{-\lambda_R t}) \qquad \text{(atoms)} \qquad (11.2.2)$$

and since the activity $A = \lambda_R N$,

$$A = Wf'Y'\,(1-e^{-\lambda_R t})\ \text{(dis/s)} = \frac{Wf'Y'}{3.7 \times 10^7}\,(1-e^{-\lambda_R t})\ \text{(mCi)}. \qquad (11.2.3)$$

In the case of activation of materials in the accelerator structure or the tungsten converter target, many radioactive products of differing half lives are produced. The realization of saturation activity for all these components is more complicated than in the case of air activation, which contains only short half life positron emitters (half lives < 21 min). One may assume that saturation is approximately reached when the operation time is about 3x the half life of the radionuclide being formed. For the activated components of the Storage Ring, the assumption that saturation is reached is reasonable for all but the very long half life products because of the almost continuous operation of the ring throughout the year. For the other accelerator components, for which the operational time is generally assumed to be only a fraction of continuous (usually taken as ~ 10%), assuming that saturation activity is reached will be conservative, except for those radionuclides which have very short half lives but do not contribute to the residual radioactivity.

To estimate the residual radioactivity in the various components of the accelerator system, the simplifying and conservative assumption that saturation is realized was made. The saturation activity, A_S, obtained from equation 11.2.3, is

$$A_S = \frac{Wf'Y'}{3.7 \times 10^7} \qquad \text{(mCi)}. \qquad (11.2.4)$$

For each of the systems of the APS, a particular material, which represents the most likely material to be activated if struck by the particle beam, was chosen. The residual activity for

this material was computed assuming that only those radionuclides, which would continue to be part of the residual radioactivity following a one year shutdown, were relevant. The residual radioactivity present at the time of shutdown (A_S) was computed for the longer-lived radionuclides without correcting for any decay during the assumed 1 year period of shutdown. The results for the various accelerator components are summarized in Table 11.6.1 (Section 11.6).

11.3 Residual Radioactivity of the Electron Linac, Positron Linac, PAR, and Injector Region

For these systems, the main component which will be activated was assumed to be copper. The relevant activities which contribute to the residual radioactivity are Co-60 and Ni-63. Assuming the power losses for the electron and positron linacs indicated in Table 5.2.1, and adding an additional 5.7 W lost in the beam compression system to the loss in the positron linac, and adjusting these losses for 10%operational time, the computed residual radioactivity for the e^- linac is 26.7 mCi of Co-60 and 11.9 mCi of Ni-63, and that of the e^+ linac is 6.43 mCi of Co-60 and 2.87 mCi of Ni-63. Because the loss rate in the PAR and Injector are assumed to be the same (Sections 6.0 and 7.2), the residual radioactivity in each of these components is 2.7 mCi of C0-60 and 1.21 mCi of Ni-63.

11.4 Residual Radioactivity of the Converter Target

The target material is tungsten (Z = 74) which has four isotopes which can be activated: W-182 (F = 0.264), W-183 (F = 0.144), W-184 (F = 0.306), W-186 (F = 0.284). Only W-182 and W-183 contribute relevant long-lived radionuclides which constitute residual radioactivity. These components are W-181 and Ta-182. Adjusting the loss rate from Table 5.2.1 for the assumed 10% operational time, the computed saturation activity of the target at the time of shutdown for these radionuclides is 340 mCi of W-181 (half life = 140 d) and 185.2 mCi of Ta-182 (half life = 115.1 d). Since the target can be easily removed, put into a shielded container and disposed of following a shutdown, it does not contribute to the residual radioactivity of the accelerator structure.

11.5 Residual Radioactivity of the Booster Synchrotron and the Extraction Region

Iron (Z = 27), present in the steel vacuum chamber, was assumed to be the important material for activation in the synchrotron system. Iron has four isotopes which can contribute to the activation: Fe-54 (F = 0.0584), Fe-56 (F = .9168), Fe-57 (F = 0.0217), Fe-58 (F = 0.0031). From the standpoint of residual radioactivity, the radionuclides of interest are Mn-54 (half life = 303 d) and Fe-55 (half life = 2.6 y). Both of these products are formed in Fe-56, 0.957 of the total activation being Fe-55, the rest is Mn-54. Of the other products which are

formed, all have half lives < 84 d and will essentially decay out in about 1 year. Using the conservative estimate that 2% of the beam is uniformly lost around the circumference, and adjusting for 10% operational time, the average power loss in the synchrotron is 0.16 W. This gives residual radioactivity of 2.02 mCi of Fe-55 and 0.09 mCi of Mn-54 in the synchrotron. Taking the total power available at the Extraction Region (Section 7.5), making the conservative assumption of 50% loss, and adjusting for 10% operational time, the average power loss in the Extraction Region is taken as 4.03 W (i.e. 80.6/2 x 0.1). The estimated activities are 50.9 mCi of Fe-55 and 2.29 mCi of Mn-54.

11.6 Residual Radioactivity of the Storage Ring

Aluminum (Z = 13) is assumed to be the important material in the Storage Ring since loss of positrons would take place in the vacuum chamber walls. The radionuclides of interest are Al-26 (half life = 7.4×10^5 y) and Na-22 (half life = 2.62 y), which are both formed from Al-27 (F = 1). The majority of the activity 0.972 is Al-26. In the case of Al-26, the half life is so long relative to the irradiation time that assuming saturation of the Al-26 activity is extremely conservative. The average power loss in the Storage Ring is taken as 0.136 W (Section 10.2.3). The estimated residual radioactivity of these components is 1.18 mCi of Al-26 and 0.034 mCi of Na-22. Since these radionuclides would be spread around the entire circumference of the ring, one would not expect a significant residual radiation field from these distributed products.

Table 11.6.1 summarizes the estimates of the initial residual radioactivity in the APS system components for those radionuclides which would constitute the major portion remaining after a 1 year shutdown.

With the exception of the tungsten target, which has a combined residual activity of 525 mCi, the maximum total residual radioactivity in the machine components is expected to be only about 112 mCi at shutdown.

11.7 Radioactivation of Cooling Water

Activation of the cooling water for the Converter Target and for the magnet cooling water in the APS System may be estimated in a manner similar to that for radioactivation in air. The primary reactions leading to activation products are bremsstrahlung interactions in O-16. In Table XXXIIb of Swanson (SWA 79), the saturation activities of photoactivation products

Table 11.6.1 - Initial Activity at Shutdown of the Important Radionuclides Contributing to the Residual Radiation

Component	Assumed Average Power Loss, W	Main Act. Matl.	Activity, mCi							
			55 Fe	54 Mn	60 Co	63 Ni	182 Ta	181 W	22 Na	26 Al
e^- Linac	2.56	Cu	-	-	26.7	11.9	-	-	-	-
Converter	46	W	-	-	-	-	185.2	340	-	-
e^+ Linac	0.616	Cu	-	-	6.43	2.87	-	-	-	-
PAR	0.259	Cu	-	-	2.70	1.21	-	-	-	-
Injection Region	0.259	Cu	-	-	2.70	1.21	-	-	-	-
Synchrotron	0.16	Fe	2.02	0.09	-	-	-	-	-	-
Extraction Region	4.03	Fe	50.9	2.29	-	-	-	-	-	-
Storage Ring	0.136	Al	-	-	-	-	-	-	0.034	1.18
	Totals		52.92	2.38	38.53	17.19	185.2	340	0.034	1.18

formed in O-16 in water are given. This table assumes that 100% of the energy is absorbed in the cooling water; whereas, a more acceptable estimate is that only 10% of this energy will be absorbed in the cooling water (SWA 79). This is reasonable since a fraction of the energy is absorbed in the accelerator components (assumed to be 0.5), and a fraction of the remaining energy escapes into the tunnels and is absorbed in air, and some energy will be absorbed in the steel of the magnets before reaching the water cooling channels.

The most important of the radionuclides which are produced is O-15. Other products which are formed include C-11 (4.4% of the O-15 production), H-3 (at saturation, 2.2% of O-15 production), N-13 (about 1% of the O-15 production), and Be-7 (0.44% of the O-15 production).

The production (yield) of O-15 may be estimated with the use of equation 11.2.1, using an effective Z of 3.34 for water, according to Schaeffer (SCH 73), and assuming that the abundance of O-16 is 100%:

$$Y' = 1.21 \times 10^{8} (1) (3.34)^{0.66} = 2.68 \times 10^{8} \text{ atoms/Ws.}$$

Because the half life of O-15 is so short (2.05 min), it will reach equilibrium (saturation) rapidly. The saturation activity of O-15, under static conditions, will be given by modified equation 10.2.3, in which f' is taken as 0.1:

$$A = \frac{Wf'Y'(1 - e^{-x/\lambda})}{3.7 \times 10^{7}} \quad \text{(mCi)}, \qquad (11.7.1)$$

in which x is the average path length through the water channel in m (assumed to be 0.02 m) and λ is the average attenuation length in m (taken as 0.5 m for the x rays that will penetrate to the water channels). Supplying values for constants in the equation, one arrives at

$$A = \frac{W(0.1)(2.68 \times 10^{8})(1 - e^{-0.02/0.5})}{3.7 \times 10^{7}} = 2.84 \times 10^{-2} W.$$

In a closed, circulating coolant system, as is planned for the APS facilities, the build-up of a given radionuclide may be estimated from the following modified expression (HOF 88, STA 89):

$$\frac{dN}{dt} = A - \lambda_R N - \frac{FRN}{V} + \frac{fFRN}{V} = A - [\lambda_R + \frac{FR}{V}(1-f)]N,$$

in which λ_R is the radioactive decay constant, FR/V is the rate of water turnover (the water flow rate, FR, divided by the irradiated volume, V), and f is the fraction of the radioactivity remaining after a complete circuit of the closed system ($f = e^{-\lambda R \tau}$, in which τ is the circuit transit time). The solution of the above for N = 0 when t = 0, is

$$N = \frac{A}{\lambda_R + \frac{FR}{V}(1-f)} (1 - e^{-[\lambda_R + \frac{FR}{V}(1-f)]t}) \qquad (11.7.2)$$

and $Act = \lambda_R N$.

For an assumed conservative transit time of 10 min. and a turnover rate of 0.08 min^{-1}, using the average power loss W in each of the system components (Table 11.6.1) to estimate the radioactivation, and assuming that saturation is reached for each of the relevant radionuclides, the estimated total saturation activities of the various radionuclides formed in the coolant water are shown in Table 11.7.1. Note that for the case of H-3 (half life 12.3 y),

the assumption of saturation activity will be quite conservative. From the estimates in the Table, any release of the radioactive gases O-15, C-11 as carbon dioxide and H-3 as water vapor into air will not contribute significantly to any on-site or off-site doses because of the small production rates.

Assuming some of the cooling water is accidentally discharged from the 250,000 gal. closed system, and all of the radionuclides in Table 11.7.1 were included, the estimated average release concentration, C_{H_2O}, in the discharge would be

$$C_{H_2O} = \frac{1.34 \times 10^{3}\ \mu Ci}{2.5 \times 10^{5}\ (gal)\, 3.785\ (l/gal)\, 10^{3}\ (cc/l)} = 1.4 \times 10^{-6}\ \mu Ci/cc.$$

This concentration is well below the discharge limits stated in DOE Order 5400.5 (DOE 88a, Chapter III) for any of the radionuclides in Table 11.7.1.

Table 11.7.1 - Estimated Saturation Activity of Radionuclides in the Cooling Water of APS Components

Component	Assumed Avg. Power Loss, W	Activity, mCi				
		^{15}O	^{11}C	^{3}H	^{13}N	^{7}Be
e^- Linac	2.56	5.91E-02	1.91E-03	1.58E-03	4.61E-04	3.15E-04
Converter	46	1.06	3.43E-02	2.84E-02	8.28E-03	5.66E-03
e^+ Linac	0.616	1.42E-02	4.59E-04	3.80E-04	1.11E-04	7.58E-05
PAR	0.259	5.98E-03	1.93E-04	1.60E-04	4.66E-05	3.19E-05
Injection Region	0.259	5.98E-03	1.93E-04	1.60E-04	4.66E-05	3.19E-05
Synchrotron	0.16	3.70E-03	1.19E-04	9.87E-05	2.88E-05	1.97E-05
Extraction Region	4.03	9.31E-02	3.00E-03	2.49E-03	7.25E-04	4.96E-04
Storage Ring	0.136	3.14E-03	1.01E-04	8.39E-05	2.45E-05	1.67E-05
	Total	1.25	4.03E-02	3.34E-02	9.72E-03	6.65E-03

11.8 Radioactivation of Soil

The potential for soil activation is limited, since the main component (bremsstrahlung), which is responsible for the majority of activation in the accelerator components, proceeds mainly in the forward direction thereby being absorbed in the accelerator components; whereas, the soil berms are at very large angles (almost at right angles) to the direction of bremsstrahlung emission. The giant resonance neutrons and the high energy neutron components may be assumed to be approximately isotropic and could potentially produce activation in the soil after passing through the shielding. However, the activation would be a second-order reaction (i.e. bremsstrahlung interacts with matter to form both GRN and HEN, which then interact with nuclei to produce radionuclides). Since these processes involve another interaction probability (cross section), the yield of products is expected to be much less than that of the activated acccelerator components which are first-order reactions so that the magnitude of any activation of soil will be insignificant.

12.0 Bremsstrahlung Doses Produced in Vacuum Chamber Residual Gas

12.1 Introduction

Loss of positrons by interaction with the atoms of the residual gas in the vacuum chamber represents an additional continuing source of bremsstrahlung production. For interactions occurring in an insertion device, all of the bremsstrahlung which is produced proceeds directly down the photon beam line and out through the shielding without attenuation. For interactions occurring in a bending magnet section of the vacuum chamber, only a portion of the path through the bending magnet will contribute to the source of the bremsstrahlung which proceeds down the photon beam line. Both of these components are generally of sufficient magnitude to require shielding in the direct path of the photon beam to reduce the radiation dose to acceptable levels.

12.2 Bremsstrahlung Dose Estimates for an Insertion Device

To achieve a beam lifetime of 10 h or more, it is necessary that the beam-on operating pressure in the storage ring be 1 nTorr or less (ANL 87). For this determination, the value of 1 nTorr (10^{-9}mm) is assumed. The differential cross section, $\sigma(E_o,k)dk$, for producing a photon in the energy range dk about k, by a positron with total energy E_o is given by (SEG 53, ICR 78, RIN 82, BAN 89):

$$\sigma(E_o,k) = \frac{4(Z)(Z+1)}{137} r_e^2 dk/k[(1+(E/E_o)^2 - 2/3(E/E_o)\ln(183Z^{-1/3}) + E/9E_o], \qquad (12.1)$$

in which Z is the atomic number of the absorbing material, $E = E_0 - k$, and $r_e = 2.82 \times 10^{-13}$ cm. This expression assumes that screening by the electric field of the atomic electrons is negligible (TSA 66, TSA 74, RIN 82), which gives an incorrect result at the high end of the bremsstrahlung spectra ($k/E_0 > 0.98$), where the number of photons drops off more rapidly than the 1/k spectrum which the "thin target" equation 12.1 predicts. According to Tsai (TSA 74), ignoring the last term in the brackets results in only a few per cent error at the low energy end of the spectrum. Inserting values into the above expression and dropping the term $E/9E_0$, the expression becomes:

$$\sigma(E_0, k)\,dk = 2.32 \times 10^{-27} Z(Z+1)\,dk/k\,[4/3 - 4/3(k/E_0) + (k/E_0)^2] \times \ln(183/Z^{1/3}) \quad (cm^2/atom\ e^+) \qquad (12.2)$$

In passing through a thickness dx (cm) of a material containing N (atoms/cc), the number of photons, produced by a beam of I (e^+/s), between energy k and k + dk, will be

$$dN_k = NI\sigma(E_0, k)\,dk\,dx \qquad (12.3)$$

in which

$$N = \frac{6.023 \times 10^{23}}{2.24 \times 10^4} \frac{(P)}{(760)} \frac{(273)}{(T)}, \qquad (12.4)$$

and P is the pressure in Torr and T is the temperature in ^oK (273 + T in ^oC). The fluence rate of photons (ph/cm^2s) is computed at a downstream distance of 30 m (the assumed minimum distance at which the photons leave the photon beam tube through a Be window). The bremsstrahlung beam will be confined to a cone of half angle

$$\theta = \frac{0.511}{7000} = 7.3 \times 10^{-5} \text{ radians.}$$

The surface area defined by the cone may be approximated by

$$A = \pi S^2 = \pi R^2 \theta^2 = \pi (3000)^2 (7.3 \times 10^{-5})^2 = 0.1507 \text{ cm}^2,$$

and the fluence rate $d\phi$ is

$$d\phi = \frac{dN_k}{0.1507} = \frac{NI\sigma(E_0, k)\,dk\,dx}{0.1507} \quad (ph/cm^2 s). \qquad (12.5)$$

Using equations 12.2, 12.3 and 12.4, and substituting values in equation 12.5 for P (= 10^{-9}mm), T (= 293 ^{o}K), dx(= 500 cm, the length of an ID), Z(= 7.26 for air) and I(= 100 mA = 6.25 x $10^{17}e^{+}$/s), one arrives at

$$d\phi = 4.326 \times 10^{4}\ dk/k[4/3-4k/3E_o+(k/E_o)^2]\ (ph/cm^2 s)\ . \quad (12.6)$$

When the right side of equation 12.6 is multiplied by a dose equivalent conversion factor $\dot{H}(k)$, which is a function of the photon energy k, and integrated from k_{min} to k_{max}, one arrives at the total dose rate produced by the bremsstrahlung beam:

$$\dot{H} = 4.326x10^{4}\int_{k_{min}}^{k_{max}} [4/3-4k/3E_o+(k/E_o)^2]\dot{H}(k)\,dk/k \quad (mrem/h)\ . \quad (12.7)$$

Utilizing dose equivalent conversion factors computed by Rogers (ROG 84) and values of k_{max} and k_{min} of $0.98E_o$ = 6860 MeV and 0.01 MeV, respectively, the final expression becomes

$$\dot{H} = 4.326 \times 10^{4}\int_{0.01}^{6860} [4/3 - 4k/21000 + k^2/(7000)^2]\dot{H}(k)\,dK/k$$

and $\dot{H}$ = 7.76 rem/h for 100 mA operation and 23.28 rem/h for 300 mA operation. These results should be conservative because Rogers' conversion factors are for a broad parallel beam of radiation incident on a slab; whereas in our case, the photon beam is confined to a very narrow cone. His results reflect the effect of radiation from the wide beam being scattered to the dose point thus increasing the contribution at the dose point.

In applying Rogers' dose conversion factors, the maximum dose factors in a 30 cm thick tissue slab were not used since it was felt that the results would give an inflated value for the expected radiation field which would need attenuation by the lead plug in the FOE. The maximum dose factors at a depth of 6 cm in tissue were used (which corresponds roughly to an irradiated tissue volume of 1 cc for the beam at 30 m) to arrive at an estimate of the dose equivalent rate. Use of factors for the maximum dose would yield values about a factor of 4 higher than those quoted above.

To reduce these radiation fields to 0.5 mrem/h would require about 24 cm of lead in direct line with the photon beam. Since more lead than this is provided in the First Optics Enclosure (FOE) beam stop, the radiation field will be sufficiently attenuated.

12.3 Bremsstrahlung Dose Rate Estimate for a Bending Magnet

In the case of a bending magnet, the total path which contributes to the bremsstrahlung that goes down a photon beam line is limited by the acceptance angle in the collimating devices.

Assuming that the acceptance angle is 2 mradians and the positron orbit radius is 175.7 m, the arc length which contributes to the bremsstrahlung will be about 35 cm. This path length represents only 0.07 of the path length in an insertion device so that scaling the dose rate gives an estimated 543 mrem/h. This result also overestimates the dose rate since the bremsstrahlung from an ID will be contained in a very narrow cone whereas the bremsstrahlung from a BM will be in a relatively wide strip, or fan, of radiation. Nevertheless, the radiation dose rate is still significant enough to require some lead shielding at the end of the photon beam line.

12.4 Bremsstrahlung Dose Resulting from Loss of Vacuum

In Sections 12.2 and 12.3, the dose rates resulting from continuing losses in an ID and a BM were estimated. In this section, an estimate of the bremsstrahlung dose which results from an instantaneous loss of vacuum in the system is estimated. Such a loss is not considered a credible incident, since there will be some elapsed time before the pressure will reach atmosphere but a dose estimate has been made to determine an upper bound for incidents which involve some loss of vacuum in the system.

Assuming that any loss of vacuum initiates shutdown mechanisms, the system will shut down in less than 50 turns. During each revolution, some of the positrons which interact will lose more energy than the bucket height (taken as 140 MeV) and will be lost from the orbit. The fraction of positrons which survive (F_{e+}) and continue to orbit may be estimated from

$$F_{e+} = \frac{\int_{.01}^{140} n(k)\,dk}{\int_{.01}^{6999.489} n(k)\,dk} = \frac{12.703}{17.112} = 0.7423, \qquad (12.8)$$

in which $n(k) = 1/k[4/3 - 4/3(k/E_0) + (k/E_0)^2]$.

For each succeeding revolution, the same fraction will survive so that the total contribution will be given by

$$\sum_{n=0}^{\infty} F_{e+}^{n} = \frac{1}{1-F_{e+}} = \frac{1}{1-0.7423} = 3.88. \qquad (12.9)$$

In effect then, each positron is counted 3.88 times. For an ID, at atmospheric pressure and 20 ^{o}C, the path length of 500 cm represents 500 (cm) 1.205 x 10^{-3} (g/cc)/37.1 (g/cm^2) = 0.0162 radiation lengths, in which 37.1 g/cm^2 is the radiation length (RL) in air (ICR 78). The total path through the ID for each positron may be expressed as 3.88 (0.0162) = 0.0629 RL.

During normal operations while the beam circulates, the total path length for the circulating beam in an ID is given by

$$0.0162(10^{-9}/760\ \text{RL/rev})(3\text{x}10^{8}/1104\ \text{rev/s})(3600\ \text{s/h})$$
$$= 2.084 \times 10^{-5}\ \text{RL/h}.$$

For a circulating current of 100 mA, the bremsstrahlung dose rate for the above conditions is 7.76 rem/h. An estimate of the dose in the case of a loss of vacuum incident can be found from

$$\frac{H}{0.0629} = \frac{7.76}{2.084 \times 10^{-5}}$$
$$H = 2.34 \times 10^{4}\ \text{rem}.$$

This dose is less than that estimated for the maximum credible incident (Section 9.5), by more than an order of magnitude, so the dose estimate will be correspondingly less.

REFERENCES

ABR 64 M. Abramowitz and I. A. Stegun, Editors, Handbook of Mathematical Functions, US National Bureau of Standards, Appl. Math. Series, Vol. 55 (1964).

ACG 88 American Conference of Governmental Industrial Hygienists, Threshold Limit Values and Biological Exposure Indices for 1988-89, ACGIH, Cincinnati, OH (1988).

ALS 67 R. G. Alsmiller, Jr. and H. S. Moran, "Electron-photon Cascade Calculations and Neutron Yields from Electrons in Thick Targets," Nuc. Inst. Meth., 48, 109 (1967).

ALS 67a R. G. Alsmiller, Jr. and H. S. Moran, "Photoneutron Production from 34- and 100- MeV Electrons in Thick Uranium Targets," Nuc. Inst. Meth., 51, 339 (1967).

ALS 70 R. G. Alsmiller, Jr. et al.,"The Energy Distribution of Photoneutrons Produced by 150 MeV Electrons in Thick Beryllium Targets," Nuc. Sci. Eng., 40, 365 (1970).

ALS 73 R. G. Alsmiller, Jr. and J. Barish, "Shielding Against the Neutrons Produced when 400-MeV Electrons are Incident on a Thick Copper Target," Particle Accelerators, 5, (1973), 155- 159.

ALS 81 R. G. Alsmiller, Jr. et al., "Skyshine at Neutron Energies < = 400 MeV," Part. Accel., 11, 131 (1981).

ANL 86 Argonne National Laboratory, "Characteristics of the Devices for the 6 GeV Synchrotron Source", ANL Report, Light Source Note, LS-52 (March 1986)

ANL 87 Argonne National Laboratory, 7 GeV Advanced Photon Source - Conceptual Design Report, Draft, ANL-87-15, ANL Report, April (1987).

BAN 89 S. Ban et al, "Estimation of Absorbed Dose Due to Gas Bremsstrahlung From Electron Storage Rings," Health Physics, 57, 407 (1989).

BAR 69 M. Barbier, Induced Radioactivity, John Wiley & Sons, Inc., New York, NY (1969).

BAT 65 G. Bathow, E. Freytag and K. Tesch, "Shielding Measurements on 4.8-GeV Bremsstrahlung," Nuc. Inst. Meth., 33, 261 (1965).

BAT 67 G. Bathow, E. Freytag and K. Tesch, "Measurements on 6.3 GeV Electromagnetic Cascades & Cascade Produced Neutrons, "Nuc. Phys., B2, 669 (1967).

BAT 70 G. Bathow, E. Freytag, M. Kobbeling, K. Tesch, and R. Kajikawa, "Measurement of Longitudinal and Lateral Development of Electromagnetic Cascades in Lead, Copper, and Aluminum at 6.0 GeV," Nuc. Phys., B20, 592 (1970).

BNL 82 K. Batchelor, Editor, National Synchrotron Light Source Safety Analysis Report, BNL 51584, Brookhaven National Laboratory, (July 1982).

BRO 78 A. Brodsky, Editor, Handbook of Radiation Measurement and Protection, Vol. 1: Physical Science and Engineering Data, CRC Press, Inc., W. Palm Beach, FL(1978).

CRO 88 E. Crosbie, "The Positron Injection Process for the 7-GeV Advanced Photon Source," ANL Report, Light Source Note LS-118, (April, 1988).

DIN 77 H. Dinter and K. Tesch," Dose and Shielding Parameters of Electron-Photon Stray Radiation from a High Energy Electron Beam," Nuc. Inst. Meth., 143, 349 (1977).

DIN 82 H. Dinter et al, "Absorbed Radiation Dose Due to Synchrotron Radiation in the Storage Ring PETRA," Nuc. Inst. Meth., 200, 437 (1982).

DIN 85 H. Dinter, "Absorbed Doses Due to Synchrotron Radiation in the Tunnel of the Storage Ring PETRA," Nuc. Inst. Meth., A239, 597 (1985).

DOE 88 Department of Energy, Radiation Protection for Occupational Workers, DOE Order 5480.11, Figure 3, Section 9.f.(5),Washington, DC (Dec. 21, 1988).

DOE 88a Department of Energy, Radiation Protection of the Public and the Environment, DOE Order 5400.5, Washington, DC (Feb. 2, 1990).

FAS 84 A. Fasso, K. Goebel, M. Hoefert, G. Rau, H. Schonbacher, G. R. Stevenson, A. H. Sullivan, W. P. Swanson, and J. W. N. Tuyn, Radiation Problems in the Design of the Large Electron-Positron Collider (LEP), CERN 84-02 (5 March 1984).

GOD 68 R. P. Godwin, "Synchrotron Radiation as a Light Source," Springer Tracts in Modern Physics, Vol 51, Springer, Berlin/New York (1968).

GOE 81 K. Goebel, Editor, The Radiological Impact of the LEP Project on the Environment, CERN 81-08 (20 July 1981).

GOL 76 P. J. Gollon, "Production of Radioactivity by Particle Accelerators," IEEE Trans. Nuc. Sci., NS-23, No. 4, 1395 (1976).

GRE 76 G. K. Green, Spectra and Optics of Synchrotron Radiation, BNL 50522, Brookhaven National Laboratory, (April 1976).

HOF 88 M. Hofert and P. Sievers, "Radiological Problems at High Energy, High Intensity Electron-Positron Converters," in End Station Radiation Control Workshop, TN-0095, CEBAF (1988).

HUB 69 J. H. Hubbell, "Photon Cross Sections, Attenuation Coefficients, and Energy Absorption Coefficients From 10 keV to 100 GeV, NSRDS-NBS 29, National Bureau of Standards, August (1969).

HUB 80 J. H. Hubbell, "Photon Mass Attenuation and Energy- absorption Coefficients from 1 keV to 20 MeV," Int. J. Appl. Radiat. Isot., 33, 1269 (1982).

ICP 21 International Commission on Radiation Protection, Protection Against Ionizing Radiation from External Sources, ICRP Publication 21, (1971).

ICR 78 International Commission on Radiation Units and Measurements, Basic Aspects of High Energy Particle Interactions and Radiation Dosimetry, ICRU Report 28, December (1978).

JAC 81 D. F. Jackson and D. J. Hawkes, "X-Ray Attenuation Coefficients of Elements and Mixtures," Phys. Repts., 70, No. 3, 169 (1981).

JEN 79 T. M. Jenkins, "Neutron and Photon Measurements Through Concrete from a 15-GeV Electron Beam on a Target - Comparison with Models and Calculations," Nuc. Inst. Meth., 159, 265 (1979).

KIM 86 S. H. Kim, "Distribution of the Bending Magnet Radiation, "ANL Report, Light Source Note LS-54, (Jan. 1986).

KNO 88 M. J. Knott and H. J. Moe, "Dose Estimates for the Heavy Concrete Ratchet Wall Configuration," ANL Report, Light Source Note LS-117, (September 1988).

KOS 80 V. O. Kostroun, Simple Numerical Evaluation of Modified Bessel Functions K_v (x) of Fractional Order and the Integral $\int_x^\infty K_v$ (n)dn," Nuc. Inst. Meth., 172, 371 (1980).

KSO 82 T. Kosako and T. Nakamura, "Air Activation by an Electron Synchrotron," Health Phys., 43, 3 (1982).

LAD 68 M. Ladu et al., "A Contribution to the Skyshine Study," Inst. Meth., 62, 51 (1968).

MOE 87 H. J. Moe, "Radiological Impacts from Operation of Argonne Synchrotron X-ray Source," ANL Report, Light Source Note LS-84 (March 1987).

MOE 87a H. J. Moe, "Shielding Estimates for the Advanced Photon Source," ANL Report, Light Source Note LS-90 (April 1987).

MOE 88 H. J. Moe, "Recalculation of Shielding for the Addition of a PAR," ANL Report, Light Source Note LS-116 (August 1988).

MOE 89 H. J. Moe, "Dose Estimates for the 1104 m APS Storage Ring," ANL Report, Light Source Note LS-139 (June 1989).

NAK 81 T. Nakamura and T. Kosako, "A Systematic Study on the Neutron Skyshine from Nuclear Facilities," Nuc. Sci. Eng., 77, 168 (1981).

NCR 77 NCRP, Radiation Protection Design Guidelines for 0.1-100 MeV Particle Accelerator Facilities, Report No. 51, NCRP, Washington, DC (1977).

NEL 68 W. R. Nelson, "The Shielding of Muons Around High Energy Electron Accelerators: Theory and Measurement," Nuc. Inst. Meth., 66, (1968), 293-303.

NEL 74 W. R. Nelson and K. R. Kase, "Muon Shielding Around High- Energy Electron Accelerators, Part I," Nuc. Inst. Meth., 120, 401 (1974).

NEL 74a W. R. Nelson et al., "Muon Shielding Around High-Energy Electron Accelerators, Part II," Nuc. Inst. Meth., 120, 413 (1974).

NIE 82 J. Nieto et al., "Ozone Hazards Incurred in Gamma-Plant Operation," Health Physics, 42, 861 (1982).

PAT 73 H. Wade Patterson and Ralph H. Thomas, Accelerator Health Physics, Academic Press, New York, NY (1973).

POO 80 J. H. Poole, "Shielding for the SRS Storage Ring," Nuc. Inst. Meth., 169, 33 (1980).

RIN 67 A. Rindi and S. Charalambus, "Airborne Radioactivity Produced at High-Energy Accelerators," Nuc. Inst. Meth.,47, 227 (1967).

RIN 75 A. Rindi and R. H. Thomas, "Skyshine - A Paper Tiger?," Particle Accelerators, 7 , (1975), 23-39.

RIN 82 A. Rindi, "Gas Bremsstrahlung From Electron Storage Rings," Health Physics, 42, 187 (1982).

ROG 84 D. W. O. Rogers, "Fluence to Dose Equivalent Conversion Factors Calculated With EGS3 for Electrons From 100 keV to 20 GeV and Photons From 11 keV to 20 GeV," Health Physics, 46, 891 (1984).

SAB 73 A. B. Sabersky, "The Geometry and Optics of Synchrotron Radiation," Part. Accel., 5, 199 (1973).

SCH 73 N. M. Schaeffer, Editor, Reactor Shielding For Nuclear Engineers, NTIS, Springfield, VA (1973).

SCW 49 J. Schwinger, "On the Classical Radiation of Accelerated Electrons," Phys. Rev. 75, 1912 (1949).

SCW 73 J. Schwinger, "Classical Radiation of Accelerated Electrons II. A Quantum Viewpoint," Phys. Rev., D, 7, No.6, 1696 (1973). Appendix gives corrections to 1949 paper.

SEG 53 E. Segre, Editor, Experimental Nuclear Physics, Volume 1, Part II. Passage of Radiations Through Matter by H. Bethe and J. Ashkin, John Wiley & Sons, New York, NY (1953).

SHE 85 G. K. Shenoy and P. J. Viccaro, "Energy and Angular Distributions of Radiation Power from Bending Magnet and Wiggler Sources at a 6 GeV Ring," ANL Report, Light Source Note LS-42, (Sept. 1985).

SHU 69 K. Shure et al., "Neutron Dose Rate Attenuation by Iron and Lead, Nuc. Sci. Eng., 35, 371 (1969).

SLA 68 D. H. Slade, Editor, Meteorology and Atomic Energy 1968, TID-24190, US Atomic Energy Commission (1968).

STA 89 G. Stapleton, "Radiolysis and Radioactivation of Beam Dump Cooling Water," in Review of the Radiological Aspects of the Conceptual Design Report for the CEBAF End Stations and Switchyard, TN-0174, CEBAF (1989).

STE 84 G. R. Stevenson and R. H. Thomas, "A Simple Procedure for the Estimation of Neutron Skyshine from Proton Accelerators," Health Physics, 46, 115 (1984).

SUL 82 A. H. Sullivan, "The Shielding of an Electron-Positron Injector," CERN, LEP Note 354 (1982).

SWA 79 W. P. Swanson, Radiological Safety Aspects of the Operation of Electron Linear Accelerators, Technical Report Series No. 188, IAEA, Vienna, (1979), and references therein.

SWA 79a W. P. Swanson, "Improved Calculation of Photoneutron Yields Released by Incident Electrons," Health Phys., 37, 347 (1979).

SWA 85 W. P. Swanson, P. M. DeLuca, R. A. Otte, and S. W. Schilthelm, "Aladdin Upgrade Design Study: Shielding," University of Wisconsin, (1985).

TAZ 84 S. Tazzari, "Synchrotron Radiation Distribution Along the Vacuum Chamber Vacuum Considerations, ESRP-IRM-32/84, ESRP Internal Report (April 1984).

TES 79 K. Tesch, "Data for Simple Estimates of Shielding Against Neutrons at Electron Accelerators," Particle Accelerators, 9, (979), 201-206.

TSA 66 Y. S. Tsai and Van Whitis, "Thick-Target Bremsstrahlung and Target Considerations for Secondary-Particle Production by Electrons," Phys. Rev., 149, 1248 (1966).

TSA 74 Y. S. Tsai, "Pair Production and Bremsstrahlung of Charged Leptons," Rev. Mod. Phys., 46, 815 (1974).

TUR 69 D. Bruce Turner, "Workbook of Atmospheric Dispersion Estimates," US Dept. of HEW,Public Health Serv.,Cincinnati, OH (1969).

WAT 48 G. N. Watson, Theory of Bessel Functions, The Macmillan Company, New York, NY (1948).

WEI 87 C. Weilandics et al, "Ozone Production at the National Synchrotron Light Source," BNL 39351, Brookhaven National Laboratory, (January 1987).

WYC 71 J. M. Wyckoff et al., "Dose Versus Angle and Depth Produced by 20 to 100 MeV Electrons Incident on Thick Targets," Proc. Int. Cong. on Protection Against Accelerator and Space Radiation,CERN 71-16, Geneva (1971).

ADDENDUM

REVIEW OF THE RADIAL RATCHET WALL SHIELDING

1.0 Introduction

In the previous computations of the necessary shielding for the APS Storage Ring, reviewed in LS-141 (MOE 90), the assumption was made that the shielding wall would be circular and run parallel to the positron orbit. With this configuration, the peak forward intensity of the bremsstrahlung for an assumed point loss would be effectively shielded due to the increased shielding thickness caused by the slant penetration of the bremsstrahlung at small angles with respect to the shield thickness. The assumed geometry of the circular arrangement is shown in Figure A1.

With the use of a ratchet-type shield wall; however, there is a possibility that the forward directed intensity of the bremsstrahlung will intercept the shield at almost normal incidence in the portion of the ratchet wall which extends radially. For this type of incidence, no enhancement of the shield thickness is realized. In the shield design of the APS, the situation just described has been somewhat taken into account by the use of an 1.5' by 1.5' Pb shield, centered around the axis of the photon beam line, in the radial sections of the ratchet wall. This Pb Shield is 25 cm thick, backed up by 55 cm of normal concrete (see Figure A2 - the Pb shield is shown as the cross-hatched region). Since this shielding does not cover the entire ratchet wall section, this study was undertaken to determine if any upstream-produced bremsstrahlung is able to intercept the section of the wall which is not covered by the Pb. Moreover, since such a situation would lead to increased dose and dose rates in the areas behind these shields, a further objective was to estimate any increase in dose, as well as any shielding modifications needed to assure the attainment of the design goals with respect to dose or dose rate limits.

The lattice arrangement of the storage ring components is not really circular, but consists of straight sections and bending magnet sections (which are circular). The actual geometry of the lattice components was used in this investigation to determine any potential upstream regions which could contribute additional bremsstrahlung radiation in the radial ratchet wall region.

2.0 Upstream Bremsstrahlung Contributions

For positron losses upstream of both the Bending Magnet (BM) and Insertion Device (ID) beamlines, regions were found for which the resulting intense, forward bremsstrahlung emitted in these regions will strike the radial section of the ratchet wall, without being

Geometry for Component Doses due to Continuous Loss around the Storage Ring

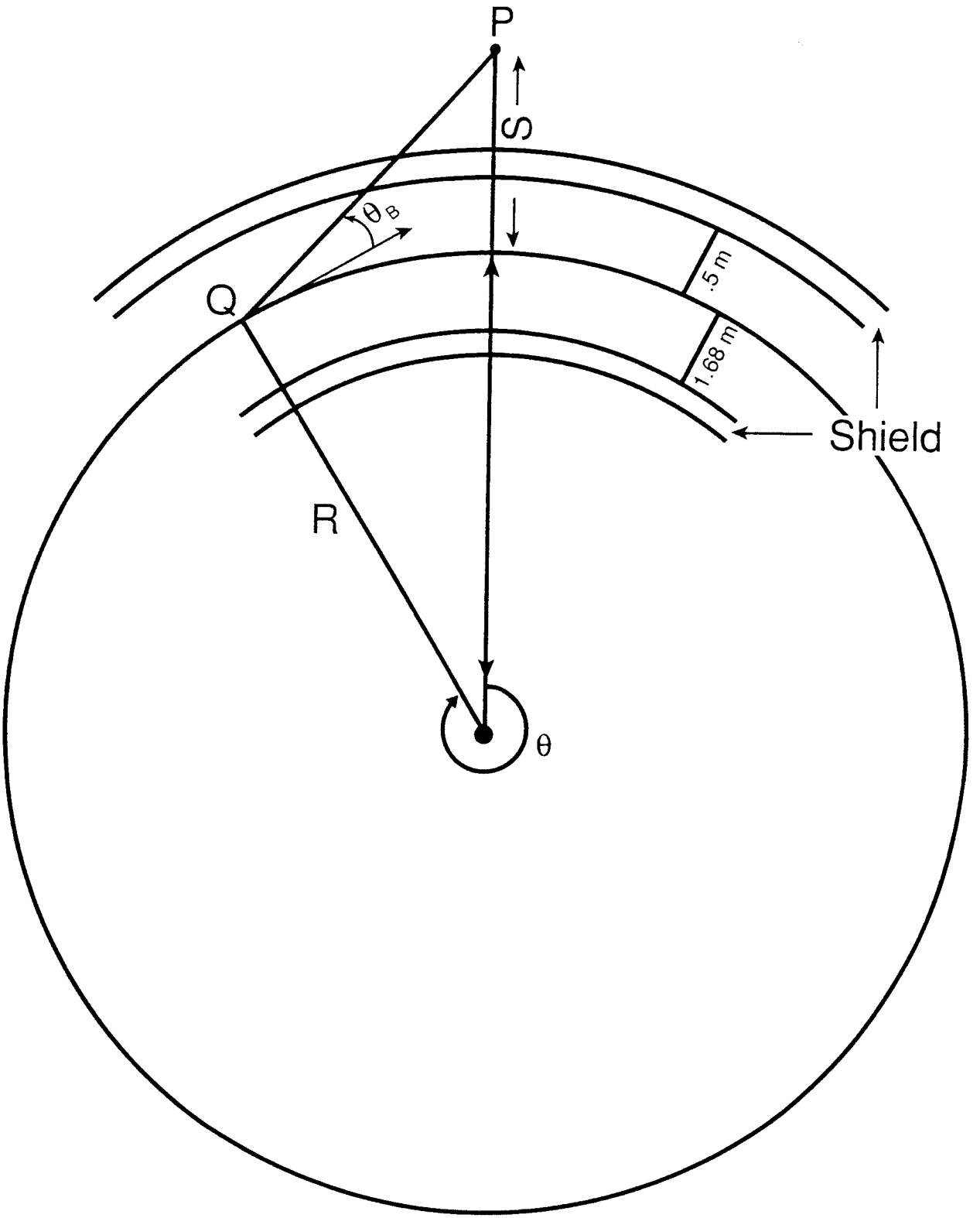

Figure A1. Geometry for Component Doses due to Continuous Loss around the Storage Ring.

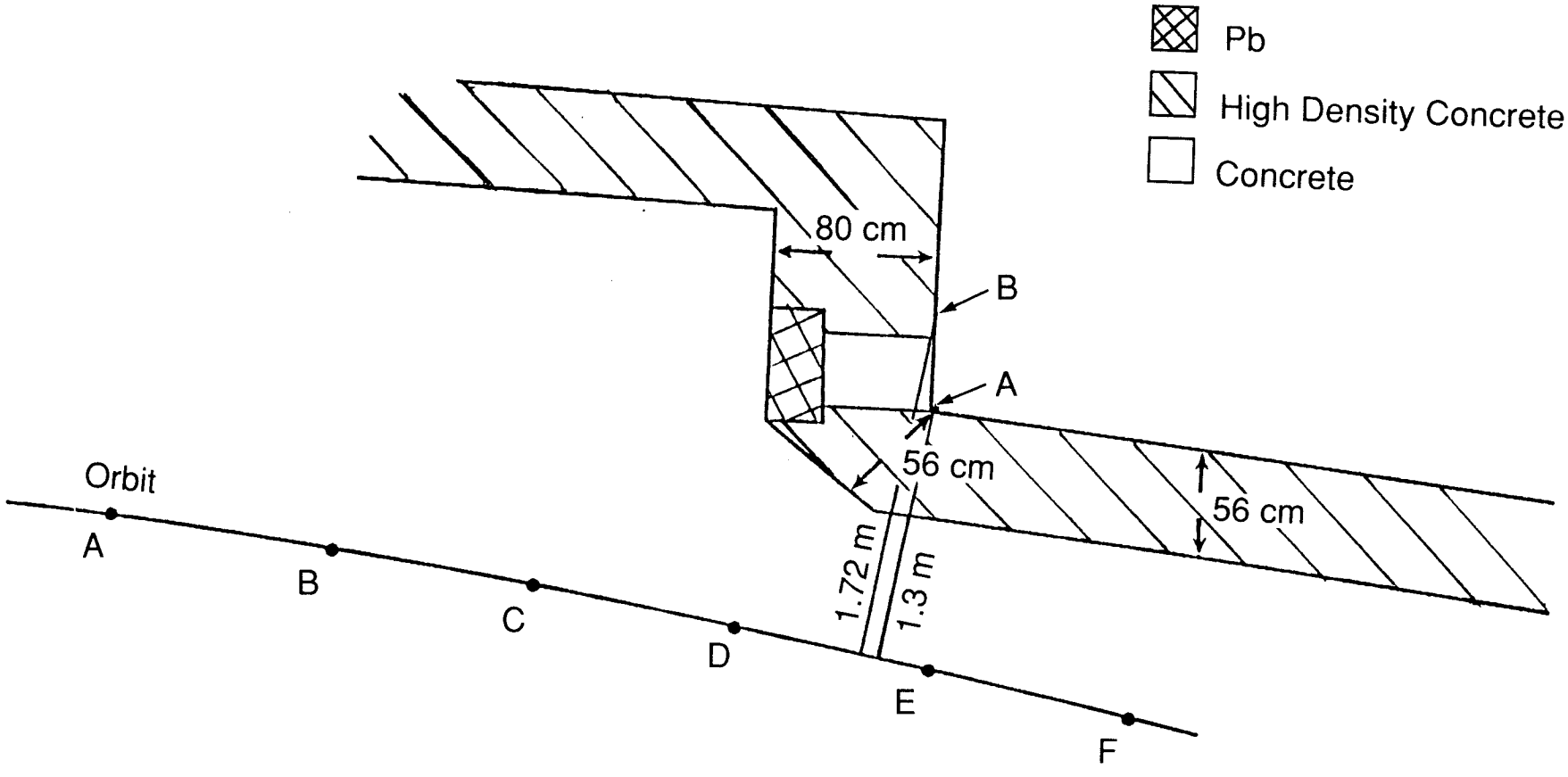

Figure A2. General ratchet-wall dimensions.

intercepted by the Pb shield in this wall. These regions are indicated in Figures A3 and A4, for the BM and ID beamlines, respectively. For an assumed point loss of the entire positron beam anywhere within these regions, the 0° bremsstrahlung beam will hit some part of the radial ratchet wall almost normally so that the shield will consist of only 80 cm of high density concrete and no lead. The shortest distance to the dose point is taken as 27.82 m (this corresponds to the worst case for the nearest assumed upstream point loss in the BM beamline - Figure A3), the computed dose contributions (for the case of 300 mA circulating current) are:

$$H_{BREM} = \frac{7728\,(J)\,8.3\,(mrem\ m^2/J\ MeV)\,7000\,(MeV)\ e^{-\frac{3.7(80)}{50}}}{(27.82)^2\ m^2} = 1558\ mrem$$

$$H_{GRN} = \frac{7728\,(0.63\ mrem\ m^2/J)\ e^{-\frac{3.7(80)}{45}}}{(1.1)^2\ m^2} = 5.6\ mrem$$

$$H_{HEN} = \frac{7728\,(0.075\ mrem\ m^2/J)\ e^{-\frac{3.7(80)}{125}}}{(1.1)^2\ m^2} = 44.9\ mrem$$

for a total dose of 1608 mrem, which is above the design goal of less than or = 100 mrem. For this computation, the neutrons are assumed to arise from bremsstrahlung interaction in the front of the ratchet wall so that the distance to the dose point is taken as only 1.1 m. On the assumption that the neutron dose component will not change much if additional Pb shielding is used to attenuate the bremsstrahlung, one may solve for the amount of Pb required to reduce the bremsstrahlung component contribution to 50 mrem:

$$50 = 1558\ e^{-\frac{11.34\ X}{25}}$$

$$X = 7.58\ cm\ of\ Pb \sim 8\ cm\ of\ Pb\ in\ the\ beam$$

direction. Since the contributing regions from the ID beamlines are at a greater distance from the ratchet wall than those for the BM lines, the above result will be conservative for the required shielding for the ID beam lines.

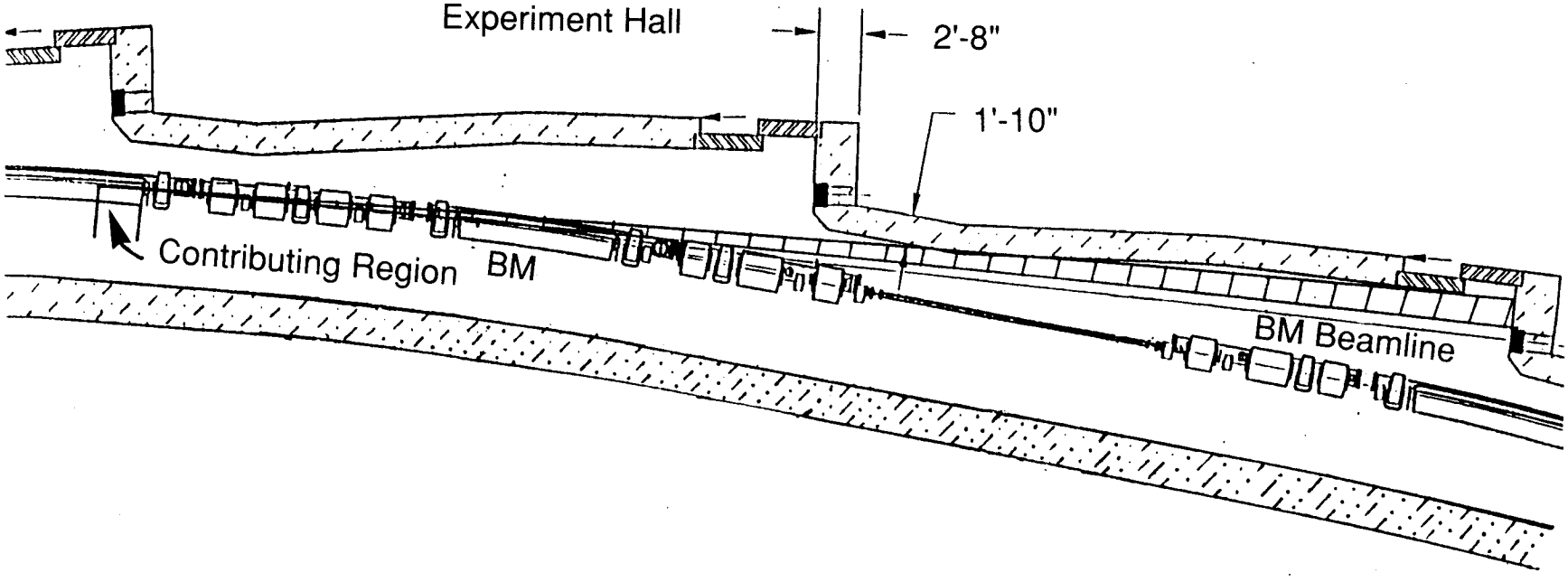

Figure A3. Upstream Bremsstrahlung Radiation Contribution from BM Beamline. Not intercepted by the Pb Stop or Ratchet Side Wall.

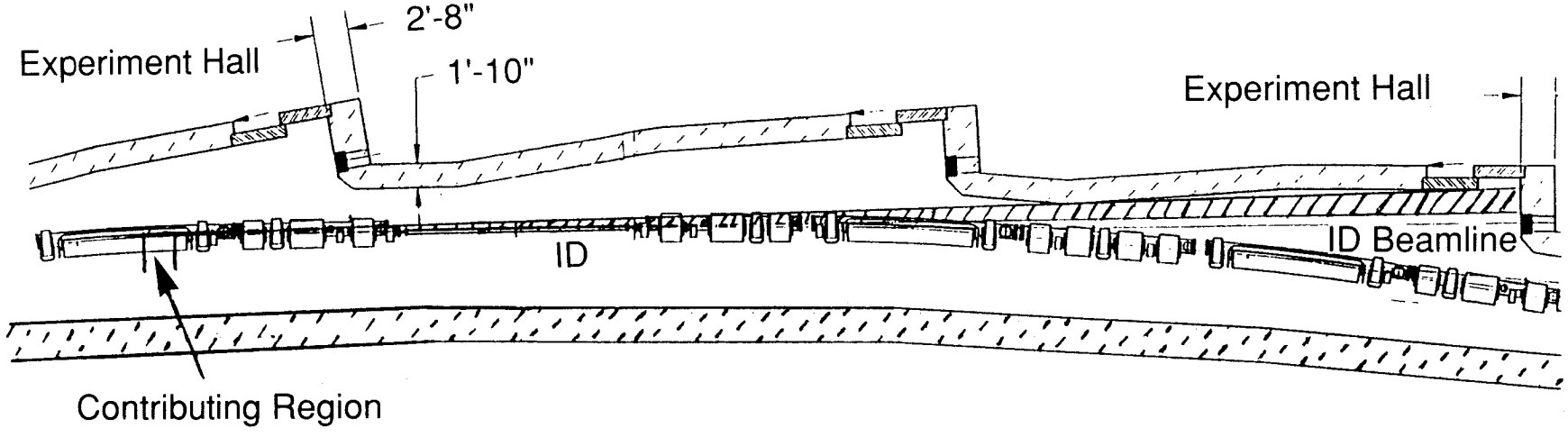

Figure A4. Upstream Bremsstrahlung Radiation Contribution from ID Beamline. Not Intercepted by the Pb Stop or Ratchet Side Wall.

3.0 Location of Additional Shielding

Figures A5 and A6 indicate the range of angles over which the upstream bremsstrahlung contributions strike the ratchet wall, missing the Pb shield for the smaller angle (marked B in Figures A5 and A6) and not absorbed by the side wall of the ratchet shield for the larger angle (marked A in Figures A5 and A6.). Although only 8 cm of lead are needed in the direction of the beam, the amount of lead shielding which is required to cover the lateral spread varies considerably with distance along the direction of the beam. In Figure A5, for example, if the additional Pb shielding is placed at a distance of 4 meters downstream from the near end of the upstream BM, the thickness of Pb needed in the lateral direction would be ~ 10 cm (i.e., ~10.5 - ~0.5) to cover the angular range of 0.05403° to 1.3387°. By adding the local Pb shielding as close to the origin of the bremsstrahlung beam as is feasible, the lateral extent of the necessary Pb can be greatly reduced. However, as indicated by curve B in Figure A5, the upstream bremsstrahlung is still very close to the synchrotron radiation beamline as far as 7 m downstream, making it difficult to shield near the point of origin. The proposed locations for the additional lead shielding for the BM and ID beamlines are also indicated in Figures A5 and A6.

With respect to Figure A5, the value of y at the front face of the ratchet is obtained from

$$y = \left[(610 + R \sin\theta)\sec\theta + \frac{R \sin .5625^{\circ} + x}{\sin(90^{\circ} - .5625^{\circ} - \theta)}\right] \sin(\theta + .5625)$$

$$-[R(1-\cos .5625^{\circ}) + 610 \sin .5625^{\circ}$$

$$+ \{R(1-\cos\theta) + R \tan .5625^{\circ} \sin\theta\}\cos .5625^{\circ}]$$

in which R is the radius of a BM (3896.11 cm), .5625° is the angle in the BM beamline at which the photon beam (synchrotron radiation) originates, θ is the angle, in degrees, in the upstream BM at which the upstream bremsstrahlung radiation originates and x is the distance from the photon beam origin to the face of the ratchet wall (2050 cm).

For Figure A6, the value of y is given by

$$y = (x + R \sin\theta)\tan\theta - R(1-\cos\theta),$$

in which θ is the angle, in degrees, in the upstream BM relative to the ID at which the upstream bremsstrahlung radiation originates and x is the distance from the start of the upstream BM to the face of the ratchet wall (3125 cm). The curves A and B in Figures A5 and A6 can be developed from the above expressions by varying the parameter x.

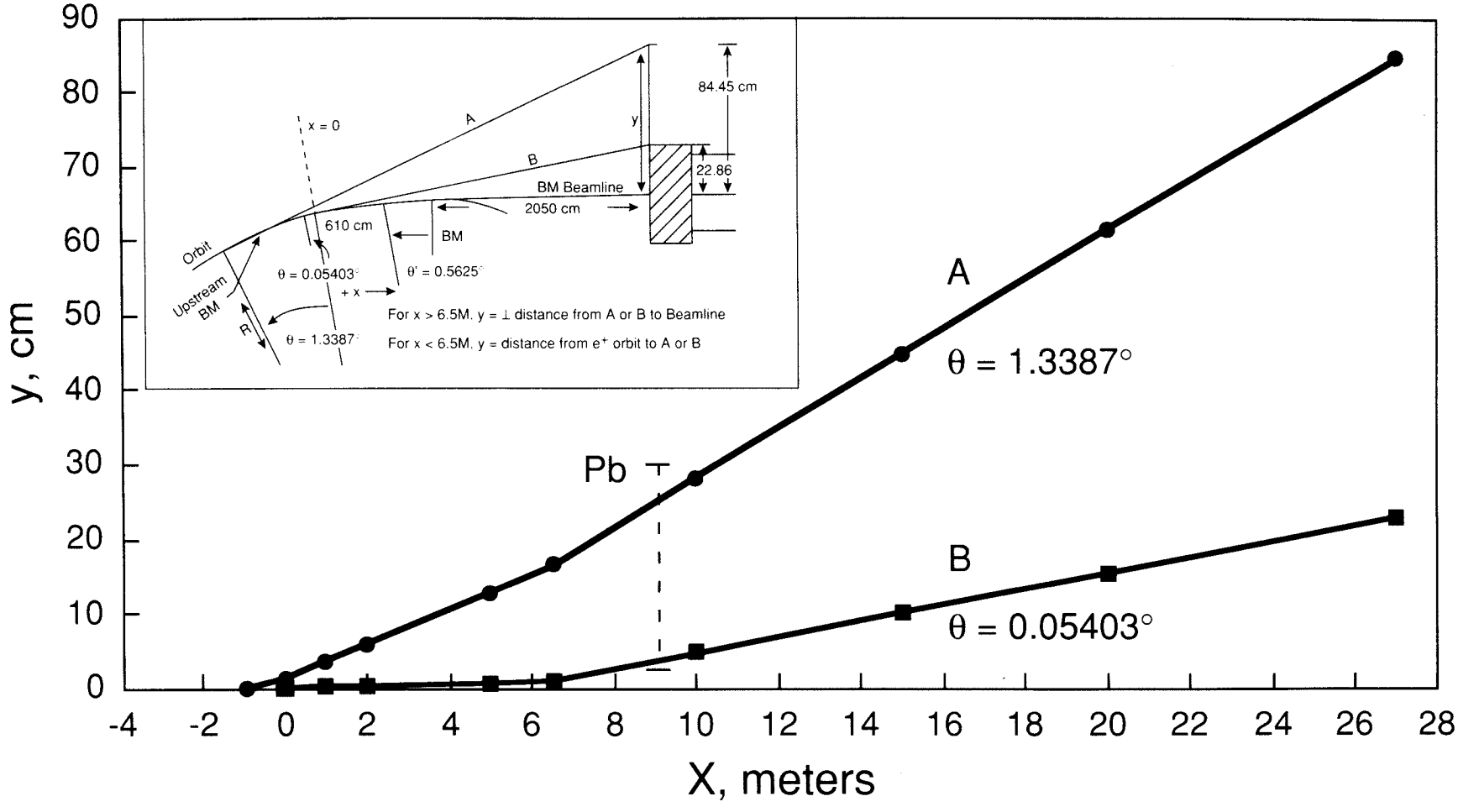

Figure A5. Angular Spread of Upstream Bremmstrahlung from a BM Line.

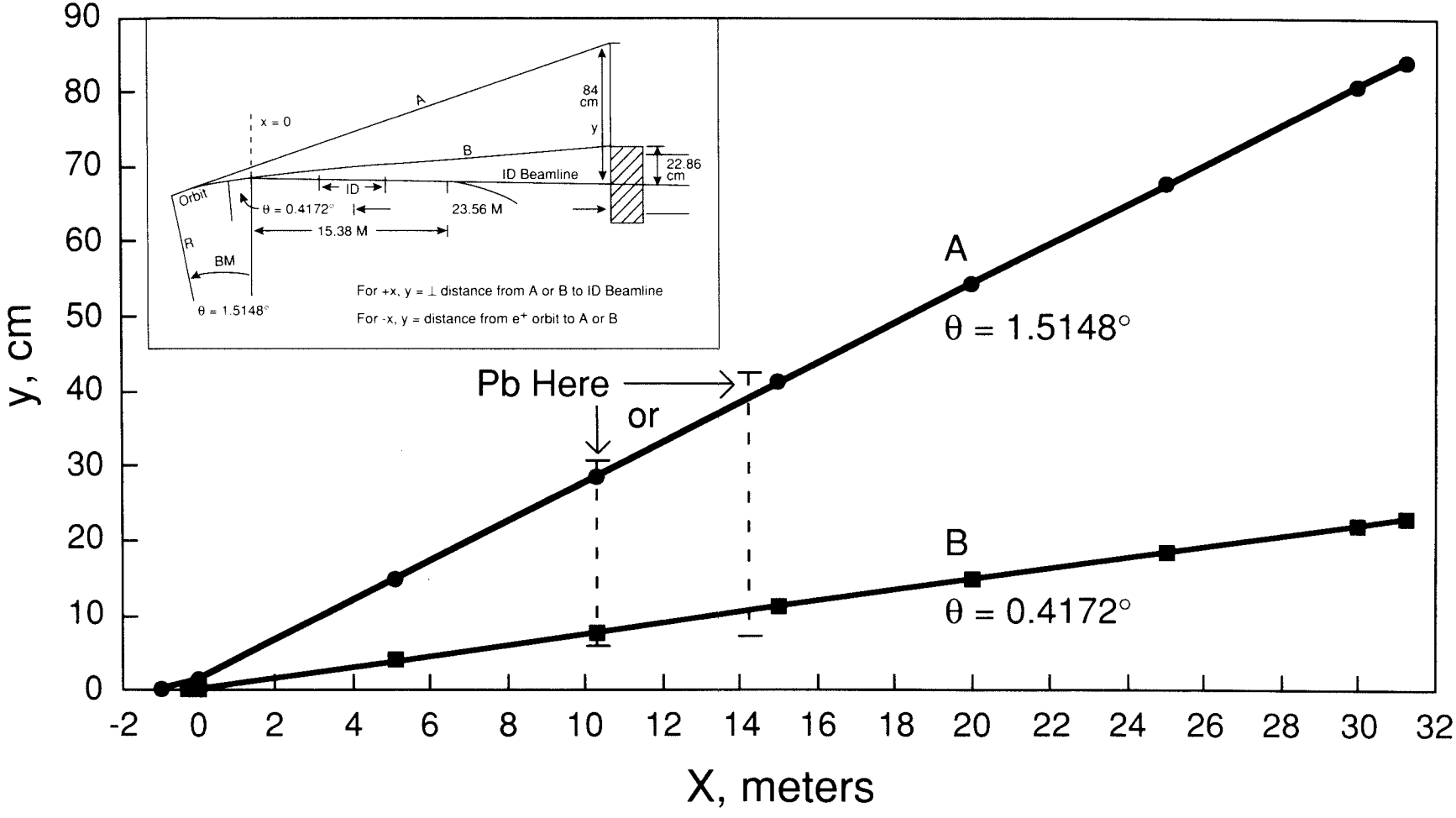

Figure A6. Angular Spread of Upstream Bremsstrahlung from an ID Line.

4.0 Dose Rate in the Radial Ratchet Sections for Continuous Losses

As part of this investigation, the dose rates in the radial ratchet sections were re-evaluated and compared to the previous estimates to determine if the design goals were still being attained. In particular, the dose rate due to the continuous loss of positrons during the assumed 10 h mean lifetime at the closest dose point of 1.3 m (designated as point A in Figure A2) was re-evaluated. In addition, the dose rate at point B in Figure A2 was also re-evaluated, since the upstream radiation generated by continuous positron loss in the previously discussed regions could make the maximum contribution to the dose at this point because it also misses the Pb shielding in the ratchet wall.

For point A in Figure A2, the Pb shield in the ratchet wall effectively shields that point from any upstream bremsstrahlung. However, the actual geometry in the vicinity of the point is significantly different from the idealized geometry of a circular shield (see Figure A1). Figure A7 shows the dose profiles for the case of a circular shield (thickness = 80 cm of normal concrete which is the shielding equivalent of 56 cm of high density concrete) and for the actual ratchet wall shield. As indicated in Figure A7, the dose profile is effectively symmetrically distributed about a peak at $\theta = 359.9°$ for the case of the circular shield. The angle θ refers to the same angle designated in Figure A1. The profile for the ratchet wall shows an irregular pattern as the slant distance through the ratchet wall varies in the vicinity of the dose point. In either case, the major contribution to the dose at a point is from only a few degrees of arc along the positron orbit. The dramatic drop-off of the ratchet wall dose profile (at about 357.5° and lesser angles) is due to the radiation being intercepted by increasing thickness of lead path occurring as the radiation encounters the Pb shield in the ratchet wall.

The bremsstrahlung dose profile was estimated from the expression adapted from Swanson (SWA 85):

$$H_{BREM} = \frac{[16.7E_o(2^{-\theta_B/\theta_{1/2}}) + 833(10^{-\theta_B/21}) + 25(10^{-\theta_B/110})e^{-\Sigma(\rho x/\lambda)_i}}{R^2} \quad \text{(mrem/J)}$$

in which $E_o = 7000$ MeV, $\theta_{1/2} = 100/E_o$ deg, R is the distance from the positron orbit to the dose point, in m, ρ_i(g/cc) is the density of the absorber material of thickness x_i (cm), and attenuation length λ_i(g/cm^2), θ_B is the angle between the forward direction of the positron beam at the point (such as A, B, C, etc in Figure A2) and the line segment from the point to the dose point (AA, BA, CA, etc).

The total contribution to the dose at the point A is obtained by integration over the angle θ. As indicated in Figure A7, the integral in the case of the circular wall is 0.03 mrem deg/J, and that for the actual ratchet wall configuration is 0.0755 mrem deg/J. This means that the

Figure A7. Dose Rate Due to Continuous Loss During SR Operation - 1.3 m Minimum Distance to Dose Point.

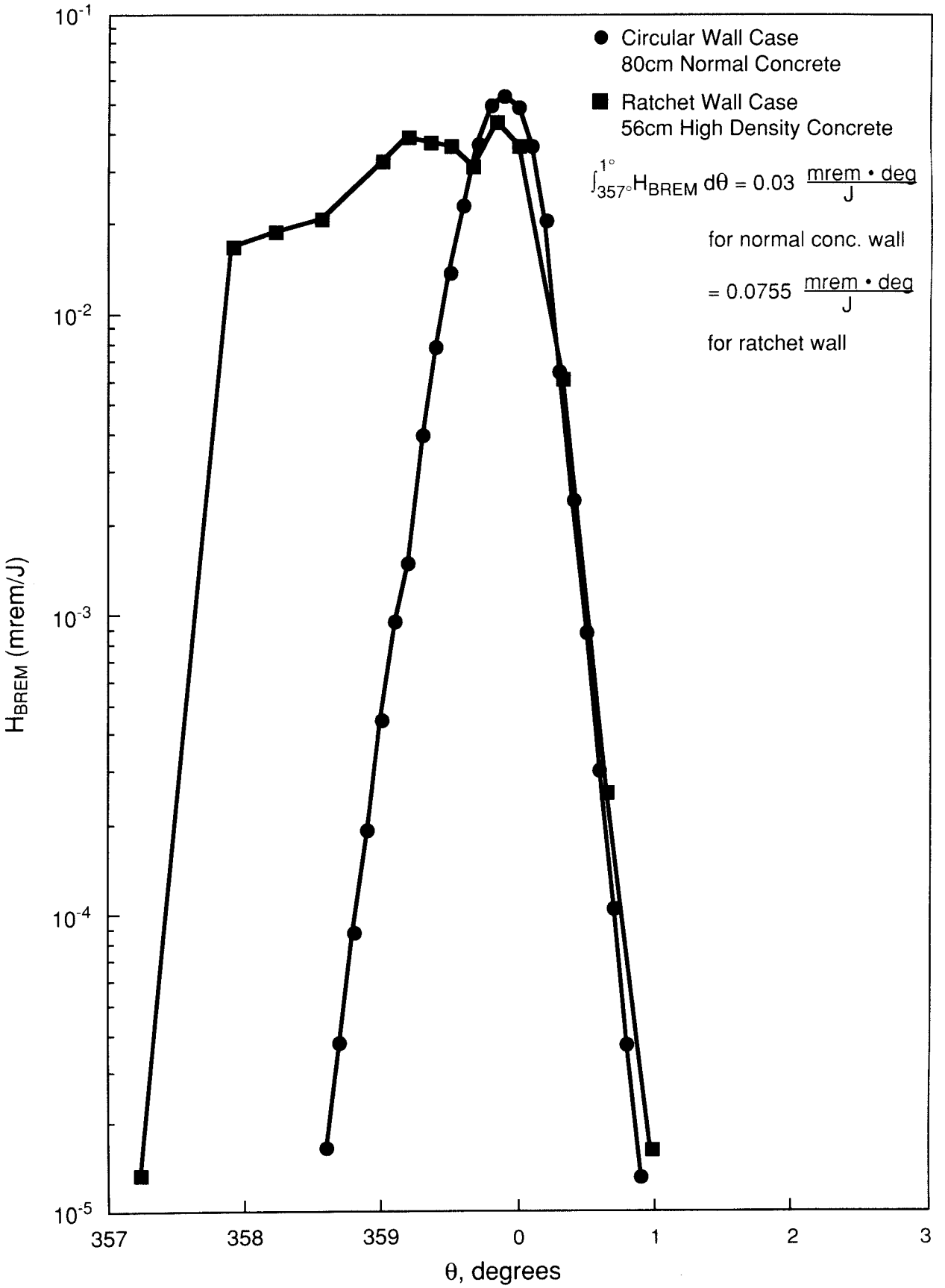

estimated occupational total dose at the closest point should be adjusted from 100 mrem/y to about 252 mrem/y, assuming no local Pb shielding is added. As already discussed in LS-141 (Section 8.3.2), additional local Pb shielding is being planned for operation at 300 mA. For operation at 100 mA, the annual dose would only be one-third of the above value.

The dose profiles for point B in Figure A2 are shown in Figure A8. In this case, the minimum distance from the positron orbit to the dose point is 1.72m. Once again, the dose profile for the case of a circular wall is almost symmetrical about the angle $\theta = 359.9°$. The distribution for the actual ratchet wall in the region around $\theta = 0°$ peaks at a value much less than that for the circular wall case, and quickly drops-off by several orders of magnitude as the Pb shield of the ratchet wall becomes effective. However, if one proceeds far enough upstream, the contribution from the upstream bremsstrahlung must be considered. This contribution causes the distribution to rise abruptly at around $\theta = 354°$ to a value greater than that for the distribution in the vicinity of $\theta = 0°$. The spike in the distribution ($\theta \sim 351°$) occurs for the case in which the 0° bremsstrahlung is directed right at the dose point. For angles less than about 351°, the distribution again drops off very rapidly from the maximum dose since the forward peak of the bremsstrahlung radiation is no longer directed right at the dose point. This rapid drop-off becomes more gradual at about $\theta = 350.9°$ and below because the peak dose component of the bremsstrahlung expression no longer contributes to the dose at the point of interest and the origin of the bremsstrahlung is farther and farther upstream thereby increasing the distance to the dose point. Figure A9 gives a more detailed picture of the structure of the bremsstrahlung spike and indicates the narrow angular range of the peak component.

The total dose contribution for this case for the circular wall assumption is 0.022 mrem deg/J and that for the actual ratchet wall case, including the upstream contribution and the bremsstrahlung spike is 0.0799 mrem deg/J, or about a factor of 3.6 higher than estimated. The dose rate produced is still well within the design goal. Local Pb shielding is needed to intercept the upstream bremsstrahlung to meet the design goal of no more than 100 mrem in a point loss of the positron beam. With this shielding in place, the dose rate for the continuous loss case will be even less than that computed for the circular wall case.

5.0 Location and Lateral Extent of the Additional Lead Shielding

Utilizing the information for the necessary lead thickness and the defined lateral extent of the contributing regions shown in Figures A5 and A6, and coordinating this information with possible places along the storage ring where one is able to place the lead, the following are the recommended lead placements:

For BM Beamlines - Place shield by bellows. The dimensions needed are 10 inches lateral (transverse to the beam), 4 inches in the beam direction and 6 inches in height.

Figure A8. Dose Rate Due to Continuous Loss During SR Operation - 1.72 m Minimum Distance to Dose point.

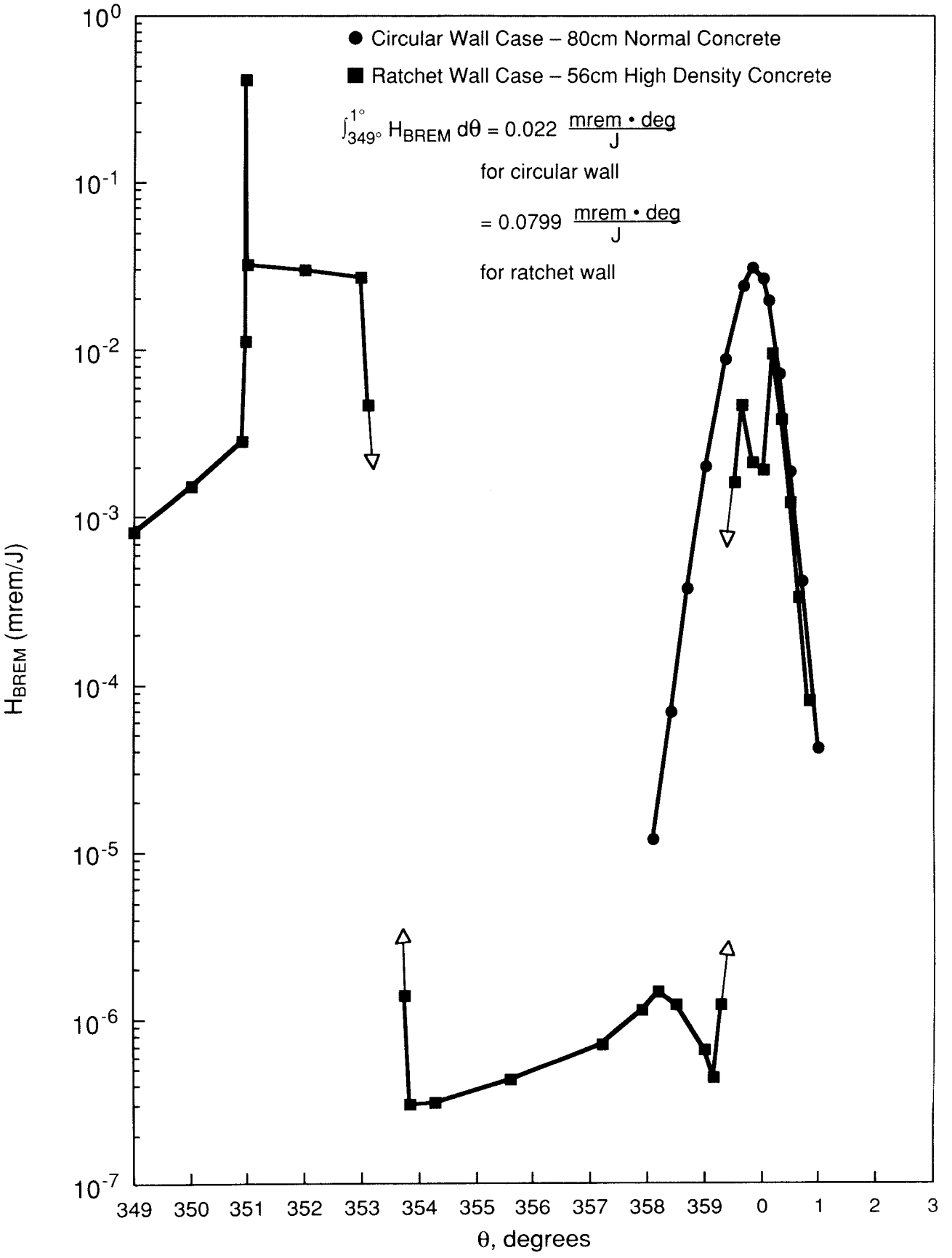

Figure A9. Contribution to Dose From Bremsstrahlung Spike.

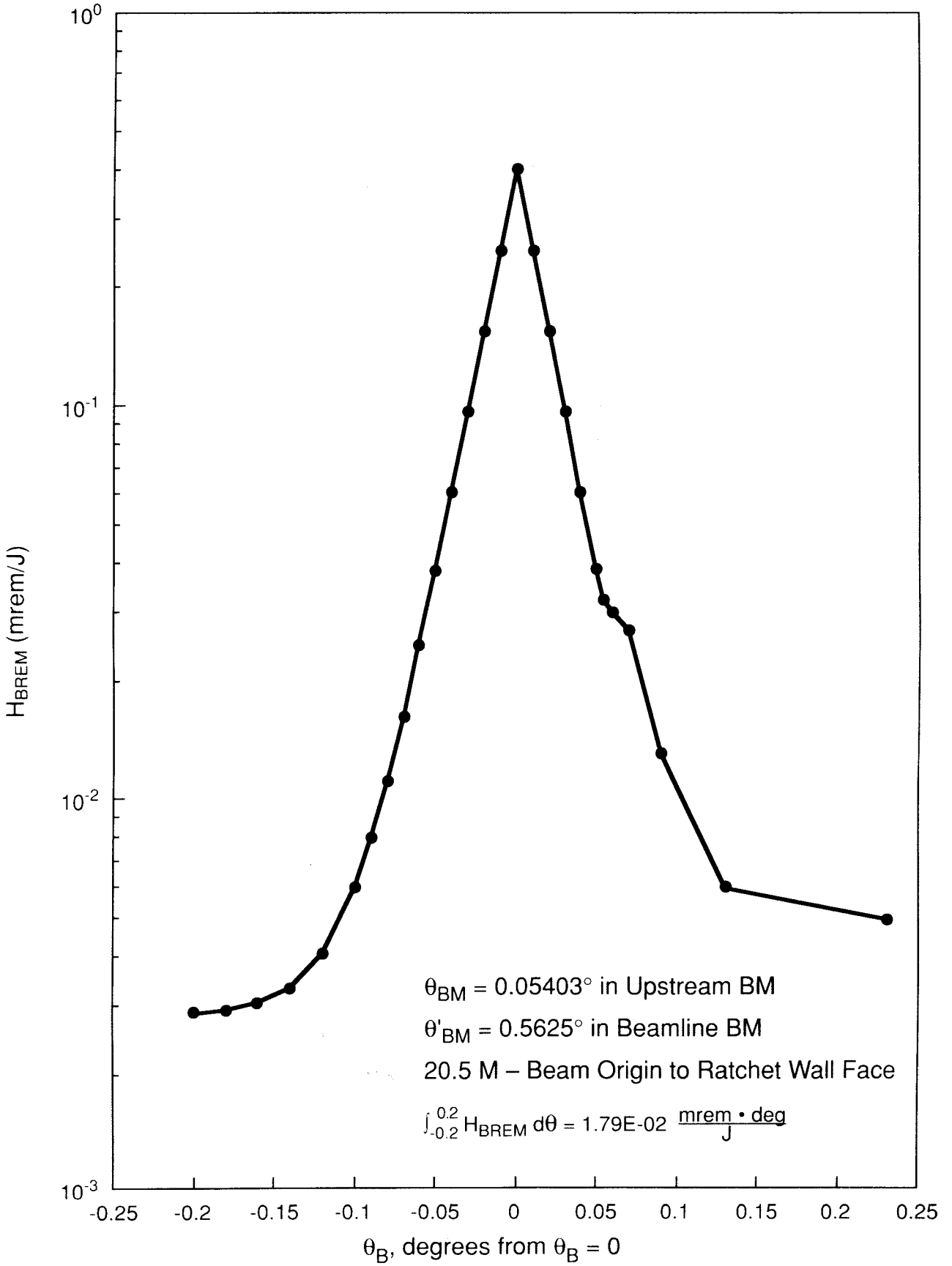

For ID Beamlines - Place shield at end of ID if lead is less than 7.5 cm from the positron orbit. The necessary dimensions are 10 inches lateral, 4 inches in the beam direction and 6 inches in height. If the lead cannot be placed that close to the orbit, the shield can be placed at the next bellows section but the lateral dimension must be increased to 14 inches.

Figure A10 shows the locations along the storage ring of the recommended lead placements for both the BM and ID beamlines. Figures A11 and A12 show the individual locations in better detail with respect to the other storage ring components. Four inches (10.16 cm) of Pb are used for the shield thickness rather than the minimum 8 cm of lead computed because the usual dimensions of available lead bricks are 2 x 4 x 8 inches. The bremsstrahlung attenuation factor in the beam direction is about 100 for the 10.16 cm of lead which also results in a lower dose or dose rate contribution.

REFERENCES

MOE 90 H. J. Moe, "Advanced Photon Source: Radiological Design Considerations." ANL Report, Light Source Note LS-141 (January 1990).

SWA 85 W. P. Swanson, P. M. Deluca, R. A. Otte, and S. W. Schilthelm, "Aladdin Upgrade Design Study: Shielding," University of Wisconsin (1985).

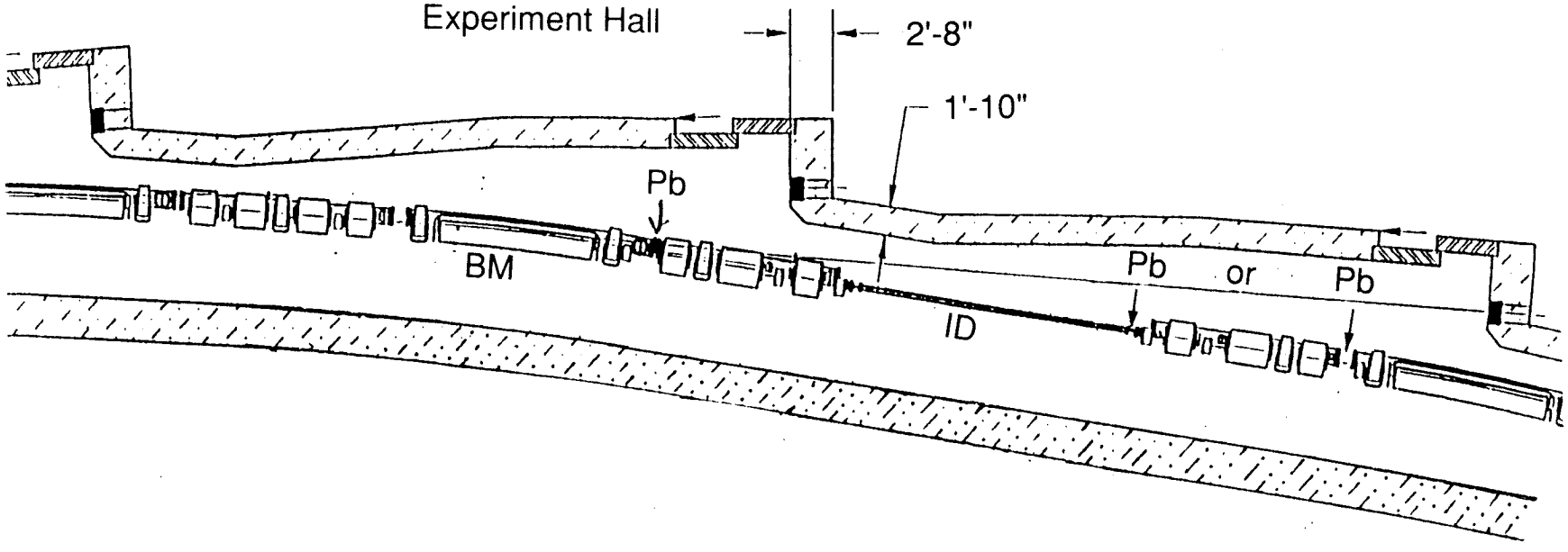

Figure A10. Recommended Locations of Additional Lead Shielding.

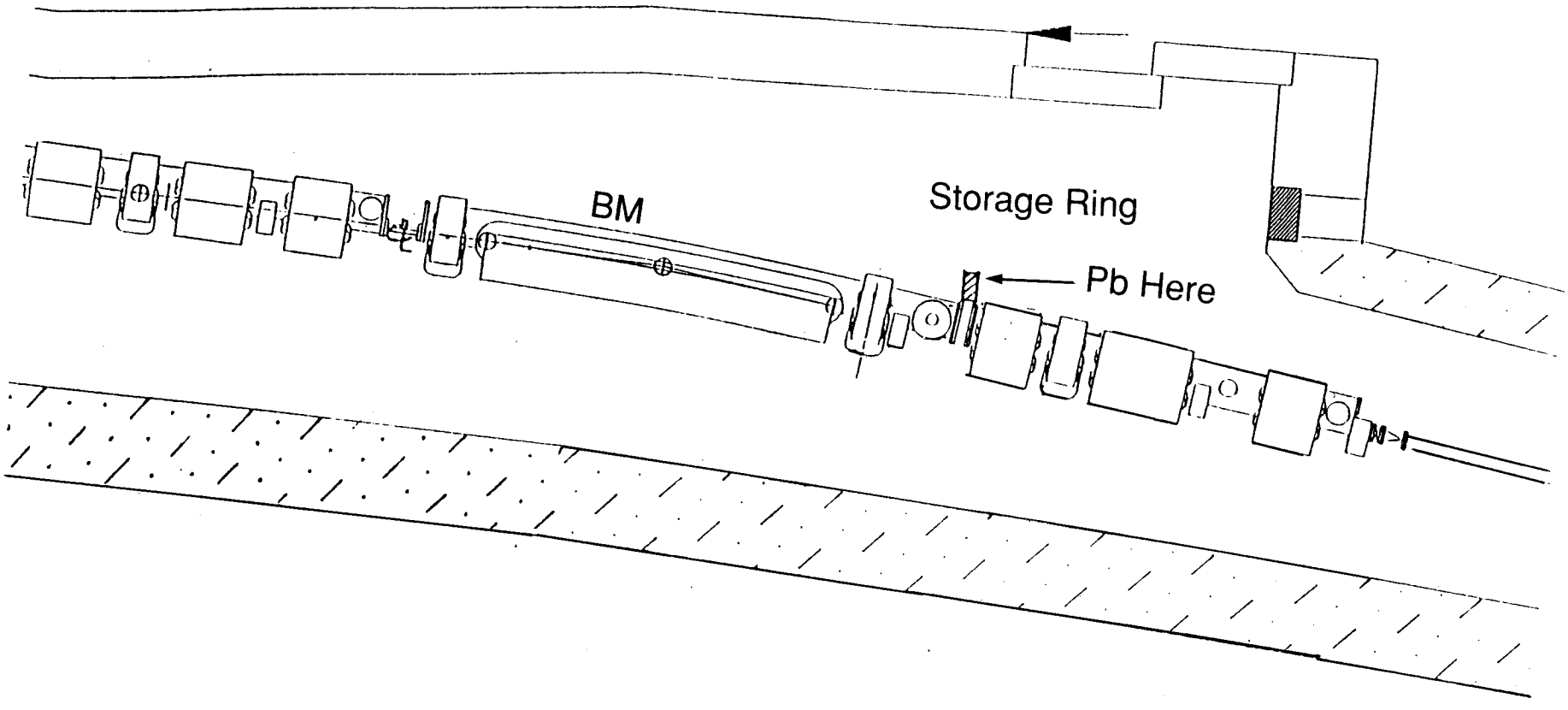

Figure A11. Placement of Lead Shielding for a BM Beamline in Order to Shield Upstream Bremsstrahlung .

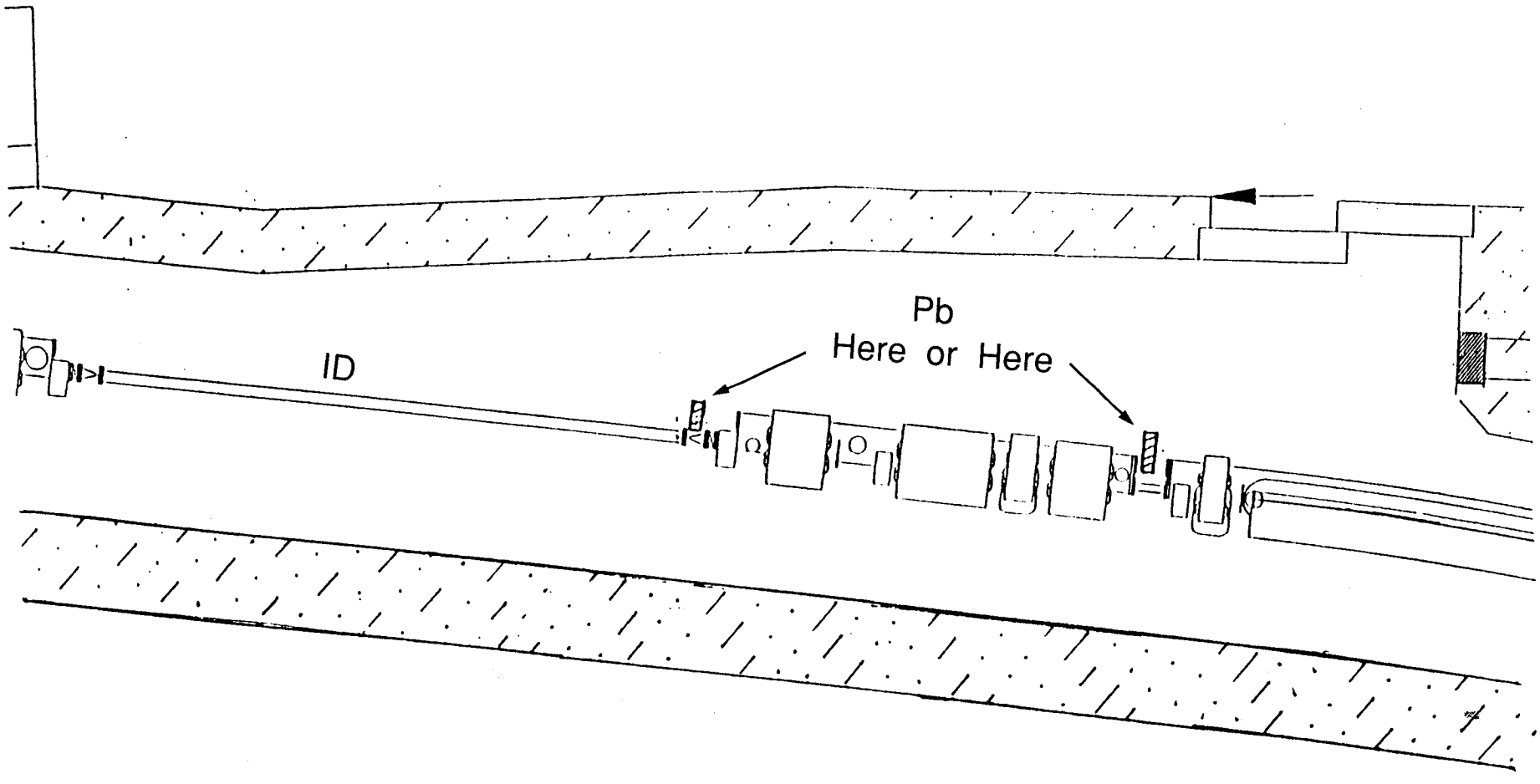

Figure A12. Placement of Lead Shielding for an ID Beamline in Order to Shield Upstream Bremsstrahlung.